Structural Controls on Geothermal Systems along the Northern Andes of Colombia: An Integrated Remote Sensing Analysis of the Dabeiba and Sibundoy Valley Geothermal Fields

Author: Nicolas Montoya Londoño, Geologist

Advisor: Professor Maria Isabel Marin-Ceron, PhD

Graduation Project

Academic Manuscript

Master in Earth's Sciences

School of Applied Sciences and Engineering

EAFIT University

August 2024

PREFACE AND ACKNOWLEDGMENTS

This project is an example not only of an exhaustive, constant, complex, and challenging document to obtain a master's degree, but it also reminds us of what a research product brings with it, when the researcher really wants to capture it. The meaning of research, from the vision of the author of this document, is not only about deciphering a complex network of geological formations, hydrological or hydrogeological processes and evolutionary proposals of millions of years and how to take advantage of it for our purposes. Our effort transcends mere scientific research; It embodies a multidisciplinary odyssey, but above all it means understanding ourselves in a context where man is part of that something that is everything, that surpasses us in size, longevity, strength, and power, and that those of us who have the privilege of investigating can transmit to those who not what it really means.

In this context, we can proudly say that we present a research project, where people participated at all types of training levels for more than 6 years and that thanks to that human capital, we can once again trust that this vision of a science is still of little value for the modern world, and even the university, acquires profound importance. It is not simply an academic search but a search for knowledge, even when assuming the implications that this has in what many call the real world.

I would like to thank those who were part of it, as always, first those who decided to have me here, my parents Adriana Londoño and Freddy Montoya, for their impeccable education, measured love and example of wisdom and resilience. To my brother Pablo, because he taught me that the beautiful thing about creating is the process and the result will be what you built as an artwork. To my future wife Elena, who taught me that when science is human, and done with the heart, it is truly science. To my brother from another mother, the one who still guides us from another earthly plane, Antonio López, my right hand, friend, and colleague, thank you for your support.

Thanks to the EAFIT University, to the teachers of the undergraduate degree in Geology and the Master's in Earth Sciences, to the administrative employees who have greeted me for more than 20 years, but above all thanks to Dr. Maria Isabel Marin, whose life is vocation and pure example of what it means to be an advisor, a teacher, and a real mentor. Thank you for trusting in what I am sure will be the opener of the future of energy science, learning along with us and filling us with arguments, motivation, and preparation to continue investigating what few want to investigate.

TABLE OF CONTENTS

LIST OF FIGURES

LIST OF TABLES

ABSTRACT

This study employs a combination of remote sensing techniques and geothermal analysis to investigate the structural and thermal characteristics of two geothermal systems in Colombia. By utilizing Mark's proposal (1992) for delimitating lineaments, and Principal Component Analysis (PCA) for generating shadow models, the research highlights regional and local structural features that are closely associated with geological structures. Fault systems and lineaments emerge as crucial elements influencing subsurface fluid flow, heat transfer, and the development of geothermal reservoirs. The integration of remote sensing data with advanced structural analysis techniques reveals significant factors shaping geothermal dynamics in the region. These findings emphasize the necessity of considering structural controls in the exploration and sustainable management of geothermal resources. The study focuses on the Dabeiba Geothermal System (DGS), potentially linked to a Miocene extensional event, emphasizing the role of fault structures, especially in the Guineales Formation, as conduits for fluid flow and heat migration from deep sources. The complex structural zones with different degrees of deformation and fracture densities directly influence the advection of the isotherms near the Dabeiba-Pueblo Rico suture zone. This geothermal play system is dominated by fault-controlled non-magmatic convection, where convection occurs predominantly along fault lines and is accompanied by meteoric water infiltration along their traces. The Sibundoy Valley Geothermal System (SVGS) as a typical example of a mixed geothermal system, where heat originates from a young magmatic source but is mainly controlled by deep faults within a pull-apart basin. These faults not only influence the distribution of monogenetic volcanoes but also shape the spatial arrangement of hydrothermal springs. The interaction between geological structures and fluid flow patterns highlights the complexity of geothermal systems. Furthermore, the presence of partial crystallizations and unique caldera geometries leads to the formation of seal layers or condensate layers, redirecting both meteoric water recharge fluxes and volcanic heat fluxes, significantly impacting hydrogeological and geothermal dynamics. This research contributes valuable insights for the geoscientific and energy exploration communities, informing decision-making processes for the assessment and development of geothermal resources.

Keywords: *Geothermal exploration, Remote sensing, Structural analysis, Automatic Lineament extraction, Principal Component Analysis (PCA), Dabeiba Geothermal System (DGS), Sibundoy Valley System (SVGS).*

RESUMEN

Este estudio emplea una combinación de técnicas de detección remota y análisis geotérmico para investigar las características térmicas y estructurales de dos sistemas geotérmicos en Colombia. Utilizando la propuesta de Mark (1992) como base para la delimitación de lineamientos y el Análisis de Componentes Principales (PCA) para generar modelos de sombra, la investigación aclara características estructurales que están estrechamente asociadas con estructuras geológicas. Los sistemas de fallas, y lineamientos emergen como elementos cruciales que influyen en el flujo de fluidos subterráneos, la transferencia de calor y el desarrollo de yacimientos geotérmicos. La integración de datos de teledetección con técnicas avanzadas de análisis estructural revela factores importantes que dan forma a la dinámica geotérmica en las zonas de interés. Estos hallazgos enfatizan la necesidad de considerar controles estructurales en la exploración y gestión de los recursos geotérmicos. Se destaca que el Sistema Geotérmico de Dabeiba (DGS), se encuentra potencialmente vinculado a un evento extensional del Mioceno, enfatizando el papel de las estructuras de falla, especialmente en la Formación Guineales, como conductos para el flujo de fluidos y la migración de calor desde las fuentes profundas. Las zonas estructurales complejas con diferentes grados de deformación y densidades de fractura influyen directamente en la advección de las isotermas cercanas a la zona de sutura Dabeiba-Pueblo Rico. Este sistema geotérmico está dominado por la convección no magmática controlada por fallas, donde el flujo ocurre predominantemente a lo largo de líneas de falla y va acompañada de infiltración de agua meteórica. El Sistema Geotérmico del Valle de Sibundoy (SVGS) corresponde a un sistema geotérmico mixto, donde el calor se origina a partir de una fuente magmática joven pero está controlado principalmente por fallas profundas dentro de una cuenca de separación. Estas fallas no sólo influyen en la distribución de los volcanes monogenéticos sino que también dan forma a la disposición espacial de los manantiales hidrotermales. La interacción entre las estructuras geológicas y los patrones de flujo de fluidos, además de la presencia de cristalizaciones parciales y geometrías únicas de caldera, conducen a la formación de capas de sello que redirigen tanto los flujos de recarga de agua meteórica como los flujos de calor volcánico, que afectan significativamente la dinámica hidrogeológica y geotérmica. Esta investigación realiza aportes valiosos para las comunidades de exploración geocientífica y energética, informando los procesos de toma de decisiones para la evaluación y el desarrollo de los recursos geotérmicos.

Palabras clave: *Exploración geotérmica, Teledetección, Análisis estructural, Extracción automática de lineamientos, Análisis de componentes principales (PCA), Sistema Geotérmico Dabeiba (DGS), Sistema Valle de Sibundoy (SVGS).*

1. INTRODUCTION

Given the increasing interest and need for the energy transition towards renewable sources, several authors have outlined fundamental parameters to improve the understanding of geothermal exploration. These parameters encompass geological-structural characterization, hydrogeological studies, geophysical investigations, and hydro-chemical analyses of hot springs (Montoya et al., 2019). Broadly, hydrothermal activity is influenced by many factors, including fluid circulation, heat sources, and pathways to the surface (Setyawan et al., 2015). Thus, developing a geothermal conceptual model requires a combination of site-specific exploration techniques to thoroughly understand the geological controls in the target area (Kenya & Oham, 2009; Moeck, 2014).

The permeability architecture within geothermal areas is typified by the geometry and kinematics of fault and fracture networks (Sibson, 1996; Roulleau et al., 2017). In hydrogeological terms, this differentiation between fractured media and porous media is based on fractures/joints properties such as continuity, persistence, aperture, and spacing, which can be quantified through fieldwork or geoprocessing (Singhal & Gupta, 2010). It is posited that fractures within the rock mass extend from the surface to depths of several tens of meters (Montoya et al., 2019), and the key to understanding it is the spatial distribution of the structures.

Modeling the thermal regimes within tectonic environments is intricate bacuase of to the rise of the geothermal gradient, rising over the footwalls of normal faults via isothermal advection during rapid exhumation. Moreover, factors such as erosion, burial, and sedimentation in the hanging walls further complicate the modeling process (Ehlers and Chapman, 1999; Gorynski et al., 2014). In fault-controlled systems (fractured medium), convection flow may occur along regional faults, and groundwater may intermix with meteoric water, needing analysis of the fractured medium at various hydro-structural processing scales (Reed, 1983).

The northwest region of Colombia presents a complex geological context derived from the interactions between the South American, Nazca and Caribbean plates (Rodríguez & Zapata, 2012). This interaction has resulted in a mosaic of tectonic blocks bounded by regional fault systems with a predominant N-S orientation. This tectonic segmentation strongly influences underground flow and hydrothermal processes. However, the attribution of the general trend on a regional based solely on the behavior of the

predominant fault structures should be complemented by the processing of remote sensing data. Automated lineament identification is more efficient, accurate, and faster than manual processing, which is inevitably influenced by subjective parameters (Muhammad and Awdal, 2012; Radaideh et al., 2016).

Generating surfaces using techniques complementary to those proposed by Mark (1992) allows detailed statistical analysis for weighted surfaces, facilitating the comparison of results related to structural trends to conclusively ascertain dominant structures in an area. Hence, in a complex tectonic environment such as the Northern Andes, exploring synergies between remote sensing techniques and structural analysis methodologies is imperative to improve the understanding of hydrogeological and geothermal characteristics in systems with limited or no exploration and characterization. Considering the objective of efficiently characterizing and classifying a geothermal system, the classification introduced by Moeck (2014) categorizes geothermal systems based on geological environment, heat transport mechanism (conduction vs. convection), and type of heat source (magmatic vs. non-magmatic).

The regional geotectonic context also strongly influences the geothermal potential and recently, Moeck et al, (2020) expands this concept by introducing a step-by-step analysis of geothermal plays, which allows understanding the geological controls at different levels within a system. However, specific differences in key geological controls and operation between contrasting types of geothermal systems, such as conventional, unconventional, and hybrid systems, are still not well understood. Evaluating these differences through the application of indirect exploration techniques, such as remote sensing, would allow the development of optimal exploration and evaluation strategies for each type of resource and geothermal play, with the aim of comparing different contexts within existing classifications.

Two study areas were selected: The Dabeiba Geothermal System (DGS) and the Sibundoy Valley Geothermal System (SVGS). DGS represents a low to medium enthalpy system, dominated by normal faults that are part of the Dabeiba-Pueblo Rico suture zone in the western part of the department of Antioquia. In contrast, SVGS is a mixed system where the heat source is young magmatic activity associated with monogenetic volcanoes, but its flow is dominated by deep faults that form the pull-apart basin where not only monogenetic volcanoes and their derived products are oriented, but also hydrothermal springs. The use of advanced remote sensing techniques, such as satellite imagery, together with structural analysis tools, aims to reveal the subsurface complexities and structural controls that influence the hydrogeological and geothermal characteristics of these regions.

2. CONCEPTUAL FRAMEWORK AND PROBLEM STATEMENT

The American Institute of Geosciences (2005) defines a geothermal system as a localized geological setting where Earth's internal heat flow is transported near the surface by circulating steam or hot water. This heat flow is exploited to extract renewable energy, either directly or by conversion to electricity (Moeck, 2014). They typically comprise a heat source, permeable reservoir, heat transport fluid, and permeable geological medium enabling fluid flow (Moeck et al., 2020). Understanding geothermal systems entails knowledge of thermal and hydrogeological regimes, fluid dynamics, chemistry, faults, fractures, stress regime, and lithological sequence, all influenced by the tectonic environment (Moeck, 2014). Traditional classifications based on temperature and enthalpy lack geological insight (Sanyal, 2005), prompting Moeck (2014) to introduce a classification scheme based on geological environment, heat transport mechanism, and heat source type. Moeck et al. (2020) further extended this concept by introducing a tiered analysis of geothermal plays, providing insights into geological controls at different levels within a system, from broad geosystem focus to local prospect scale (Genter et al, 2012).

In general, geothermal fields are dominated by either a convection or conduction heat transfer regime and said transfer mechanism defines the type of geothermal system (Moeck et al., 2020; Montoya et al., 2019). In convection-dominated geothermal plays, upward circulation of fluids transports heat from depth to shallower reservoirs or to the surface (Moeck, 2014). These play systems occur in areas of active tectonism (Nukman & Moeck, 2013), active volcanism (Deon et al., 2012), young plutonism (less than 3 Ma), and elevated heat flow caused by extensional tectonics (Faulds et al., 2009). Convection of thermal fluids induced by a heat source or elevated heat flow transports heat from deeper levels to the surface, and structural controls have a major effect on fluid flow pathways in high-temperature convection-dominated play systems.

In the Colombian Andes, there are three types of geothermal systems that differ significantly due to the unique geological environments of pull-apart basins, active volcanic regions, and suture zones. According to the classification of geothermal systems presented by Moeck (2014) in Figure 1, the Dabeiba geothermal system (DGS) is part of the extensional domains dominated by convection, apparently controlled by regional faults, and the Sibundoy geothermal system (SVGS) could be considered as a

mixed system between an extensional and a volcanic one. It features long-distance fault heat transport but also has a shallow magmatic heat source, which is suggested to be currently inactive.

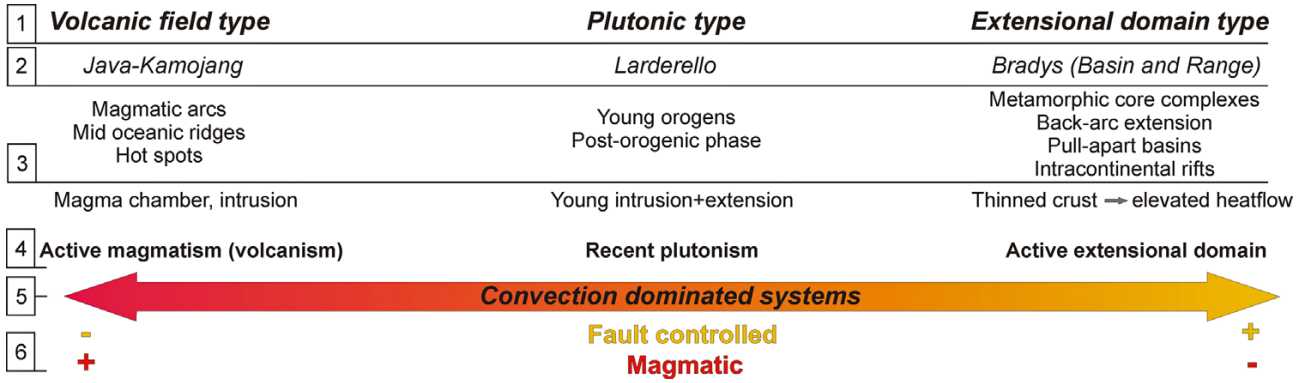

FIGURE 1. CATALOG SCHEME FOR CONVECTION DOMINATED GEOTHERMAL PLAY SYSTEMS BASED ON THE GEOLOGIC CONTROLS OF IGNEOUS ACTIVITY AS MAGMATISM (VOLCANIC TYPE WITH TYPUS LOCALITY JAVA, INDONESIA), RECENT PLUTONISM (INTRUSION TYPE WITH TYPUS LOCALITY LADERELLO ITALY IN THE PERIPHERY OF THE ALPINE OROGENY), AND ABSENT IGNEOUS ACTIVITY BUT SIGNIfiCANT ACTIVE EXTENSION (EXTENSIONAL DOMAIN TYPE WITH TYPUS LOCALITY BASIN AND RANGE, WESTERN USA.). 1 – PLAY TYPE, 2 – TYPUS LOCALITY, 3 – PLATE TECTONIC SETTING, 4 – GEOLOGIC HABITAT OF POTENTIAL GEOTHERMAL RESERVOIRS, 5 – HEAT TRANSFER TYPE, 6 – GEOLOGIC CONTROLS. TAKEN FROM MOECK, 2014.

Magmatic geothermal plays encompass volcanic fields and are typically situated in regions characterized by active basaltic volcanism at divergent plate margins, basaltic to andesitic volcanism along island arcs, or recent andesitic to dacitic volcanism along continent-continent convergent margins, often with recent plutonism (McCoy-West et al., 2011; Deon et al., 2012). Within volcanic fields, magma chambers having parental melts influence fluid chemistry, fluid flow, and the overall geothermal play system, through processes such as recharge of basalt and crystallized melts (Moeck, 2014). Such systems are commonly divided into distinct upflow and outflow zones (Hochstein, 1988). In these upflow zones, the hydrothermal products are typically characterized by near-neutral pH and chloride-rich chemical composition. Mixed systems involve the migration of heat from a young magmatic source primarily dominated by volcanism, helped by a network of regional faults that regulate fluid flow as presented in Figure 2. These systems may exhibit zones of upward flow where temperature gradients typically increase at shallow depths but decrease below the outflow layer, as outlined by Moeck (2014).

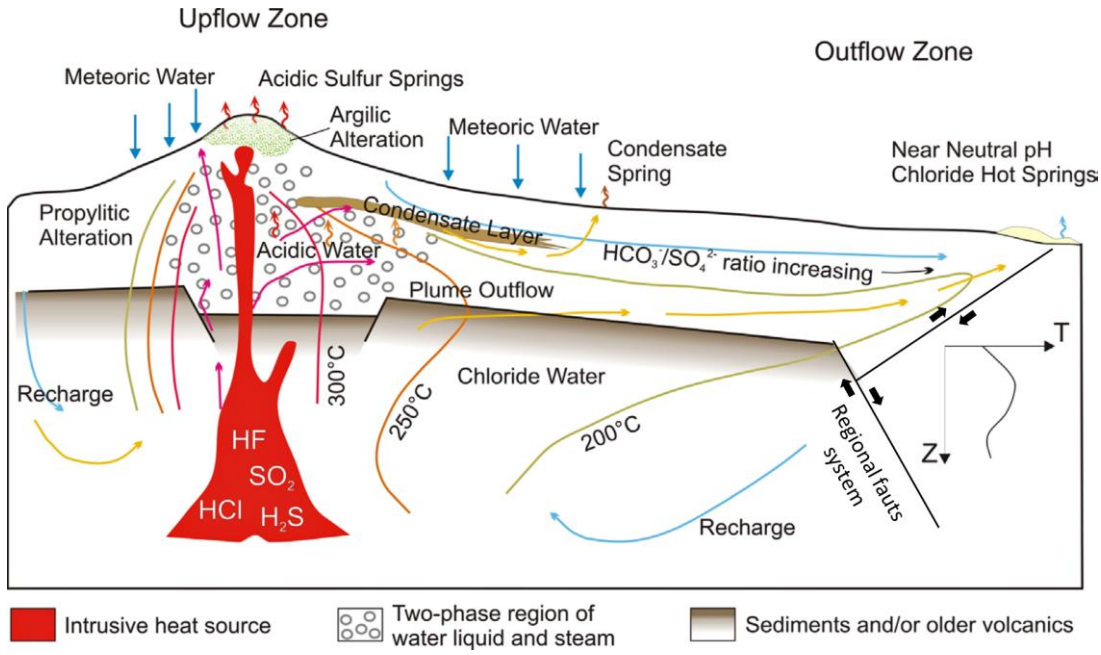

FIGURE 2. GEOTHERMAL PLAY TYPE RELATED TO AN ACTIVE VOLCANIC FIELD TYPICAL FOR A MAGMATIC ARC SETTING ABOVE A SUBDUCTION ZONE. TWO HEAT FLOW ZONES AND RELATIONSHIP BETWEEN THERMAL EMANATIONS AND REGIONAL STRUCTURAL SYSTEMS. MODIFIED FROM MOECK, 2014.

In contrasting manner, non-magmatic convection-dominated geothermal play systems show two primary control mechanisms: fault-controlled and fault-leakage controlled. In fault-controlled systems, convection predominantly occurs along fault lines, often accompanied by infiltration of meteoric water along these fault zones (Reed, 1983). Conversely, fault-leakage controlled systems involve fluid leakage from faults into permeable concealed layers. Subsequently, fluids may migrate from these permeable layers into fault zones and eventually reach the surface (Moeck, 2014).

As thermal fluids disperse away from the upwelling zone along fault zones, they undergo mixing with cooler groundwater or meteoric water (Figure 3). This mixing process is shown by observable changes in chemical composition, such as an increase in bicarbonate and magnesium levels, coupled with a decrease in boron, sulfate, and chloride concentrations (Flynn & Ghusn, 1983); (Nicholson , 1993).

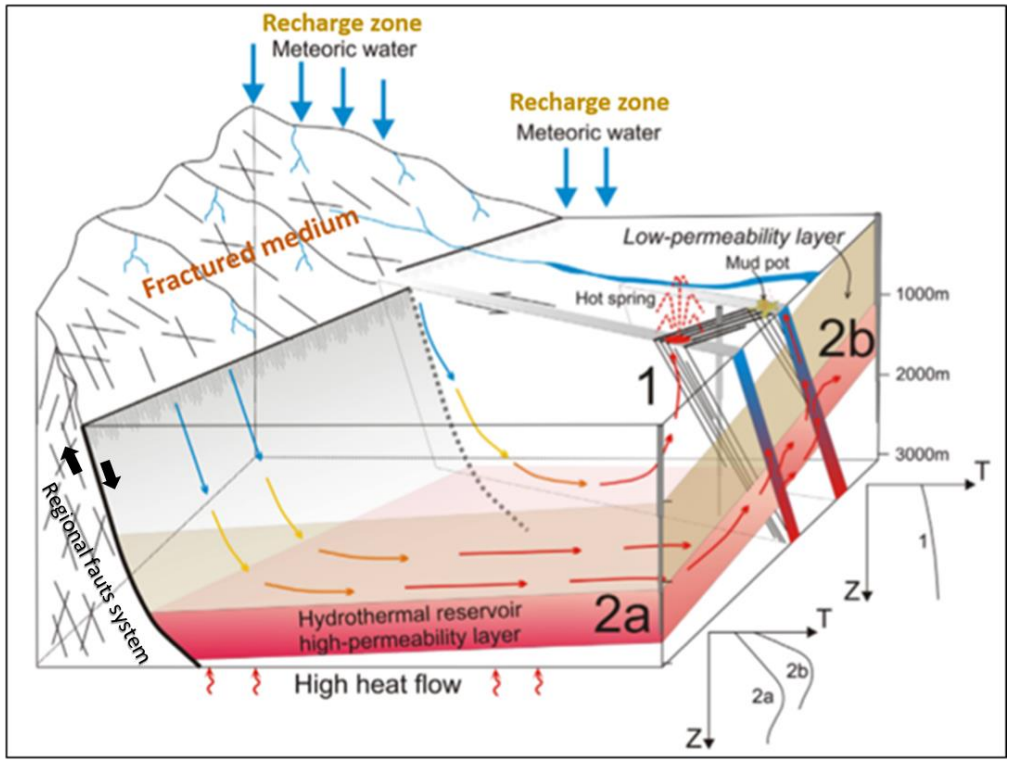

FIGURE 3. NON-MAGMATIC ACTIVE GEOTHERMAL PLAY SYSTEM IN ACTIVE EXTENSIONAL TERRAINS WITH DIFFERENT TYPES OF RESERVOIRS (1, 2A AND 2B). TYPE 1 IS A CONVECTION CELL FROM INFILTRATION TO DISCHARGE ALONG ONE FAULT. TEMPERATURE GRADIENT IS GRADUALLY INCREASING AT WELL SITE 1. TYPE 2A AND 2B ARE FAULT LEAKAGE-CONTROLLED PLAYS. THE TEMPERATURE GRADIENT OF A WELL DRILLED INTO SUCH AN AREA RISES TO THE PERMEABLE LAYER AND DROPS BELOW THE LAYER (WELL 2A AND 2B). MODIFIED FROM MOECK, 2014; MONTOYA ET AL, 2019.

Some basic parameters have been defined to better understand geothermal exploration, such as geological-structural characterization, hydrogeological and geophysical studies, along with hydrochemical analysis of thermal waters. In general, hydrothermal activity depends on numerous factors, including understanding fluid circulation, heat sources, and pathways (Setyawan et al., 2015). Therefore, a combination of multi-technique approach with a set of modern site-specific exploration techniques must present a preliminary geothermal conceptual model (Kenya & Oham, 2009) for a deep understanding of the geological controls of the play (Moeck, 2014).

The starting point of the different analyses is the hydrogeochemical characterization of the thermal springs, with the aim of identifying the types of water sources, finding the origin and temperature profile of the geothermal fluids, establishing their relationship with local hydrology and hydrogeology and understanding the fluid-rock interactions crucial for the exploration of the geothermal system (Gómez Díaz, 2017). This analytical approach involves investigating whether the fluids derive from meteoric

water, volcanic water, or a combination thereof, while also examining the processes of water-rock interaction that influence their chemical composition.

Additionally, hydrogeochemical analysis allows the identification of mixing and dilution processes by evaluating conservative and non-conservative solutes in fluids, and the study of stable and radiogenic isotopes provides information on fluid circulation and recharge processes, including areas of recharge, elevations, and deep circulation patterns. Its importance lies in the possibility of identifying when a geothermal play presents the percolation of meteoric waters from the recharge zones of the system that, when heated, react with the host rock, dissolving and adding many chemical components to the geothermal fluid (Giggenbach, 1991; Gómez, 2017). The geochemical characterization of hot springs becomes the key background for the delimitation of a geothermal system, its association with the type of heat source, and allows us to propose the first hypotheses of the heat flow, recharge flow lines, and associated processes in the geothermal play.

In this way, by relying on the geometry of the regional structural systems and on the preliminary context generated by geochemistry in relation to the thermal behavior of a specific system, it is possible to propose, through distributed surfaces of lineament density with geostatistical support, the flow directions of a geothermal play, its controls, and the factors that differentiate them from systems with other characteristics. The effectiveness of using surfaces and images for lineament studies has been proven by many case studies of hydrogeological mapping (Corgne et al., 2010), groundwater resource assessment (Koch & Mather, 1997), and latent fault detection for risk models and neotectonics (Bonforte et al., 2013).

To find geothermal zones, an index is necessary that quantifies the spatial concentration of lineaments such as the density of faults and fractures (Soengkono, 1999). As proposed by Saepuloh et al. (2017), it is common to obtain from the linear characteristics, a series of indices or surfaces distributed in relation to the intersection, frequency, and length of lineaments. The first two indices were used to correlate hydrogeological characteristics with geology (Corgne et al., 2010), and the third index was used to specify the degree of fracturing (Hung et al., 2005). Then, by obtaining the correlation between the three indices and the high permeability zones, the different fluid paths within a system can be inferred.

While clear classification strategies exist, specific differences in key geological controls and operations between contrasting types of geothermal systems, such as conventional, unconventional, and hybrid systems, are still poorly understood. Therefore, **our research question is**: What is the relationship

between the identified geological structures, as revealed through the integration of remote sensing and structural analysis, and the hydrogeothermal flow paths in the DGS and SVGS?

This research question aims to delve into the specific mechanisms through which geological structures influence the hydrogeological and geothermal characteristics of geothermal fields. By understanding the interactions between identified structures and subsurface processes, the research aims to provide insights that can inform geothermal resource assessment, development, and sustainable management strategies. To answer this question, **we hypothesize** that the structural features detected by remote sensing and structural analysis are indicators related to the distribution and direction of hydrogeothermal flow paths in the Dabeiba and Sibundoy Valley geothermal systems. This flow control hypothesis could relate both to meteoric water infiltration processes and possible volcanic water flows from deep sources in regional migration routes. The **main objective** of this study is to investigate how geological structures found by integrating remote sensing and structural analysis influence hydrothermal dynamics in two geothermal systems with contrasting geological characteristics and environments. This overarching goal encompasses several specific aims that are related at a methodological level within the comparative characterization of systems. These **specific objectives are**:

(1) Define the mechanism and type of geothermal Play: Using available basic and thematic cartography, as well as hydrogeochemical characterization of thermal sources and classifications proposed in the literature, each geothermal system will be evaluated based on the background research conducted by the Geothermal Research Group in recent years, enabling the definition of the heat transfer regime.

(2) Acquisition of remote sensing data: Downloading digital elevation models from the ALOS PALSAR satellite and later processing to gather comprehensive information on surface features and topography in the mentioned geothermal systems. The primary product will be the basin-scale digital elevation model represented on a raster surface with a pixel size of 10 x 10 meters.

(3) Structural Analysis Techniques and data integration: Applying advanced structural analysis methods, including lineament extraction, fracture density mapping, and Principal Component Analysis (PCA), to identify and characterize the structural components influencing hydrogeological and geothermal processes. This involves integrating remote sensing-derived data with structural analysis results to create a comprehensive understanding of the subsurface conditions, fault systems, and structural controls within the study areas.

3. ANALYTICAL METHODS

For the proper development of the research and to accurately align the appropriate results with each specific objective to address the research question, the methodology was divided into four main stages.; (1) Search and analysis of secondary thematic information, to define the mechanism and type of geothermal play; (2) Acquisition and process of remote sensing data; (3) Structural Analysis techniques and data integration; (4) Integration of information and proposal of geothermal signatures. The methodological flow chart is presented in Figure 4.

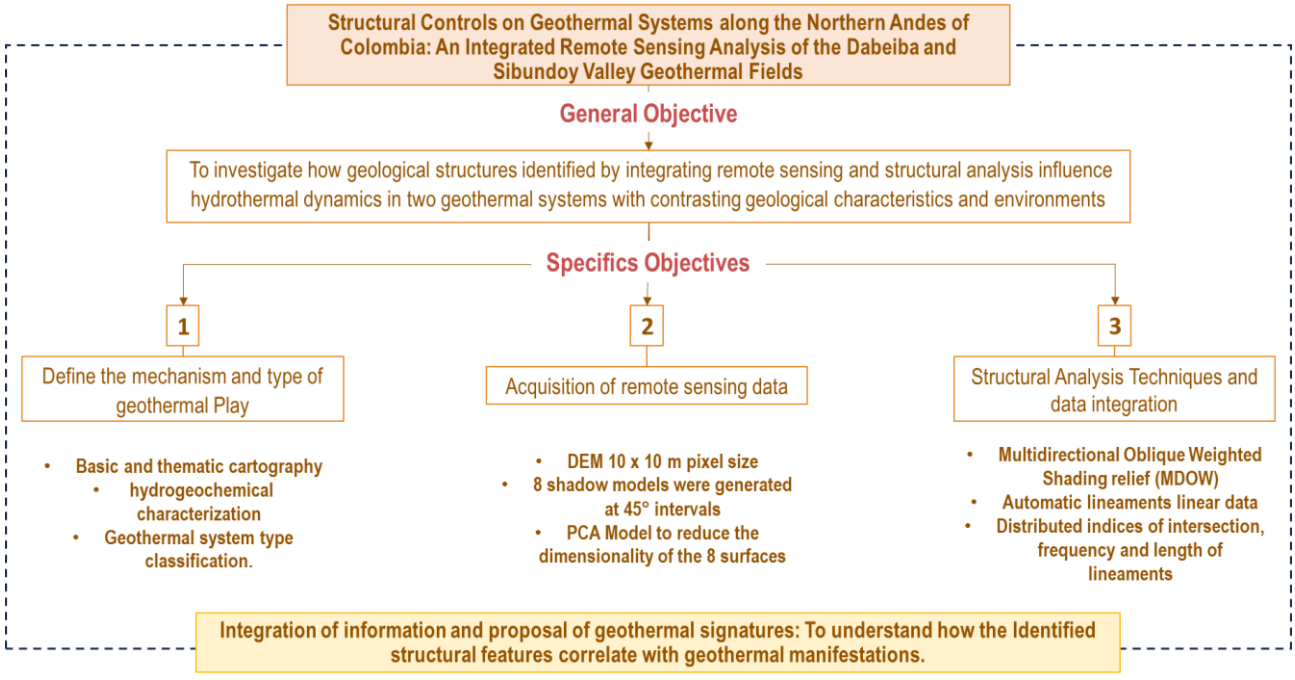

FIGURE 4. METHODOLOGICAL SUMMARY TO ADDRESS THE PROBLEM STATEMENT. STAGES AND PRINCIPLES RESULTS.

3.1.Search and analysis of secondary information.

Based on the secondary information available and previous research results on geothermal plays, the main objective of this section is to classify each system according to Moeck's proposal (2014), using litho-structural blocks. The compilation of all relevant bibliographic information related to this goal is presented in Table 1.

The method analyses secondary information related to basic geological cartography, evolutionary models, conceptual diagrams and key tectonic and structural findings of the study areas, to define the conceptual geometry of the geothermal play, considering the relationship between stratigraphic units and regional structural systems.

Subsequently, this conceptual geology is correlated with the locations of thermal springs inventoried by the Colombian Geological Survey in 2014, along with hydrogeochemical analyses conducted in 2018 and 2021 for each geothermal play. The methodological approach for both plays follows a similar framework, starting with the calculation of the charge balance error (CBE) for all springs to ensure the reliability of the chemical dataset obtained by the SGC and remove from the analysis samples with ionic imbalances.

The general classification involves generating Piper and Stiff diagrams to show the type of water in each thermal spring. The Cl-SO_4-HCO_3 diagram is then utilized to characterize water types and classify and correlate geothermal fluids with geology and subsurface processes. Additionally, Cl-Li-B and Cl-Sr-B diagrams are generated using 'conservative' elements. Lithium and boron are considered conservative elements due to their behavior in geothermal systems. Subsequently, the Na-K-Mg diagram proposed by Giggenbach (1991) is applied to set up physicochemical equilibrium between the fluid and the host rock, providing a first estimate of reservoir temperature and showing if they are suitable for solute geothermometers. All diagrams and solute geothermometer calculations are performed and adapted according to Gómez (2019), based on the spreadsheet of Powell & Cumming (2010).

3.2.Remote Sensing Data Acquisition and Processing

Remote sensing structural analyses rely on satellite elevation data obtained from the ALOS-PALSAR satellite in GeoTIFF format. The data acquisition process involves direct download into NASA's Vertex-Alaskan Viewer, easing access to high-resolution digital elevation models (DEMs) and complementary datasets. Preprocessing of the acquired data is conducted using ArcMap v10.8 software. The elevation data, initially captured at a pixel scale of 12.5 meters, undergo resampling to 10 meters to enhance representation accuracy and optimize computational efficiency during next analyses. This resampling is carried out using the "resampling" tool, which implements an interpolation algorithm based on the B-

Spline technique—a method that uses piecewise polynomial functions to create smooth and flexible curves through a set of data points.

TABLE 1. BIBLIOGRAPHIC DATA COLLECTED FOR THE CLASSIFICATION OF THE TYPE OF GEOTHERMAL PLAY. SUMMARY OF OBJECTIVE 1.

Name	Author	Year
POMCA Rio Sucio Alto Basin	CORPOURABÁ	2018
Geology and geochemistry of sheet 114-Dabeiba. Scale 1:100.000	Servicio Geológico Colombiano (SGC)	2014
Geology and geochemistry of sheet 115-Toledo. Scale 1:100.000	INGEOMINAS	1987
Geology and geochemistry of sheet 129-Cañasgordas. Scale 1:100.000	Servicio Geológico Colombiano (SGC)	2005
Geology and geochemistry of sheet 130-SantaFe De Antioquia. Scale 1:100.000	Servicio Geológico Colombiano (SGC)	2016
Comprehensive Research of the Colombian Pacific Platform. Cartographic sources of geology, geomorphology, soils, and threat sheets 101, 102, 103, 104, 112, 113, 128. Urabá, Antioquia.	IGAC e INGEOMINAS	2001
Provenance and Structural Style of the Penderisco Formation and Beibaviejo Sedimentites in the Uramita-Dabeiba Cut: Relationship to the Evolution of the Panama–Chocó Block (PCB)	Botero	2018
Geological mapping and geochemical sampling of sheets 144, 145, 128, 129, 113 and 114	INGEOMINAS	2009
National Water Study - ENA. Colombia	IDEAM	2018
Potential and prospects for hydrogeological exploration according to lithostructural criteria in Antioquia department, Colombia.	Betancur & Martinez	2022
Low Enthalpy Geothermal System at Dabeiba, Colombia; an Assessment Through the Hydrogeochemistry of Thermal Waters	Gómez	2019
Geothermal conceptual model for the low enthalpy geothermal play at Dabeiba-Antioquia, Colombia	Montoya et al	2019
SGC Hot Springs Inventory. Location and physico-chemical description of the three hot springs of the Dabeiba thermal system.	Servicio Geológico Colombiano (SGC)	2014
Regional geological reconnaissance of sheets 411 La Cruz, 412 San Juan de Villalobos, 430 Mocoa, 431 Piedmont, 448 Monopamba, 449 Orito and 465 Churuyaco. Departments of Caquetá, Cauca, Huila, Nariño and Putumayo. Scale: 1:100,000.	Servicio Geológico Colombiano (SGC)	2003
Zoning of potential infiltration and flow lines in the Sibundoy geothermal play	López et al	2023
The current tectonic motion of the Northern Andes along the Algeciras Fault System in SW Colombia	Velandia et al	2005
Preliminary geothermal conceptual model at the Sibundoy geothermal play, SW Colombian volcanic arc. A conventional or non-conventional geothermal play?	Ramirez et al	2021
Late Cenozoic to Modern-Day Volcanism in the Northern Andes: A. Geology and Tectonics of Northwestern South America	Marín-Cerón et al	2019

Analytical relief shading techniques are commonly employed in regions characterized by tectonic activity to find linear features with specific orientations (Radaideh et al., 2016). To achieve this, the resampled

DEM is processed to evaluate terrain response under varying angles of light incidence. Utilizing the "Hillshade" tool, eight shadow models are generated at 45° intervals, following the methodology proposed by Mark (1992), with a constant inclination of 30°. Additionally, the "Aspect" tool is used to create a terrain appearance model, which assesses the direction of slope to reveal elements that may not be visible under other lighting angles.

3.3.Statistical Model: Principal Component Analysis (PCA)

To enhance the assessment of shadow surfaces in automatic lineament analysis, a statistical approach was employed, drawing upon concepts from data analysis. Principal Component Analysis (PCA) is a statistical technique used to reduce the dimensionality of a dataset by transforming the original variables into a smaller set of uncorrelated components, known as principal components, which capture the maximum variance in the data. The PCA Model was utilized to reduce the dimensionality of the eight shadow surfaces, aiming to address potential redundancy in terms of directional frequency. By statistically grouping the data, PCA found two distinct groups of shadow models, from which definitive surfaces were derived to replicate Mark's (1992) proposed procedure. This technique enables a more detailed examination of areas within an image that would otherwise be either illuminated or left in darkness by a single lighting source (Mark, 1992).

Traditional shaded relief maps generated by conventional models tend to emphasize structures obliquely illuminated while excluding those illuminated along the structural domain (Mark, 1992). To address this limitation, a statistical analysis was conducted in accordance with the scale of the cartographic information, starting with a correlation matrix including 986 points associated with the centroid of each 1 km x 1 km cell within the study area for the Sibundoy case, and 1716 points for the Dabeiba case. The resulting values, organized into a database of 986/1716 rows and 8 columns, formed the basis for the correlation matrix. Values close to 1 or -1 say high correlation between surfaces, suggesting complementarity, while values close to 0 signify differences between surfaces, highlighting terrain features that may show trends in different directions.

Subsequently, using MATLAB processing code, the two principal components were derived from the correlation matrix. The first principal component was represented by a combination of models at 135°, 180°, 225°, and 270°, grouping complementary surfaces from 45°, 90°, 315°, and 360°.

3.4.Digital Processing for Identification of Linear Features

The method employed simulates the effect of artificial light from a point source of illumination with specific altitude and azimuth, drawing upon established techniques (Radaideh et al., 2016). Using a Multidirectional Oblique Weighted Shading (MDOW) relief shading method, shaded images are generated from multiple azimuthal angles, each weighted according to the general terrain aspect model (Radaideh et al., 2016). This approach combines different lighting angles within a single image, providing valuable insights into diverse spatial patterns of linear features that may not be discernible with a single illuminated image (Radaideh et al., 2016).

Mark's (1992) proposal typically implements four shadow models at 225°, 270°, 315°, and 360°, weighted by the oblique factor obtained from equation 1. However, to align with the findings of the principal component analysis, a comparative model is run for PCA surfaces, following the MDOW model (Mark, 1992) with surfaces at 135°, 180°, 225°, and 270°, as outlined in equation 2.

$$W(225°) = sin2aspect - 225°$$
$$W(270°) = sin2aspect - 270°$$
$$W(315°) = sin2aspect - 315°$$
$$W(360°) = sin2aspect - 360°$$

Equation 1. MDOW Weighting Proposal. Taken from Mark, 1992.

$$W(135°) = sin2aspect - 135°$$
$$W(180°) = sin2aspect - 180°$$
$$W(225°) = sin2aspect - 225°$$
$$W(270°) = sin2aspect - 270°$$

Equation 2. MDOW + PCA Weighting Proposal. Adapted from Mark, 1992.

To obtain the shadow models weighted by the oblique factor, map algebra is implemented following equations 3 and 4 for Mark's proposed model and the model adjusted to PCA analysis, respectively.

$$Mark's\ weighted\ image = W(225°) * Shades225° + W(270°) * Shades270° + W(315°) * Shades315° + W(360°) * Shades360°$$

Equation 3. Obtaining Weighted Image. MDOW Weighting Proposal. Taken from Mark, 1992.

$$PCA\ Model\ \ weighted\ image = W(135°) * Shades135° + W(180°) * Shades180° + W(225°) * Shades225° + W(270°) * Shades270°$$

Equation 4. Obtaining Weighted Image. MDOW + PCA Weighting Proposal. Adapted from Mark, 1992.

After generating the shadow models, automatic lineament extraction was performed using Geomatics 2016 software with the "LINE EXTRACTION" algorithm, configured according to the parameters proposed by Radaideh et al. (2016): RADI (Filter Radius) =24, GTHR (Edge Gradient Threshold) =70, LTHR (Curve Length Threshold) =30, FTHR (Line Fit Threshold) =3 , ATHR (Angular Difference Threshold) = 7, and DTHR (Link Distance Threshold) =70. These parameters were selected to ensure high sensitivity in the extraction model, with Radaideh et al proposal (2016) considered the most suitable adaptation for analysis models in intra-montane reliefs after testing various configurations.

Following extraction, the data were validated, and any lineaments with lengths less than 100 meters, considered as "noise" at the working scale of 1:100,000, were removed. It's important to note that while determining the dominant direction based on lineament frequency is common, it may not always be accurate and should be cross-referenced with local and regional trends defined in cartography. Automated extraction has limitations, including difficulty distinguishing between geological and non-geological lineaments, leading to imprecise mappings that may include non-geological features such as railways and roads (Leech et al., 2003; Sarp, 2005; Radaideh et al., 2016). The processed results from the two weighted surfaces were combined with the traces of the main faults to create a single file of linear characteristics for each study area. Using the 1 x 1 km matrix proposed for PCA analysis, metrics such as the quantity, length, and number of intersections of linear structures were obtained to map three lineament density

indices proposed by Saepuloh et al. (2017): Ll (Length of lineaments), Lf (frequency of occurrence), and Li (density of intersections). Distributed surfaces were generated using ordinary kriging interpolation adjusted to either the spherical or exponential model according to the methodological proposal.

4. CASE 1: DABEIBA GEOTHERMAL SYSTEM (DGS)

The Dabeiba Geothermal System was suggested as a play of interest by Montoya et al. (2019) and is part of the 122 hydrothermal emanations found outside the blocks and areas of geothermic interest in Colombia (Alfaro et al., 2021). This system falls within the municipalities of Cañasgordas, Uramita, Dabeiba, and Mutatá, located in the northwestern region of Antioquia, Colombia. It spans elevations ranging from 180 to 3200 meters above sea level on the northwestern slope of the Cordillera Occidental. Hydrographically, the study area is located within the Riosucio basin, which is part of the Caribbean Hydrographic Area, specifically the Caribbean Coastal Hydrographic Zone and the Atrato-Darién Hydrographic Subzone (CORPOURABA, 2018).

For this study we are focused on the extension associated with the Upper and Middle of the rio Sucio Basin within the area of the department of Antioquia, in the vicinity of the Aquifer System and the Gulf of Urabá. The system contains three selected thermal waters of the SGC inventory: the Manantial Guineales, located near the Riosucio River, approximately 12 km (7.5 miles) from the urban area of Dabeiba; the Chobar spring, which appears on the slope approximately 3 kilometers northwest of the road to Urabá Antiqueño; and the Mohán Spring, the southernmost point located near the Mohán School, about four hours upstream from the Chimurró stream. The location of the DGS influence zone, in relation to the Alfaro et al. (2021) prospecting proposal, is presented in Figure 5. Surface hydrogeochemical data of hot springs compiled by the SGC (2014) record temperatures ranging between 27 and 30°C., suggesting a low to medium enthalpy geothermal play, which according to Alfaro et al. (2021), is related to geothermal areas outside the blocks of greatest interest and that are possibly associated with fractured/faulted hydrothermal systems. In general, geothermal resources have been evaluated only along magmatic-geothermal systems, and the so-called “blind” geothermal systems, associated with fractured media, are unexplored and represent a scientific challenge with high potential to contribute to knowledge (Gorynski et al., 2014).

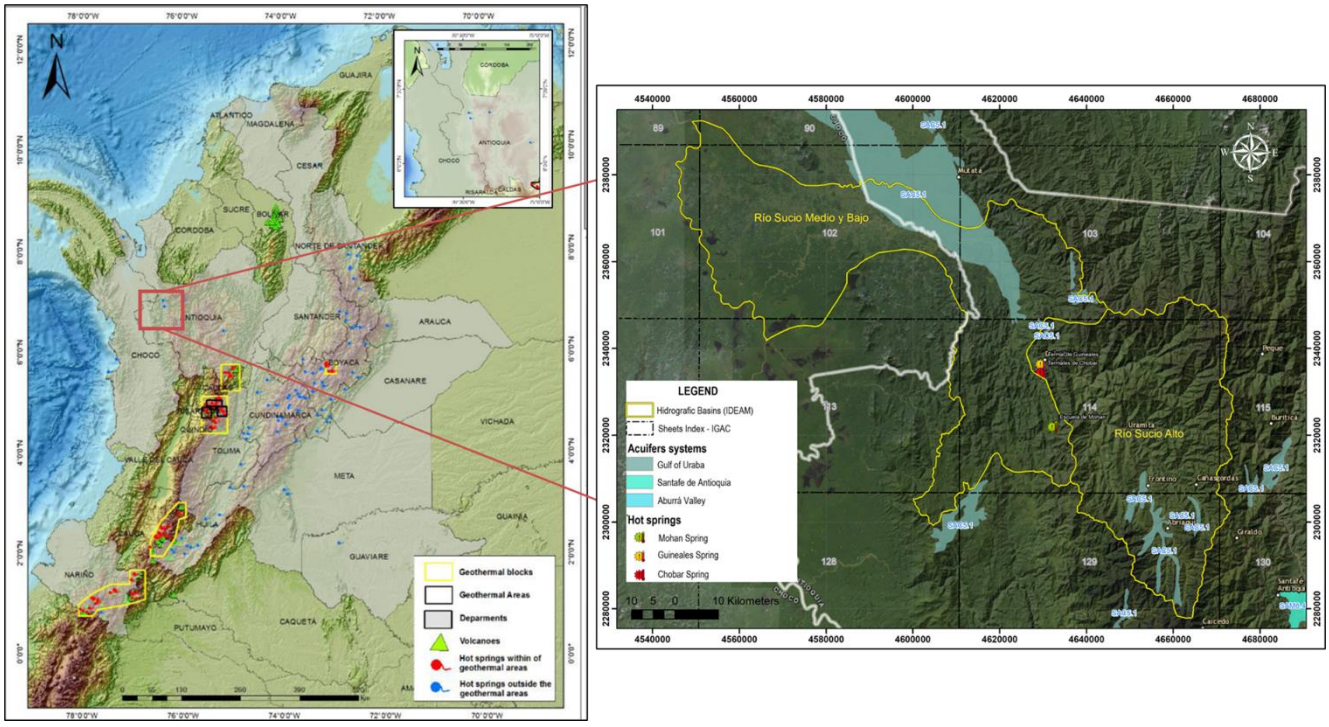

FIGURE 5. LOCATION OF PRELIMINARY GEOTHERMAL AREAS (BLACK POLYGONS) AND BLOCKS (YELLOW POLYGONS) IN COLOMBIA. IN THE RED RECTANGLE, THE LOCALIZATION OF DABEIBA GEOTHERMAL SYSTEM (DGS). GREEN DOT MOHAN HOT SPRING, RED DOT CHOBAR HOT SPRING, YELLOW DOT GUINEALES HOT SPRING. ADAPTED FROM MONTOYA ET AL., 2019; ALFARO ET AL, 2021.

4.1.Geological framework and tectonic setting

The tectonic environment in this region is linked to the triple junction of the Nazca, Caribbean, and South American plates, resulting in a mosaic of large and deformed lithotectonic blocks bounded by faults oriented in a regional N-S direction (Rodríguez & Zapata, 2012). This tectonic interaction between two regional blocks creates a context of deformed rocks composed of the Chocó-Panamá Block (PCB) and the Cañas Gordas Block (CGB). In Colombia, the Chocó-Panamá Block consists of the Mandé Batholith (Álvarez, 1970), the Santa Cecilia-La Equis Complex (Calle & Salinas, 1986), and the Cañas Gordas Block. The latter is characterized by a basaltic oceanic affinity basement represented by the Barroso Formation (Rodríguez & Arango, 2013) and a set of Cretaceous sedimentary units known as the Penderisco Formation (Álvarez & Gonzalez, 1978).

Structurally, the region is dominated by transpressive fault systems, with significant movement along the N-S trending Romeral Fault System (RFS) and the trends of the Dabeiba Pueblo Rico Fault System

(DPRFS) (Rodríguez et al., 2012). These two systems are considered the main sutures defining the trend and dominant structural regime within the study area. Locally, they are represented by the Cañasgordas Fault, Chimurro Fault, and Cerrazón Fault from west to east (Rodríguez & Zapata, 2012), also controlling lithological contacts.

Figure 6 shows the lithological units that appear in the study area. From east to west consist of Cretaceous sedimentary rocks of the Penderisco Formation (K2alu) (Álvarez & González, 1978), interspersed with basaltic flows from the Barroso Formation (JRK1du). These complexes associated with the Cañasgordas Complex are faulted in contact with the Guineales Formation (E3N1g) (SGC, 2014) and the Boton´s Basalts (N4N5bb), along a series of N-S structures. These structures also affect the rocks of the Santa Cecilia-La Equis Complex (E1csce) and lead to the emplacement of intrusive bodies to the south and west of the basin, such as the Mandé Batholith (E1tm), and felsic bodies associated with early Miocene volcanism

Two predominant regional fault systems with a north-south orientation prevail: (1) The Western Edge System of the Central Cordillera, which encompasses the Cauca-Romeral System and includes several faults such as Cauca-Almaguer, Cauca Occidental, Tonusco, Espíritu Santo, Santa Rita, and Sabanalarga, along with their associated satellite faults; (2) The Dabeiba Fault System, which includes, among others, the faults of Dabeiba, La Herradura, San Ruperto, Urrao, and Río Verde. To the west of the Dabeiba-Pueblo Rico Fault is the Amparradó-Murindó fault system. Together, these two fault systems exert considerable influence on the regional tectonics of the northern part of the Cordillera Occidental, resulting in a predominantly compressive style in the area. While the Western Edge System of the Central Cordillera shows dextral movement, the Dabeiba Fault System shows a sinistral part with normal and reverse displacements (INGEOMINAS, 2010). Additionally, there are also faults with northeast and northwest orientations, which are younger in their formation than the regional system. These faults are crucial as they fracture the blocks, interrupt, and displace the N-S trending faults.

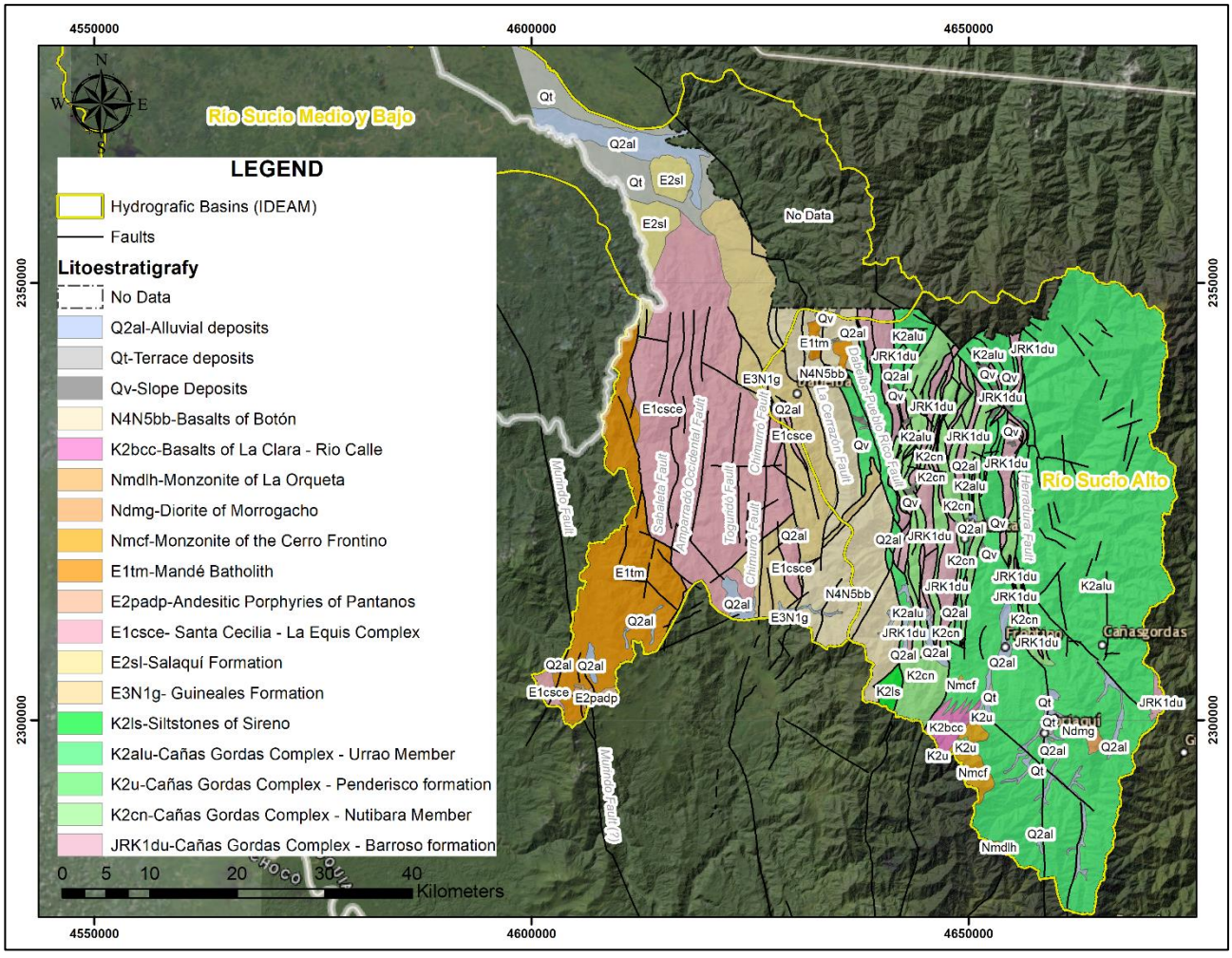

FIGURE 6. LITHOSTRATIGRAPHIC UNITS OF THE RIO SUCIO BASIN IN ANTIOQUIA DABEIBA GEOTHERMAL SYSTEM (DGS). ADAPTED FROM SGC, 2012; BOTERO, 2018 Y MONTOYA ET AL, 2019.

4.2.Hydrogeochemistry and low temperature thermochronolgical data

As part of the context and background mentioned in the introduction, this chapter reports the chemical data of the Dabeiba hot springs obtained from the National Hot Springs Inventory (2014) by the SGC, compiled and plotted by Gómez (2019), and analyzed for context geothermal by Montoya et al., 2019. The summary of the data is presented in Table 2. The cations, using average data, were Na^{+}, K^{+}, Ca^{+2}, Mg^{2+}, Li^{+} and Sr^{2+}, while the anions were HCO_3-, F-, SO_4- and Cl^{-}.

TABLE 2. MAIN CHEMICAL COMPONENTS, PH, AND TEMPERATURE OF DABEIBA HOT SPRINGS. LABEL ASSOCIATED FOR THE FIGURES. THE SPECIES OF THE SOLUTION IN MG/L. MODIFIED FROM (GÓMEZ, 2019 AND MONTOYA ET AL., 2019).

Sample Name	Label	CE	T ° C	pH	Li	Na	K	Ca	Mg	SiO_2	B	Cl	SO_4	HCO_3
Mohan	Mh	17930	30.0	7.4	7.5	4029.3	118.5	23.6	22.7	122.9	84.2	3446.2	2469.0	1439.8
Chobar	Ch	16290	28.4	7.8	2.1	3122.0	41.3	30.7	23.5	84.5	71.1	4405.0	725.9	1751.0
Guineales	Gui	15200	26.1	8.0	1.4	3332.0	40.0	24.0	18.4	27.0	75.0	5072.5	636.0	1415.2

The hot springs of the Dabeiba Geothermal System (DGS) are slightly diluted sodium-chloride type and close to mature waters as it is shown in Figure 7, whose interpretation suggests flows associated with the opening of discontinuities that allow fluid circulation (Kresic & Stevanovic, 2010). These rupture surfaces generated by the structural system also allowed meteoric water to seep to greater depths, collecting heat from the system and producing convective processes with evident ion exchanges.

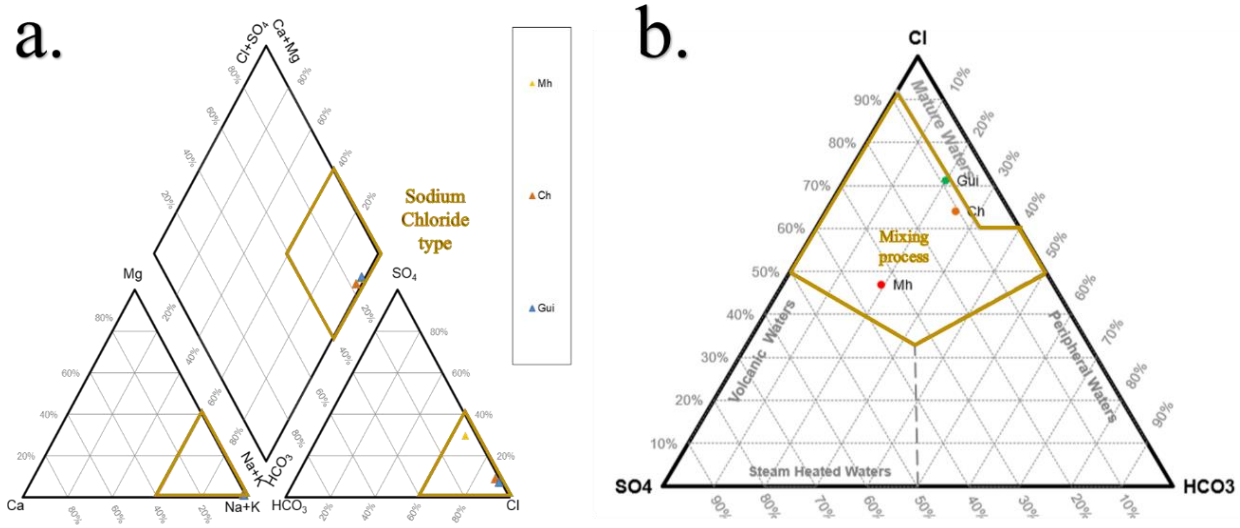

FIGURE 7. PIPER DIAGRAM OF DABEIBA HOT SPRINGS. SODIUM-CHLORINATED TYPE. THE MOHÁN THERMAL SPRING IS REPRESENTED BY AN ORANGE DOT, GUINEALES BY A BLUE DOT AND CHOBAR BY A BROWN DOT. ADAPTED FROM (MONTOYA ET AL., 2019). DABEIBA GEOTHERMAL SYSTEM (DGS).

The Stiff diagrams show a clear ion-exchange of the sources, supporting the compositional classification as sodium chloride in the three cases and evidencing, in turn, a decrease in the Cl anion as it moves towards the south, increasing the concentration of SO_4 in the Mohán spring and a notable increase in electrical conductivity, as shown in the Figure 8.

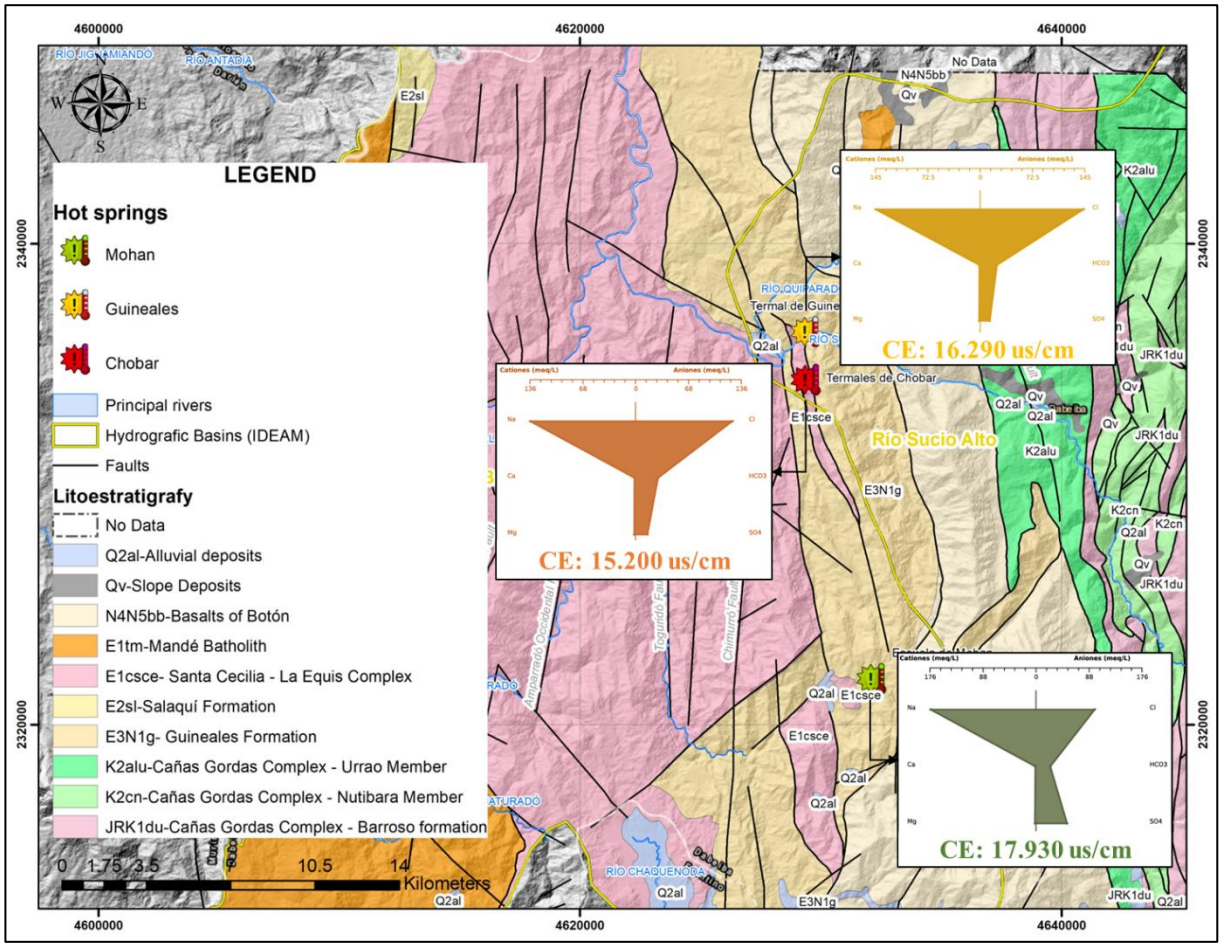

FIGURE 8. STIFF DIAGRAMS OF THE DABEIBA SPRINGS. SPATIAL DISTRIBUTION ON THE GEOLOGICAL MAP. THE GREEN DIAGRAM REPRESENTS THE GUINEALES SPRING, THE BLUE DIAGRAM REPRESENTS THE CHOBAR SPRING AND THE PURPLE DIAGRAM REPRESENTS THE MOHÁN SPRING. ADAPTED FROM (MONTOYA ET AL., 2019). DABEIBA GEOTHERMAL SYSTEM (DGS).

Conceptually, Montoya et al. (2019) proposed that the water emerging on the surface has cooled as it rose from the cold groundwater reservoir, disrupting the chemical equilibrium process. To verify this hypothesis, the Figure 9 shows that the hot springs of the DGS are positioned to the right of the GWML (Global Meteoric Water Line) and CML (Colombia Meteoric Line) with a slight inclination. This result suggests that the hot springs may have been influenced by slight mixing, possibly with groundwater containing magmatic or fossil waters trapped in marine sediments. During the mixing process, water-rock interaction could occur, leading to an exchange of oxygen between the geothermal waters and the rock, especially if the temperature higher than 220°C, where the percentage of oxygen depleted from the rock equals the oxygen enrichment in the geothermal water (Chandrasekharam & Bundschuh, 2008).

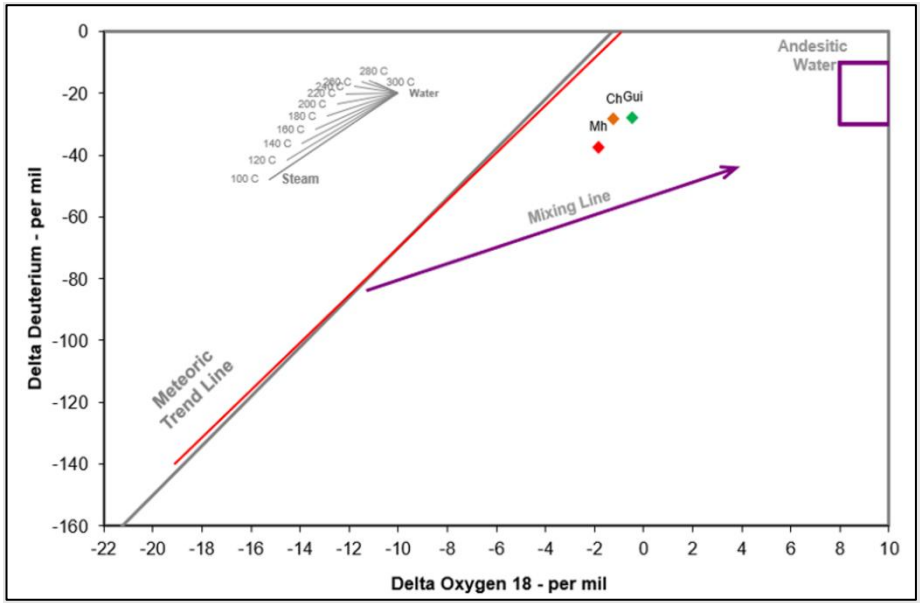

FIGURE 9. DIAGRAM OF STABLE ISOTOPES OF WATER (O_{18} – OD). THE RED LINE IS THE SEGMENT OF THE COLOMBIA METEORIC LINE (CML) AND THE GRAY LINE IS THE GLOBAL METEORIC WATER LINE (GWM). THE RANGE OF ANDESITIC WATERS PROPOSED BY GIGGENBACH (1991). THE POINTS OF THE DABEIBA SPRINGS REFLECT A SLIGHT ELEVATION TO THE RIGHT. THE MOHÁN FOUNTAIN IS REPRESENTED BY A RED DOT, GUINEALES BY A GREEN DOT AND CHOBAR BY AN ORANGE DOT. ADAPTED FROM (GÓMEZ, 2019 IN MONTOYA ET AL., 2019). DABEIBA GEOTHERMAL SYSTEM (DGS).

The Na-K-Mg diagram (Figure 10) shows that all springs fall within the range of partial equilibrium, around 110°C for Guineales and Chobar, and approximately 150°C for the Mohán spring. Diluted waters with a moderate concentration of HCO_3 are influenced by the mixing process and proves the preliminary hypothesis supported throughout the present study.

Finally, the selected silica geothermometers are shown in Table 3. Using the chalcedony geothermometer, the maximum calculated temperature is 120°C at the Mohán spring, while the lowest is 44°C at the Guineales spring. The Na-K-Ca geothermometer indicates a reservoir temperature of around 125-170°C. However, this geothermometer in low-temperature environments (<100-120°C) and/or with fluids relatively rich in CO_2 or Mg may provide misleading temperatures (Nicholson, 1993). The Na/K geothermometer indicates a reservoir temperature between 106 and 150°C, contrary to the calculation of K/Mg generated by Gómez, (2019), which shows values below 122°C, with Mohán being the highest in all geothermometers.

To validate the geothermometer data, we use the available Low Temperature Thermochronology dataset from Botero (2018), specifically the (U-Th)/He in apatites from sediments of the Guineales Formation. The reported ages by Botero have its place to the range of 1.7 to 2 Ma. This thermochronometer closure temperature range is above 80°C and below 40°C for AHe retention in a geothermal gradient of 25 °C/km (Ehlers & Chapman, 1999). Therefore, the AHe can be used in small-scale geological processes (e.g. tectonics and erosion). In this case, the data from the Guineales Formation on the hanging wall of the Chimuro Normal Fault highlighted a long-term conductive equilibrium since the late Pleistocene, with a temperature that cannot exceed 80°C, indicating the the DGS belongs to a low-medium enthalpy play.

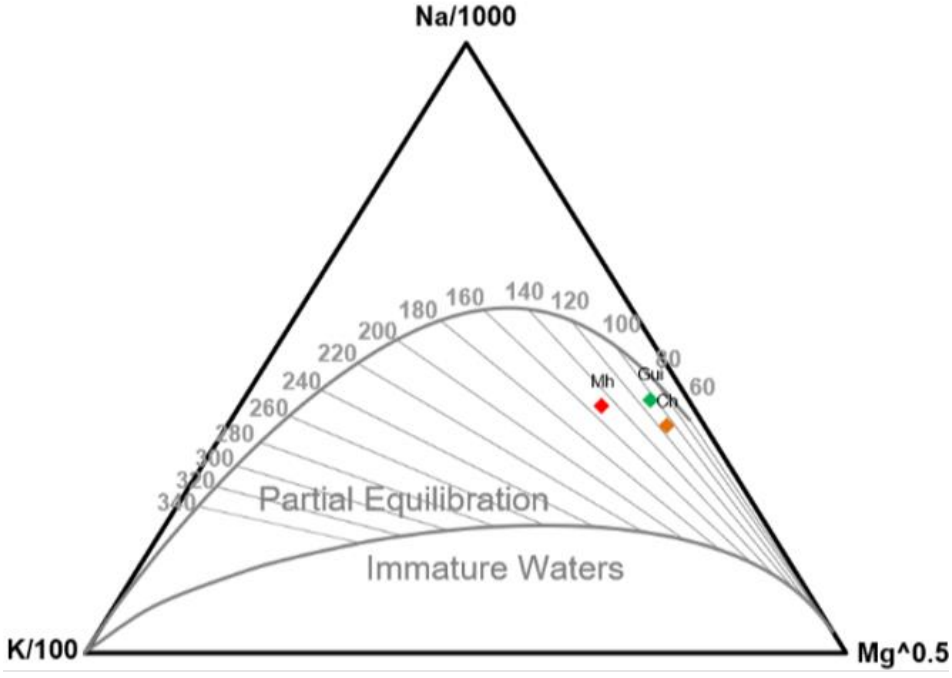

FIGURE 10. NA-K-MG DIAGRAM. THE MOHÁN SPRING IS REPRESENTED BY A RED DOT, GUINEALES BY A GREEN DOT AND CHOBAR BY AN ORANGE DOT. GRAPHS WERE MADE USING THE LIQUID ANALYSIS V3 SPREADSHEET (POWELL & CUMMING, 2010).ADAPTED FROM (GÓMEZ, 2019 IN MONTOYA ET AL., 2019). DABEIBA GEOTHERMAL SYSTEM (DGS).

TABLE 3. RESERVOIR TEMPERATURES (°C) ESTIMATED BY SOLUTE GEOTHERMOMETERS IN THE DGS. MODIFIED FROM (GÓMEZ, 2019 AND MONTOYA ET AL., 2019).

Hot spring	Chalcedony Fournier & Potter, 1982	Na-K-Ca Fournier and truesdell, 1973	Na/K Giggenbach, 1988	K/Mg Giggenbach, 1988
Mohan	124	170	150	122
Chobar	100	127	110	92
Guineales	44	125	106	94

4.3.Acquisition of satellital information and processing of shaded surfaces

The assessment of relief through quantifiable attributes allows for the characterization, grouping by similarities, and qualification of a system according to the research objectives. This numerical relationship of terrain characteristics reduces subjectivity in the conclusions derived from these attributes and enables a spatial and numerical assessment of the conditions of a particular area (Carvajal, 2012). As outlined in the methodology section, the analysis of the morphometric conditions of the terrain is conducted using geographic information system processing of the information provided by the Digital Elevation Model (DEM) mosaic of the ALOS-PALSAR satellite at a resolution of 12.5 x 12.5 meters. This surface was reprojected and adjusted to the extension of the indirect influence zone (Rio Sucio Basin around the department of Antioquia), resulting in a surface of 10 x 10 meters, on which the orientation model of the slopes and shadow maps of the area were obtained.

As expected, the highest elevation areas coincide with the high points marking the limit of the Rio Sucio basin, situated to the east, southeast, and northeast of the area. Elevation values reach a peak within a range of 3800 to 4000 meters above sea level, consistent with the westernmost foothills of the western cordillera. Conversely, the lowest elevation areas correspond to the beginning of the Gulf of Urabá in Antioquia, where values do not exceed 1000 meters above sea level and tend to decrease towards the west of the area, bordering the department of Chocó. The digital elevation model of the zone is presented in Figure 11.

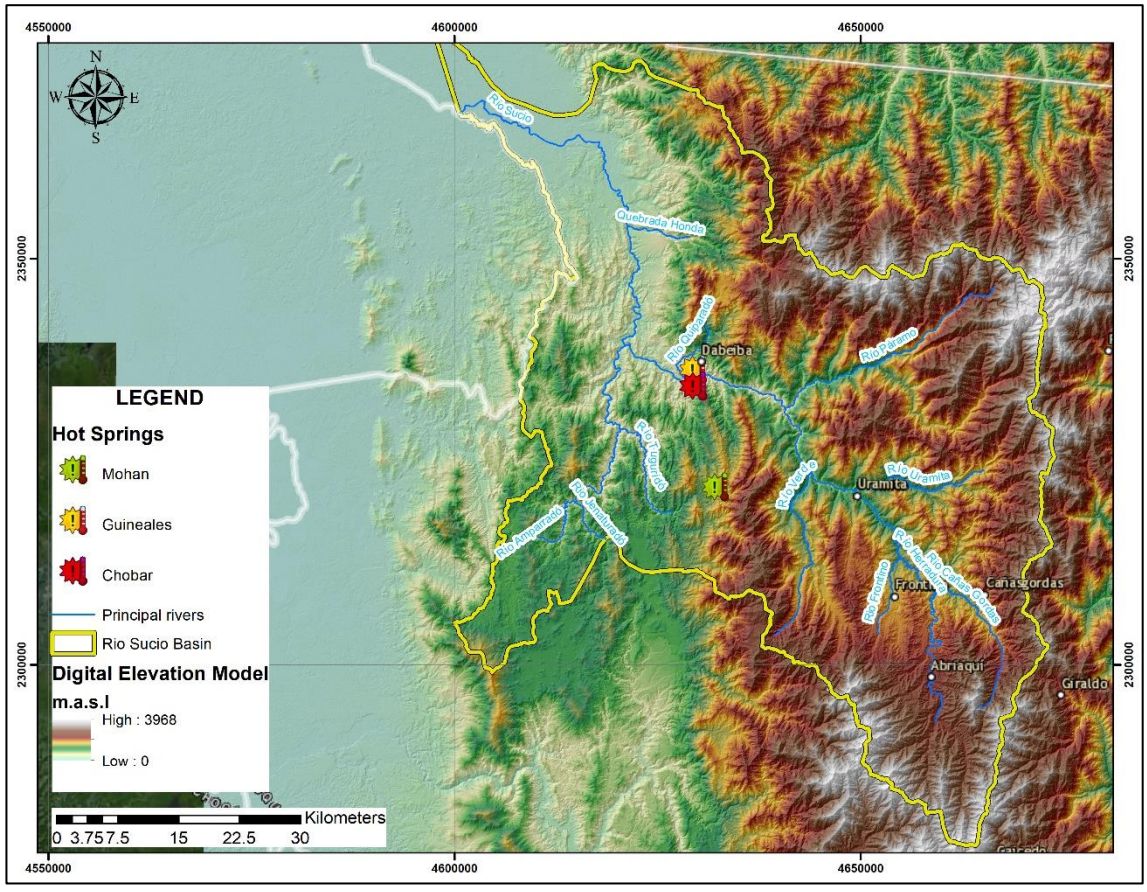

FIGURE 11. DIGITAL ELEVATION MODEL . ALOS PALSAR SURFACE REPROCESSED IN 10 X 10 PIXEL SIZE. HIGHER VALUES IN EARTH COLORS, LOWER VALUES IN PASTEL COLORS. DABEIBA GEOTHERMAL SYSTEM (DGS).

The proposed methodology entails generating the aspect model to determine the orientation of slopes relative to geographic north. The final aspect raster layer contains values ranging from 0° to 360°, representing the slope direction of specific hillsides. Like other processing steps, this is carried out pixel by pixel, with values starting from the north (0°) and continuing clockwise as an azimuthal distribution. This model primarily impacts hydrological delimitation rather than hydrogeological delineation, showing that most flow tends to move in an east, northeast, or southeast direction. Approximately 43% of slopes in the basin flow towards the east, southeast, and northeast, while about 34% flow north, and 12% flow south. Flat areas, as delineated throughout the morphometric analysis, are primarily located in the northwestern part of the study area, constituting approximately 1% of flat areas without slopes. The spatial distribution of the terrain aspect model is depicted in Figure 12.

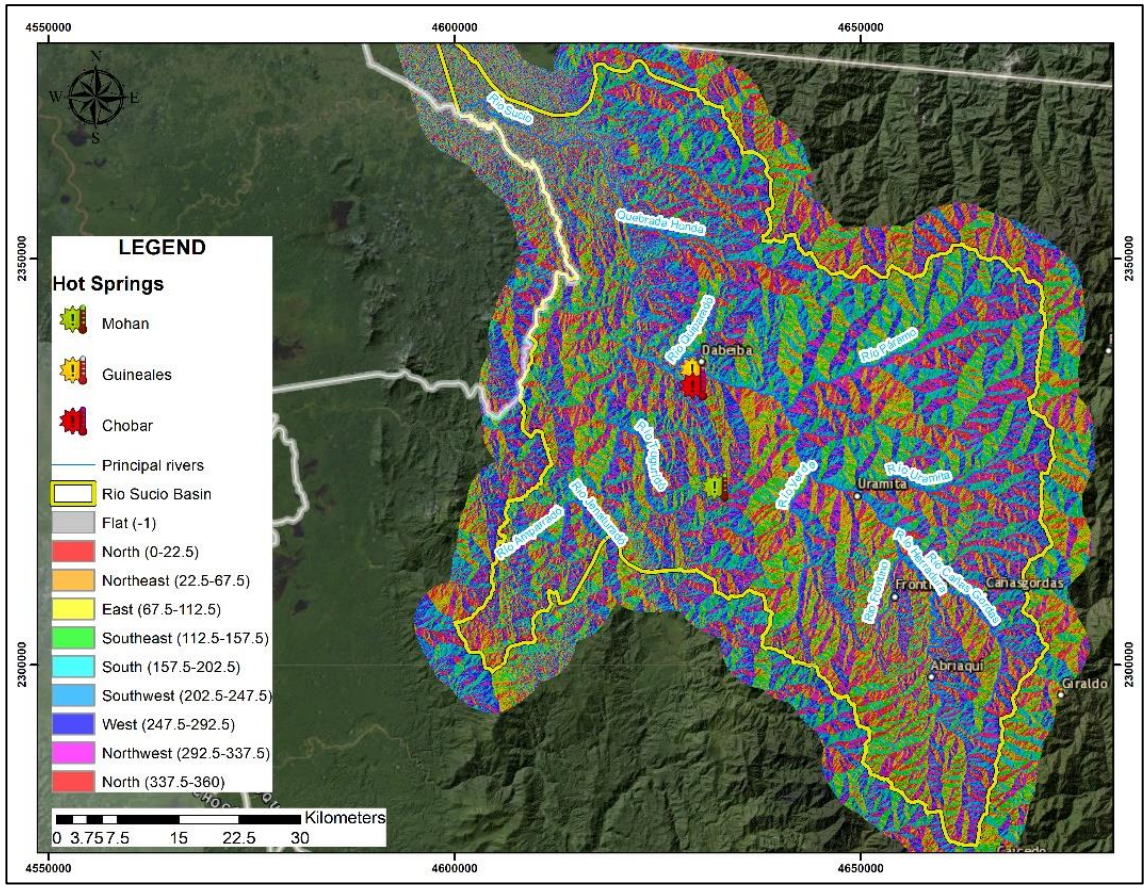

FIGURE 12. ASPECT MODEL. PRODUCT DERIVED FROM ALOS PALSAR SURFACE REPROCESSED IN 10 X 10 PIXEL SIZE. DABEIBA GEOTHERMAL SYSTEM (DGS).

A terrain shadow model is the spatial distribution of shadows cast by terrain features, delineating areas of sunlight exposure and those in shadow due to topographical elements like hills, valleys, and slopes. This model is constructed by assessing the angle and orientation of terrain surfaces relative to the position of a theoretical lightning source, resulting in semi-dimensional visualization.

Following the proposed methodology, eight shadow models were generated, with orientation intervals every 45° and a constant inclination of 30°. The results are depicted in Figure 13. Surfaces labeled as a, b, g, and h (0°, 45°, 270°, and 315°) denote positive relief features in weighed images, representing elevated topographies such as ridges and scarps. Conversely, the remaining orientations (90°, 135°, 180°, and 225°) correspond to negative relief features, primarily being faults, valleys, trenches, and joints (Radaideh et al., 2016).

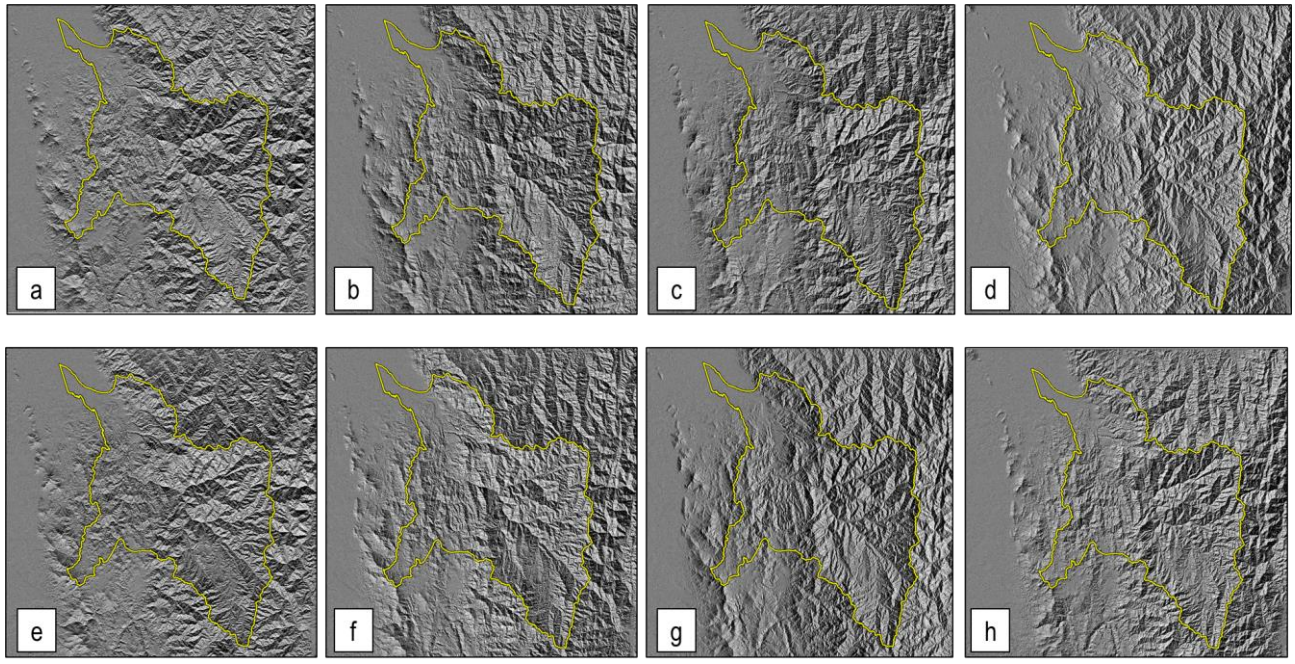

FIGURE 13. SHADOW MODELS EVERY 45° AZIMUTH WITH CONSTANT INCLINATION OF 30°. RIO SUCIO BASIN IN THE DEPARTMENT OF ANTIOQUIA. A. 0° AZIMUTH MODEL. B. 045° AZIMUTH MODEL. C. 090° AZIMUTH MODEL. D. 135° AZIMUTH MODEL. E. 180° AZIMUTH MODEL. F. 225° AZIMUTH MODEL. G. 270° AZIMUTH MODEL. H. 315° AZIMUTH MODEL. DABEIBA GEOTHERMAL SYSTEM (DGS).

4.4.Statistical model: Principal Components analysis

To statistically complement the assessment of the shadow surfaces involved in the analysis of automatic lineaments, a PCA (Principal Components Analysis) statistical model is performed to reduce the dimensionality of the eight surfaces, which may show redundancy in terms of frequency associated with a specific direction. PCA statistically groups the data, showing two groups of shadow models from which the final surfaces are derived to replicate the procedure proposed by Mark (1992). The combination of individual shadow maps enhances detail in areas of an image that would otherwise be illuminated by direct light or left in darkness by a single illumination source (Mark, 1992).

It's worth noting that shaded relief maps generated in traditional models emphasize structures that are illuminated obliquely but exclude structures illuminated along the structural domain (Mark, 1992). Following this premise, a statistical analysis begins with a correlation matrix (Figure 14b), composed by 1716 points associated with the centroid of a 1 km x 1 km cell within the zone (Figure 14a). Each model's

value returned configures a database of 1716 rows x 8 columns. Values close to 1 and -1 in this matrix indicate surfaces with high correlation, suggesting they are similar. Values close to 0 indicate surfaces that differ from each other, possibly representing terrain features that can be combined when analyzing trends in different directions. Subsequently, using a processing code in MatLab software, two surfaces grouped into two main components are obtained: the first, represented by the combination of the 135°, 180°, 225°, and 270° models, and the second, grouping the 45°, 90°, 315°, and 360° models as a complementary surface, as depicted in Figure 14c.

By processing the shadow models to derive different weights (W) and executing the weighted models, two surfaces are obtained, presented in the Figure 15, summarizing the most expressive features according to different proposals. In Mark's proposal, where light incidence angles correspond mainly to NW-W-SW directions, emphasizing shaded features that depend on weights, the algorithm is induced to capture the main trends along a N-S to NNW-SSE regional axis (Figure 15b). Conversely, the PCA model adapts surfaces with light incidence angles in SE-S-SW directions, which, complementarily to the former surface, highlight shaded features at similar angles to the incidence, with the main trends being NW-SE and E-W (Figure 15a)

Visually, the models respond in a nearly complementary manner, emphasizing features associated with different morphotectonic characteristics. Both multiple illuminated shaded images, when analyzed independently, yield results with noticeable differences. For the purposes of this research, these surfaces are considered visually and statistically complementary, supported by the analysis of the second principal component obtained in the correlation matrix in section 3.3, suggesting PCA-2 type surfaces in the directions proposed by Mark (1992) (225°, 270°, 315°, and 360°).

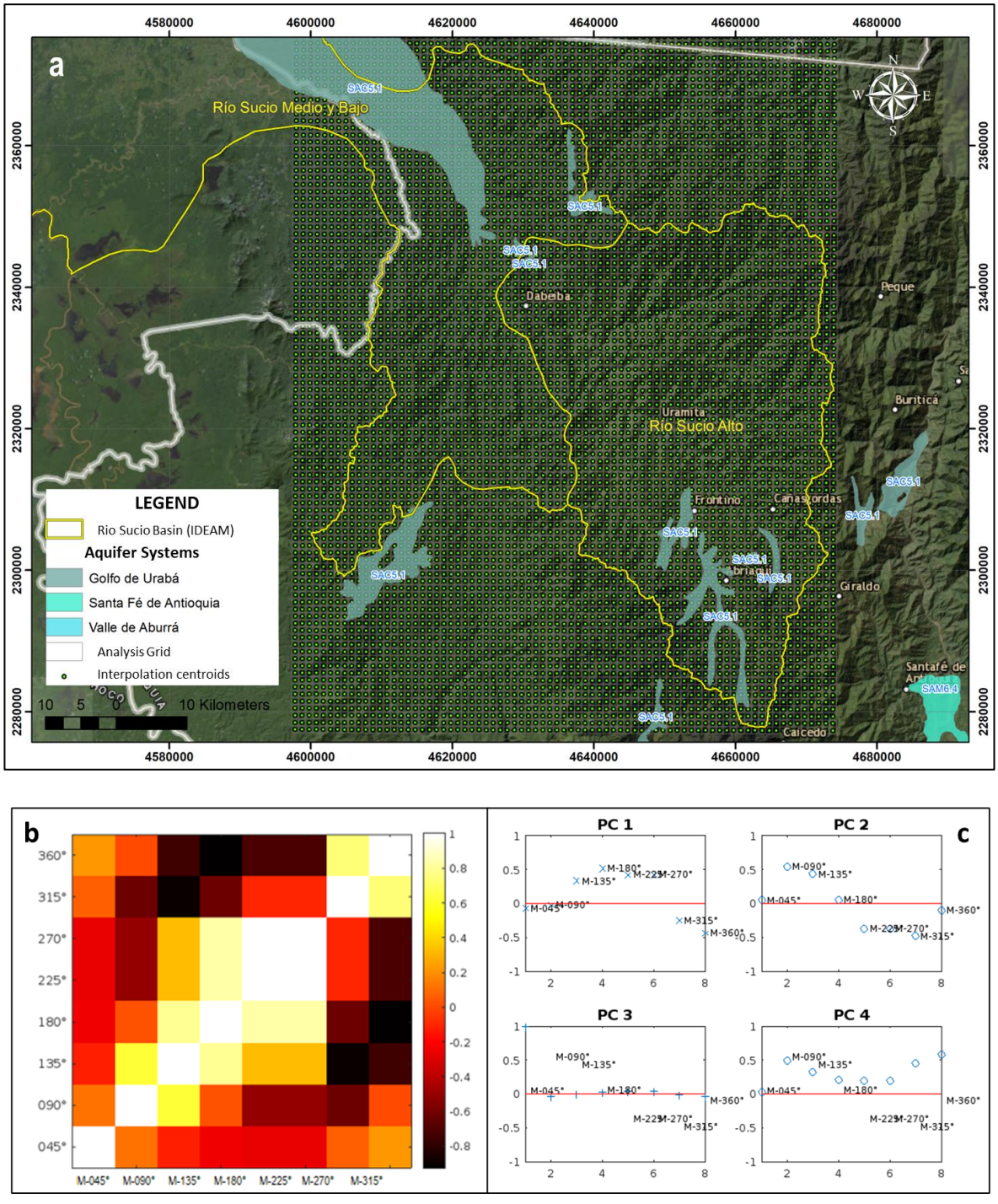

FIGURE 14. PCA ANALYSIS PROCESSING. (A) 1X1 KM GRID AND SAMPLING CENTROIDS. (B) CORRELATION MATRIX FOR THE 8 SHADOW MODELS. (C) PRINCIPAL COMPONENTS AND CLUSTERS OF INTEREST. DABEIBA GEOTHERMAL SYSTEM (DGS).

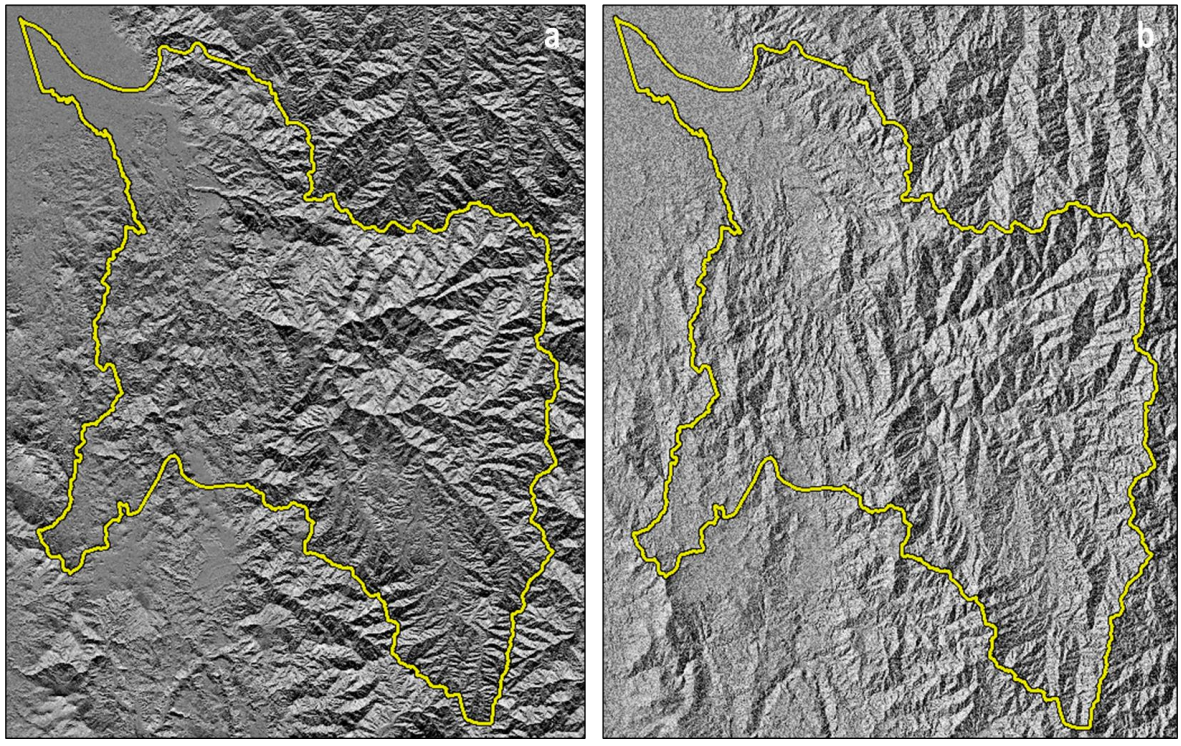

FIGURE 15. WEIGHTED MODELS DERIVED FROM PCA ANALYSIS. (A) WEIGHTED MODEL ACCORDING TO PCA MODEL . (B) WEIGHTED MODEL ACCORDING TO MARK´S PROPOSAL. DABEIBA GEOTHERMAL SYSTEM (DGS).

4.5.Analysis of Lineament Trends at DGS

As mentioned earlier, independent analyses of shadow surfaces exhibit differences in predominant directions. However, they share a pronounced tendency towards a greater concentration of lineaments in regions of rugged terrain, particularly in the central and eastern areas. Here, fault systems and the complex geological environment associated with the upper part of the basin delineate the linear features highlighted in the surfaces.

The lineaments obtained on each of the surfaces are joined within ArcGIS Pro, generating a unified lineament product that encompasses areas of combined lithologies, excluding recent and sub-recent deposits from the analysis. In total, the combined model yielded 8021 lineaments ranging from 500 to 7625 meters (about 4.74 miles) in length (Figure 16a). The general trends, weighted by the length of the

segments, are depicted in Figure 16b, predominantly showing an NNW-SSE orientation, while without weighting by segment length (Figure 16c), a trend of NNE-SSW is evident.

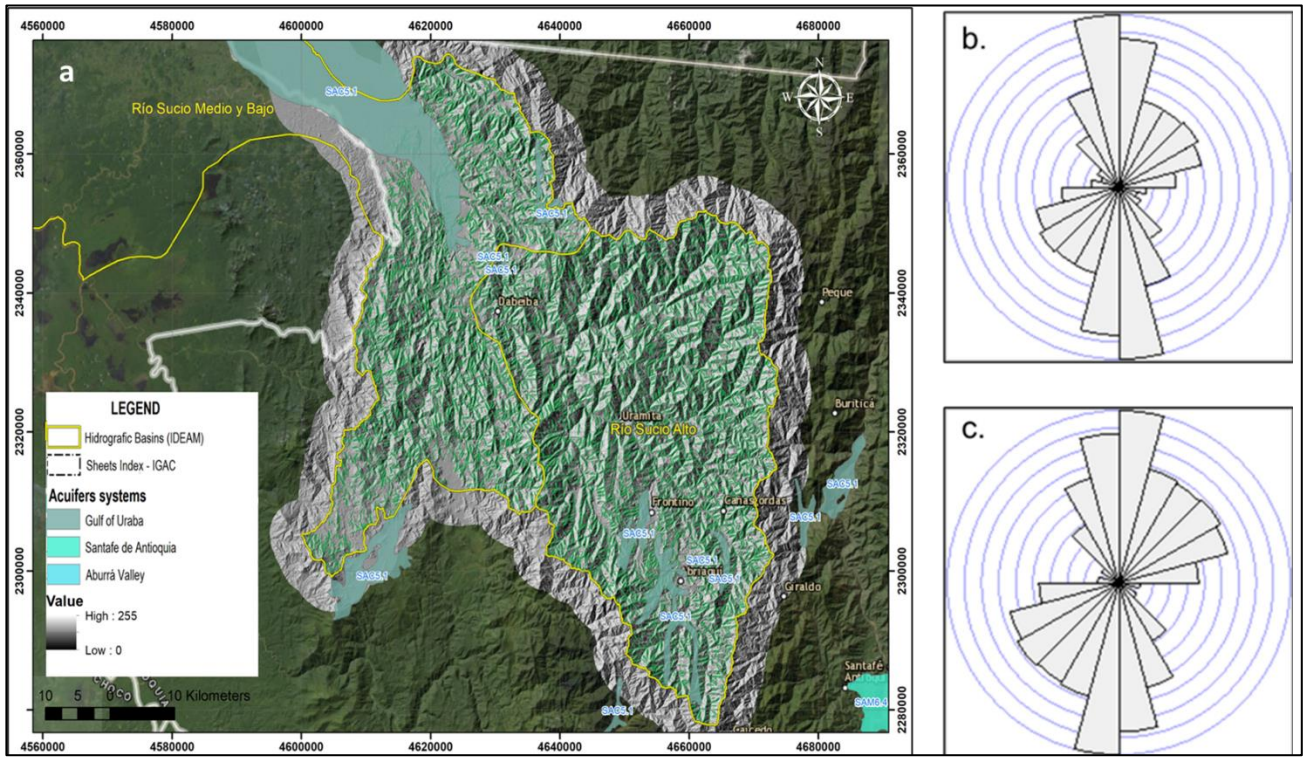

FIGURE 16. AUTOMATED LINEAMENT FINAL PROCESSING. (A) UNION OF THE WEIGHTED SURFACES PRODUCT. (B). TREND OF THE LINEAMENTS WITH LENGTH WEIGHTING. (C) TREND OF THE LINEAMENTS WITHOUT LENGTH WEIGHTING. DABEIBA GEOTHERMAL SYSTEM (DGS).

The analysis of the main trends associated with the behavior of automatic lineaments in the upper part of the Rio Sucio basin suggests that intrusive units such as the Frontino Hill Monzogranite, the Horqueta Monzonite, and the extrusive rocks associated with the Calle River basalts show a predominant orientation of their structures in the NE-SW direction, with minor trends in NW-SE. Conversely, the associated rocks of the Cañas Gordas complex display orientations of approximately N-S, with minor trends in NE-SW, aligning with the dominant orientations of regional structures that contact the different lithologies of the complex, as presented in Figure 17c and 17d.

In the southern zone of the basin, sedimentary lithologies of the Guineales Formation and the Sireno Limonite exhibit N-S trends with a slight NE trend, while hypabyssal rocks like the Pantanos Porphyries

display NW-SE orientations and vergences of the minor directions almost N-S, following the behavior of the regional fault system. Notably, in this area, the structures associated with the Morrogacho Diorite demonstrate an approximately E-W trend (Figure 17a).

Lastly, to the north of the middle zone of the Rio Sucio basin in Antioquia, the obtained lineaments for igneous lithologies such as the Mandé Batholith, the Button Basalts, and the Santa Cecilia - La Equis complex show predominantly NE-SW trends and some minor ones in approximately N-S directions. The latter is consistent with the structural response of the lineaments obtained in the Salaquí Formation. The trends in the middle part of the basin are presented in Figure 17b.

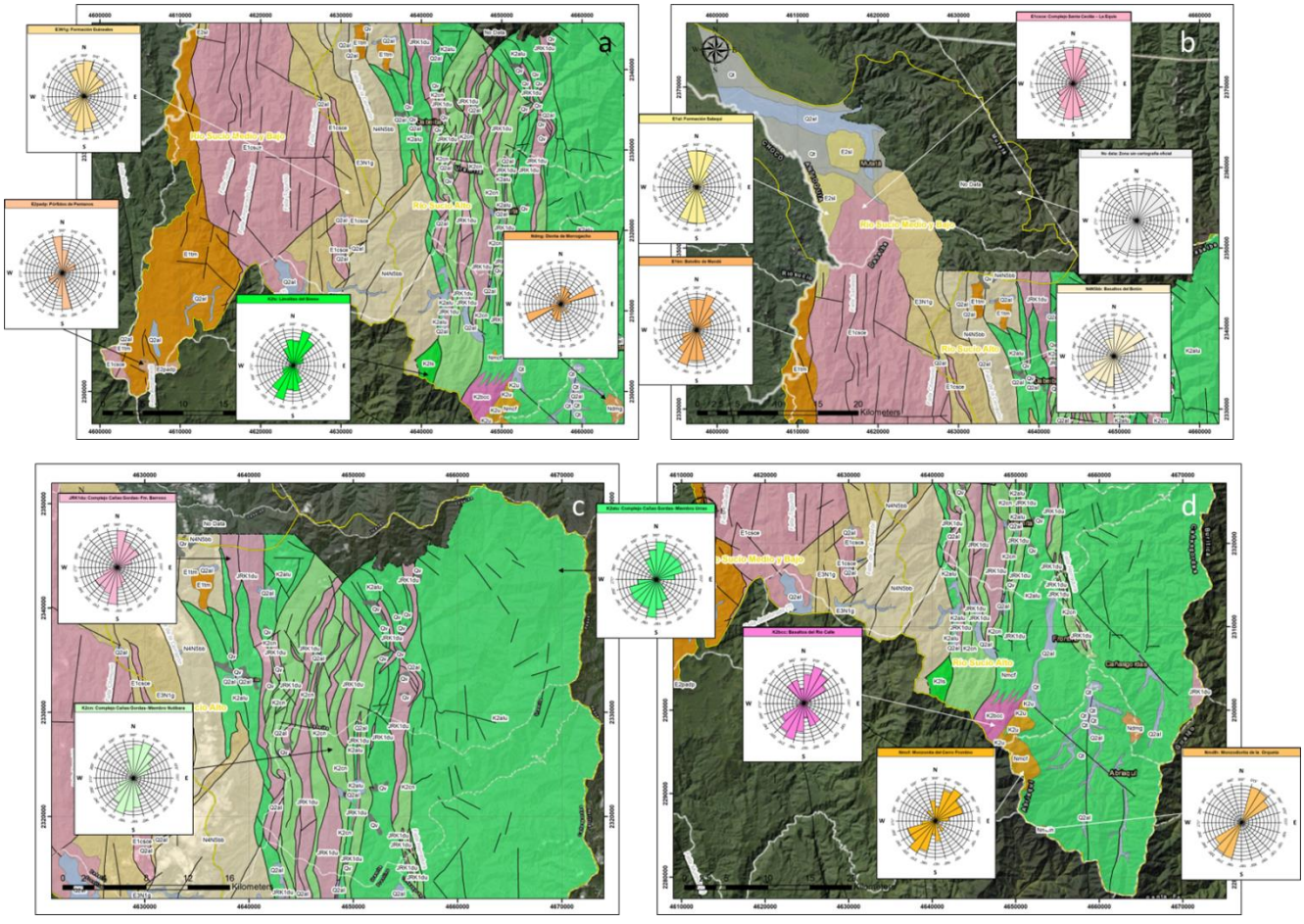

FIGURE 17. ROSE DIAGRAMS OF THE AUTOMATIC LINEAMENTS OBTAINED FOR THE LITHOLOGIES OF THE RIO SUCIO BASIN. (A) SOUTHERN AREA OF THE RIO SUCIO BASIN. (B). NORTHERN AREA OF THE SUCIO RIVER BASIN. (C) SOUTH OF THE UPPER PART OF RIO SUCIO BASIN. (D) NORTH OF THE UPPER PART OF RIO SUCIO BASIN. DABEIBA GEOTHERMAL SYSTEM (DGS).

4.6.Distributed surfaces and structural blocks at DGS

To fulfill the main objective of delineating flow zones based on the degree of fracturing within the constituent units of the geothermal system, it is important to consider that, given its environment characterized by faults and fractures, it is expected that the flow paths of groundwater will predominantly follow these characteristics. These predictions require validation through more extensive research. Para mapear los tres índices de densidad de lineamientos propuestos por Saepuloh et al. (2017) – Ll (Longitud de lineamientos), Lf (frecuencia de ocurrencia), Li (densidad de intersecciones) – se realizó una interpolación kriging ordinaria ajustada según la propuesta metodológica al modelo esférico o exponencial.

As presented in Figure 18, the zoning of the length of the lineaments oscillates in a range of approximately 0 to 5 km, with a high concentration of values that tend to increase towards the northeast and southcentral zones of the basin. This behavior is repeated on the number of lineament's map, with values ranging from 0 to 12 segments per km^2. Additionally, the number of intersections presents a range from 0 to 6, with the highest values in the southwestern of the study area. The concentration of lineaments is consistent with the area of greatest concentration of regional faults, mainly associated with the traces of the Dabeiba Pueblo Rico and Chimurró faults, highlighting the number of intersections as the most coherent surface with the location of the thermal springs of interest.

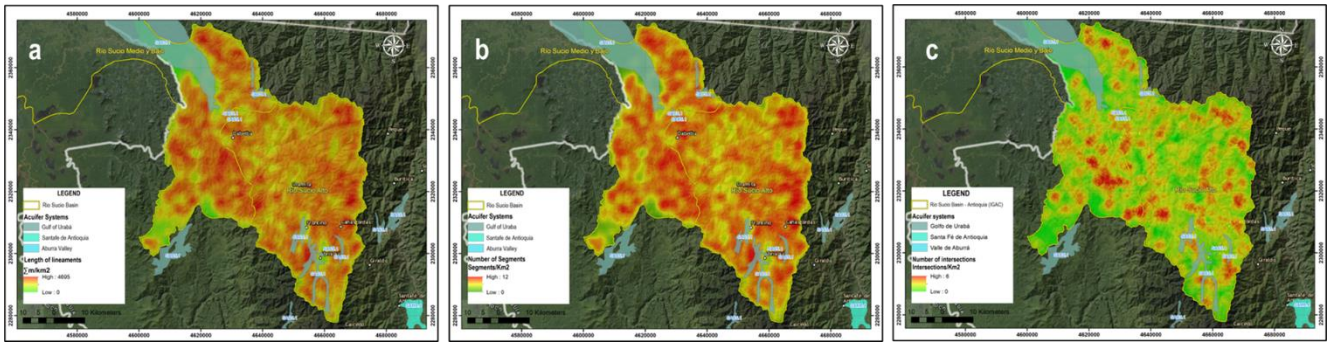

FIGURE 18. DISTRIBUTED MAPS OF FRACTURING DENSITY ANALYSIS OF THE RIO SUCIO BASIN. (A) MAP OF LENGTH OF LINEAMENTS – LL INDEX, (B) MAP OF NUMBER OF LINEAMENTS – LF INDEX, (C) MAP OF NUMBER OF INTERSECTIONS - LI INDEX. DABEIBA GEOTHERMAL SYSTEM (DGS).

According to the conclusion drawn from the analysis of surfaces associated with fracturing density, groundwater is expected to descend rapidly towards reservoirs along prominent faults and fractures in certain regions. However, in other regions of the basin, it may gradually change, mainly following regional flow patterns. Near the discharge areas, particularly, upward flow could occur, possibly influenced by the advective motion of the isotherms of the hydrothermal system. The advective movement of isotherms in a hydrothermal system refers to the displacement of temperature lines due to the flow of fluids, like water or steam, which transport heat within the geothermal reservoir. This process alters the temperature distribution, impacting the thermal dynamics and efficiency of the system.

Therefore, it is relevant to limit the analysis to a series of structural blocks (Figure 19a), considering that it is the fractured medium that conditions how the recharge processes advance towards major faults and fractures, reaching storage areas previously delimited in balances of humidity from works such as that of Montoya et al., 2019. The fracture density analysis is based on the interpolation of segment number for each block of interest for each sector and reveals the relationships between different units present within a single tectonic-structural block.

The first sector of the area, found between the localities of Cañasgordas and Uramita, bounded to the east by the watershed limits and to the west by the trace of the westernmost fault of the La Herradura system, shows low-intensity deformation. As proposed by Botero (2018), certain areas exhibit nearly vertical stratification with gentle folding. Generally, the layers predominantly dip towards the ESE, with a smaller proportion inclining towards the WNW. This zone is related to moderately important secondary porosity units, mostly composed of Miembro Urrao sediments, and some alluvial and colluvial deposits in the upper parts. It generally presents two important recharge zones, south and north, in the highest elevation areas of the system, which are consistent with the proposal of Montoya et al., 2019 (Figure 19b).

The second block extends from the town of Uramita near the La Herradura fault system to the Rio sucio river, limited to the west by the Cerrazón – Dabeiba Pueblorico fault system. In general, it is a sequence of cherts and limestones intercalated with elongated segments of diabase from the basement, heavily tectonically affected, giving rise to zones of high importance secondary porosity for sedimentary sequences and of moderate to low importance for the San José de Urama diabase bodies. The relationship between volcanic rock blocks and cherts is interpreted as a series of basement slabs exposed at the surface through high-angle faults, suggesting the concentration of flow towards the main slopes and the capture

of part of it towards deeper layers of the hydrogeological system. In the middle part, due to intense fracturing, very localized flow behavior is inferred, with more important recharge areas in the middle part of the block, controlling part of the system flow in the S-N direction, until accumulating over the central zone of the block. A second flow in the NW-SE direction is seen in a smaller proportion, as shown in Figure 19c.

The third block, found between the Rio Sucio River on the limits of the Cerrazón fault system and the lower part of the basin in the department of Antioquia, stands for the zone of greatest structural complexity. Surfaces that separate deformed domains from those with minor disturbance, and even without structural influence, are found in this sector. In this sector, units with significant primary porosity are combined, such as the extensive alluvial and colluvial deposits in the northwest, together with areas of sedimentary rocks with moderate to high porosity, which are intertwined within a structural context that includes rocks of the Santa Cecilia-La Equis complex, which are conceptually classified as having moderate to low secondary porosity, depending on their lithology. This block could stand for the zone with the greatest intensity of deformation, absorbing the most stress, and corresponds, in turn, to the region that provides a clear determination of the vergence of structures towards the E-SE (Botero, 2018). It concentrates both local flows in free aquifers and possibly regional flows that discharge over the northwestern due to the trends of the structures. The behavior of the block is presented in Figure 19d.

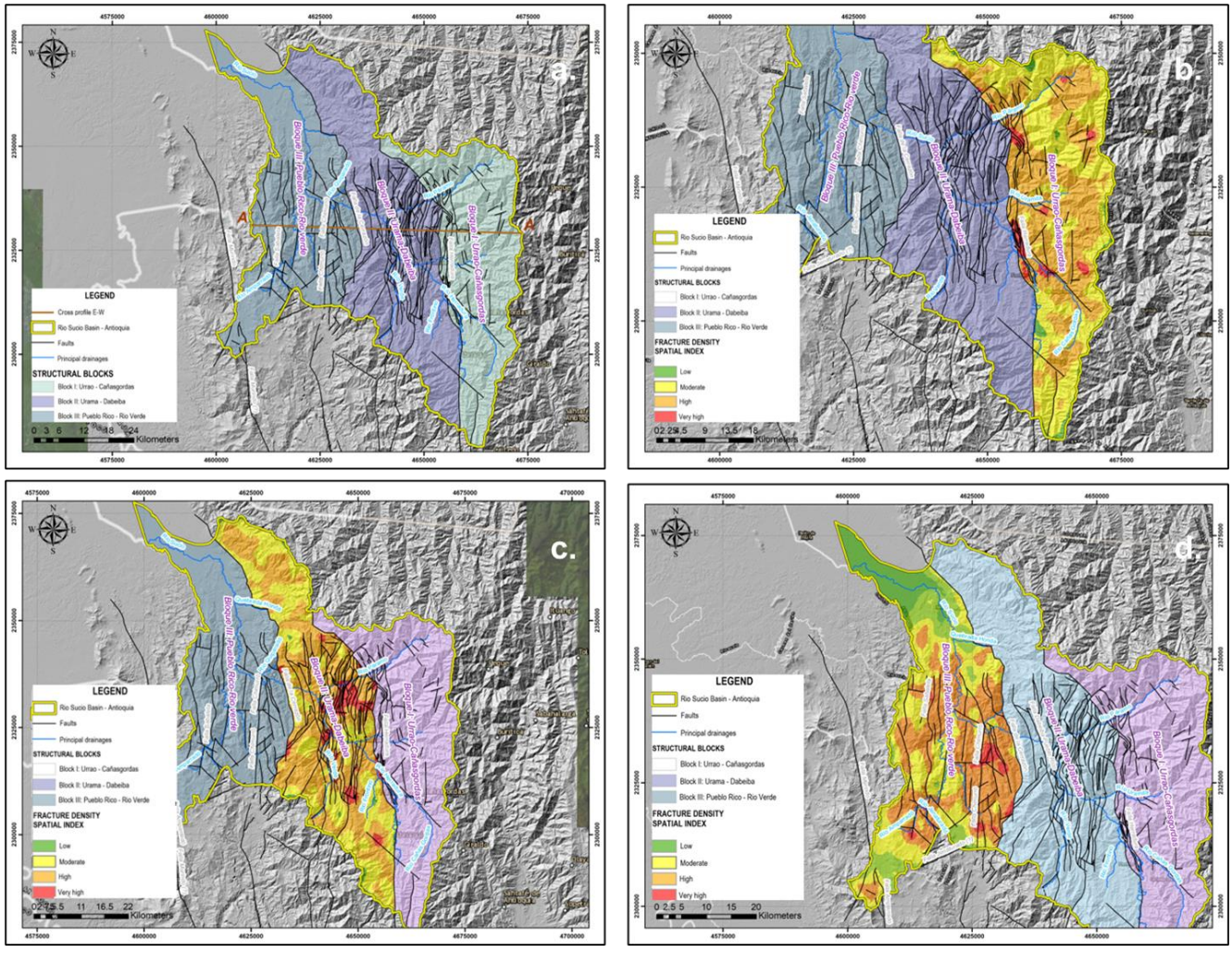

FIGURE 19. STRUCTURAL BLOCKS AND FRACTURE DENSITY OF THE RIO SUCIO BASIN. (A) DELIMITATION OF THE BLOCKS OF INTEREST AND FAULT SYSTEMS. (B) FRACTURE DENSITY FOR BLOCK I: URRAO-CAÑASGORDAS. (C) FRACTURE DENSITY FOR BLOCK II: URAMA-DABEIBA. (D) FRACTURE DENSITY FOR BLOCK III: PUEBLO RICO-RIO VERDE. DABEIBA GEOTHERMAL SYSTEM (DGS).

4.7.The geothermal model at DGS

In the hydrothermal analysis, recharge zones correspond to assessments of the medium's capacity to allow mixing processes found in spring geochemistry. The existence of higher recharge potential is related to processes of accumulation in the medium. This zoning and potential identification process is complemented by the analysis of possible water flow, which is hypothetically influenced by the heat flow present in the medium, concentrating different zones with the potential to generate inflow-outflow processes that characterize the hydrogeological-geothermal environment where it is found.

Based on the context presented within the POMCA of the Upper Río Sucio, this study affirms as a unit of analysis a continental basin, characterized by a predominantly ESE-W-NW surface flow. Atmospheric, surface, and groundwater are integral parts of the same hydrological cycle, constantly interacting between systems. CORPOURABA (2018) affirms that the main source of groundwater recharge is meteoric water resulting from the recharge-discharge balance processes among the mentioned contexts.

The approach through remote sensing effectively combines surface geomorphological features with structures that may project into the subsurface (Radaideh et al., 2016). The similarity in azimuthal directions shows that lineaments are preferred zones for surface water runoff, fluvial incision, and likely downward percolation of water during rains (Radaideh et al., 2016). In many cases, these lineaments align with the main drainage patterns of the area, forming escarpments in response to structural stresses. High lineament density is generally associated with high topographic relief rather than drainage density, suggesting areas of complex structural deformation involving not only geomorphological expressions derived from structural stresses but also overlying volcanic flow features.

This complementary context is reflected in the acquisition and combination of the two shadowed surfaces implemented for analysis. In general, Mark's proposal (1992) adequately stands for structures of a regional nature, while the PCA shadow model suggests the delineation of a more local context associated with jointing, changes in drainage courses, and, as a hypothesis, fracturing due to the cooling of volcanic material. This premise is primarily supported by the differences in the orientation of the lineaments and their correlation with regional systems and major fault traces.

Thus, it can be affirmed that geothermal fluids appear to flow through fault structures, and these permeable zones play a crucial role in the vertical flow of the geothermal system. They act as a regime for meteoric water entry from the surface, in conjunction with upward heat flows through these same systems. From the understanding of distributed potential recharge related to fracture density, water fluxes through these zones within the medium become a precursor to mixing processes, as supported by hydrochemical evidence from the proposed Dabeiba Geothermal System (DGS).

Following this line of thought, the fundamental premise is that the DGS is probably related to a Miocene extensional event that led to the formation of sedimentary rocks of the Guineales Formation. This was followed by an emplacement event associated with the accretion of the Panama-Choco block, resulting in a series of high-angle normal faults. The flow of fluids along these faults is controlled by the stress state in the different tectonic zones found in the literature.

The flow of groundwater could be associated with the regional fault system, which, together with various automatic trend analyses, reflects a predominantly N-S direction with a slight NE vergence as we approach the collision front proposed by Botero (2018). These systems affect the rocks of the Mandé Batholith, the Nutibara Member (K2cn), the Barroso Formation (K2bb), and the Urrao Member of the Cañasgordas Complex (K2alu), transforming them into rocks with secondary porosity of significant importance for understanding the flow. They share the same structural patterns in their drainage systems, lineaments, and overall regional orientation of the bodies.

The Guineales Formation (E3n1g) is perhaps the unit of greatest geothemal interest, as the primary porosity resulting from diagenetic processes is enhanced by the presence of a superimposed fracture density that accounts for the structural control marked by an orientation N-S approximately. This orientation coincides with the location of the three thermal water sources on the surface, suggesting that the transfer of heat from the deep source to thermal emanations is strongly influenced by deep and intermediate subsurface flows. It is worth noting that the approaches made through the creation of weighted images imprint a broader and statistically supported context. This allows connecting hypotheses associated with the origin of geomorphological expressions with trends in local features in terms of direction and length of lineaments. However, this tool is a simple approximation to trends on a regional scale and is considered a starting point for deeper analyses such as fracture density and dilation models that must be compared with field data in future research phases.

4.8.Concluding remarks

Dabeiba is recognized for its geothermal potential, particularly the Dabeiba Geothermal System (DGS), which spans various municipalities in Antioquia, Colombia. Studies suggest that the region hosts thermal waters with temperatures ranging from 27 to 30°C. The geological context of Dabeiba is characterized by its location within the triple junction of the Nazca, Caribbean, and South American plates, resulting in a mosaic of large lithotectonic blocks bounded by faults oriented in a regional N-S direction. Transpressive fault systems dominate the region, influencing the distribution of lithological units and controlling fluid circulation.

Chemical data from the Dabeiba hot springs indicate a slightly diluted sodium-chloride type of water, suggesting flows associated with the opening of discontinuities and meteoric water seepage to greater depths. Stiff diagrams illustrate ion-exchange processes, supporting the classification of hot springs and providing insights into the hydrogeochemical characteristics of the system. Through complementary analysis of apatites from sediments of the Guineales Formation (Botero, 2018), the study confirms long-term conductive equilibrium since the late Pleistocene, with temperatures below 80°C. This indicates that the DGS is within a low-to-medium enthalpy play.

In general, areas exhibiting convergence of aligned elements in two or more directions coincide with sectors conducive to generating parallel structures across their influence zones. This phenomenon enables distributed analyses to identify regions of higher density. These zones are interpreted as Structural Block III, characterized by the highest fracture density concerning the automatically generated structures. Through the amalgamation of structural system traces with those produced by the methodological approach, sectors with the greatest fracturing become distinctly delineated as areas prone to facilitating bidirectional flows, encompassing meteoric water ingress and heat dissipation.

Structural analysis reveals the presence of major fault systems such as the Romeral Fault System and the Dabeiba Pueblo Rico Fault System, which exert considerable influence on the regional tectonics. The orientation of fault systems correlates with the distribution of lithological units and controls fluid flow pathways. The presence of fault structures facilitates the flow of fluids and the transfer of heat within the

subsurface, thereby influencing the formation of potential recharge zones and the emergence of thermal water sources. In the context of Dabeiba, understanding the regional tectonic framework holds paramount importance for optimizing strategies related to geothermal resource assessment and development.

Overall, Dabeiba is a significant area for geothermal exploration, with its geological and hydrogeochemical characteristics offering valuable insights for sustainable energy production and resource management initiatives (e.g. agricultural productivity, industrial processes, tourism, and environmental sustainability). Additionally, Dabeiba's geothermal hot springs attract tourists to spa and wellness resorts, boosting the local economy and promoting leisure and relaxation.

5. CASE 2: SIBUNDOY VALLEY GEOTHERMAL SYSTEM (SVGS)

The Sibundoy Geothermal System (SGSV), situated in the Putumayo subregion of the Central-Eastern Cordillera in southwest Colombia, encompasses six geothermal areas within the Las Ánimas - Chiles Block. These areas include the Doña Juana Volcanoes - Las Ánimas, Galeras - Volcanoes of Morazurco, Sibundoy Volcano, Azufral Volcano, Cumbal Volcano, and Chiles-Cerro Negro Volcanic Complex (Alfaro et al., 2021). At a local level, the Sibundoy volcanic system, which extends between the departments of Nariño and Putumayo, has an area of approximately 283 square kilometers and is home to four hot springs: Balsayaco hot spring, Colón hot spring, Josefina hot spring and Sibundoy hot spring. These springs are in the municipalities of San Francisco, Sibundoy, Mocoa and Villagarzón, with altitudes ranging from 3,930 to 220 meters above sea level.

Hydrographically, the Sibundoy valley marks the onset of the Amazon hydrographic area, situated in the eastern foothills of the Andes Cordillera in Colombia. It falls within the hydrographic subzone of the Putumayo River and extends over geological sheets 410, 411, 429, 430, 448, and 449 of the Colombian Geological Survey. Apart from Balsayaco Thermal, these thermal sources are located on Quaternary deposits surrounding the Sibundoy Valley and the Sibundoy monogenetic field (Marin-Cerón et al., 2019).

The presence of these thermal springs is linked to low-order tributaries feeding into the San Pedro and Putumayo rivers (CORPOAMAZONIA, 2006), where heat flow is facilitated along the San Francisco-

Yunguillo fault system, involving lithologies within the geology of the 430 Mocoa sheet of the Colombian Geological Service (SGC, 2021). The influence zone of the SVGS, as proposed by Alfaro et al. (2021), is depicted in Figure 20.

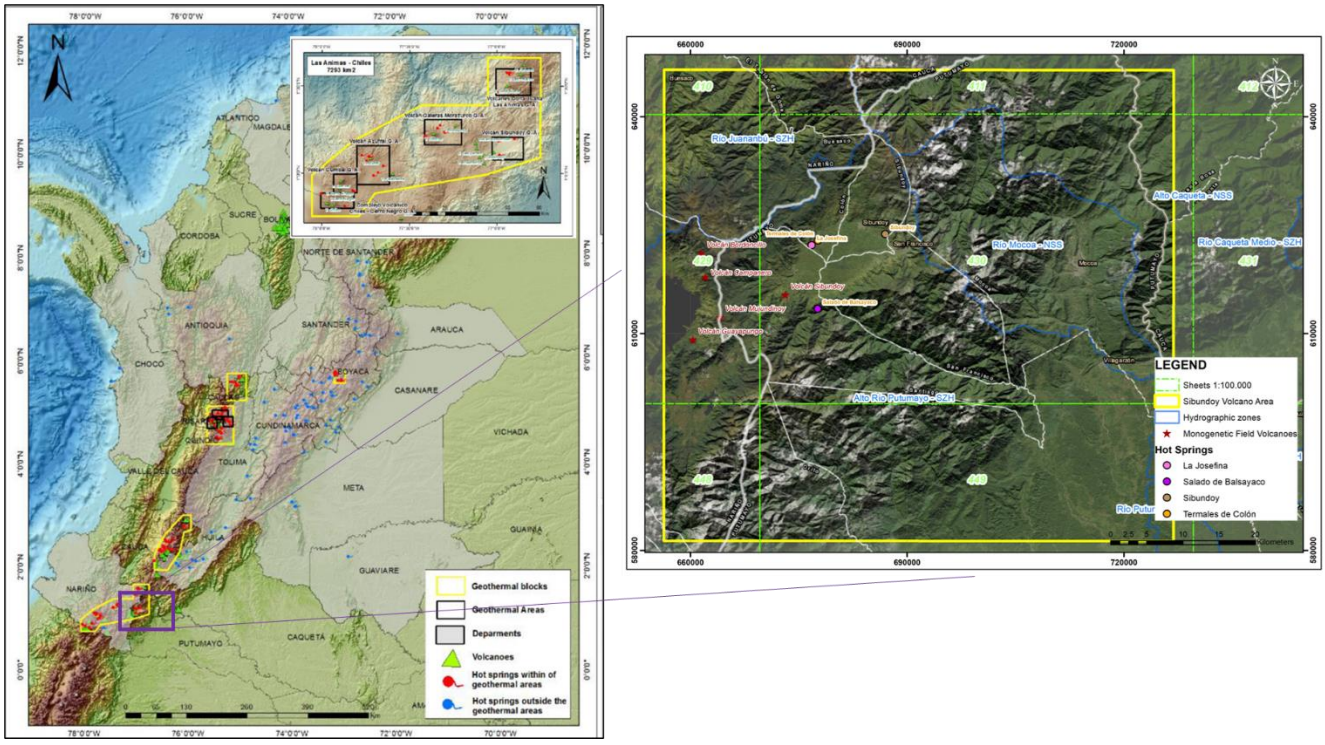

FIGURE 20. LOCATION OF PRELIMINARY GEOTHERMAL AREAS (BLACK POLYGONS) AND BLOCKS (YELLOW POLYGONS) IN COLOMBIA. IN THE PURPLE RECTANGLE, THE LOCALIZATION OF SIBUNDOY VALLEY GEOTHERMAL SYSTEM (SVGS). PINK DOT JOSEFINA HOT SPRING, PURPLE DOT BALSAYACO HOT SPRING, BROWN DOT SIBUNDOY HOT SPRING, ORANGE DOT COLON HOT SPRING . ADAPTED FROM MONTOYA ET AL., 2019; ALFARO ET AL, 2021.

The cartographic sources utilized as the foundation for subsequent processing are detailed in Table 1, aligning with the primary objective. The index study map consolidates various studies pertaining to the area, facilitating the establishment of a comprehensive geological context. This context encompasses the structural configuration proposed by Velandia (2005), validation of a subduction zone-associated context featuring the "Sierra-type" trace element pattern proposed by Marín-Cerón (2019), and the geothermal characterization linked to overthrust fault zones facilitating advection processes of isotherms (Ramírez et al., 2021). Collectively, these studies contribute to the development of an initial base characterization of the study area.

5.1.Geological framework and tectonic setting

The geodynamic setting of the northern Andean Block (BNA) is shaped by the interplay among the Nazca, South American, and Caribbean Plates, fostering a subduction zone along the northwestern South American continental margin. Marín-Cerón et al. (2019) propose that this area hosts processes involving fluid/melt interaction of the subducted plate, mantle metasomatism, partial melting, and interaction of magma with the lower crust and upper mantle.

The Sibundoy Valley, characterized by tectonic complexity, features the Algeciras Fault System, marked by lateral reliefs or jumps often challenging to correlate due in part to transverse faults in the NW direction (Velandia et al., 2005). Geological lineaments associated with the Algeciras Fault configure a system with significant vertical components, with the San Francisco Fault controlling the southern flank morphology of the basin. The resulting Sibundoy monogenetic field, linked to the rear-arc position of the SW volcanic segment, exhibits alkaline compositions, characterized by ash cones, scoria, and basaltic lavas (Marín-Cerón et al., 2019; Monsalve et al., 2020). This geological context spans from Proterozoic to Quaternary deposits, encompassing metamorphic rocks like the La Cocha-Río Téllez Migmatitic Complex and intrusive plutonic bodies such as the Mocoa and Sombrerillos Batholiths. The spatial distribution of these geological units in the Sibundoy valley geothermal area is illustrated in Figure 21.

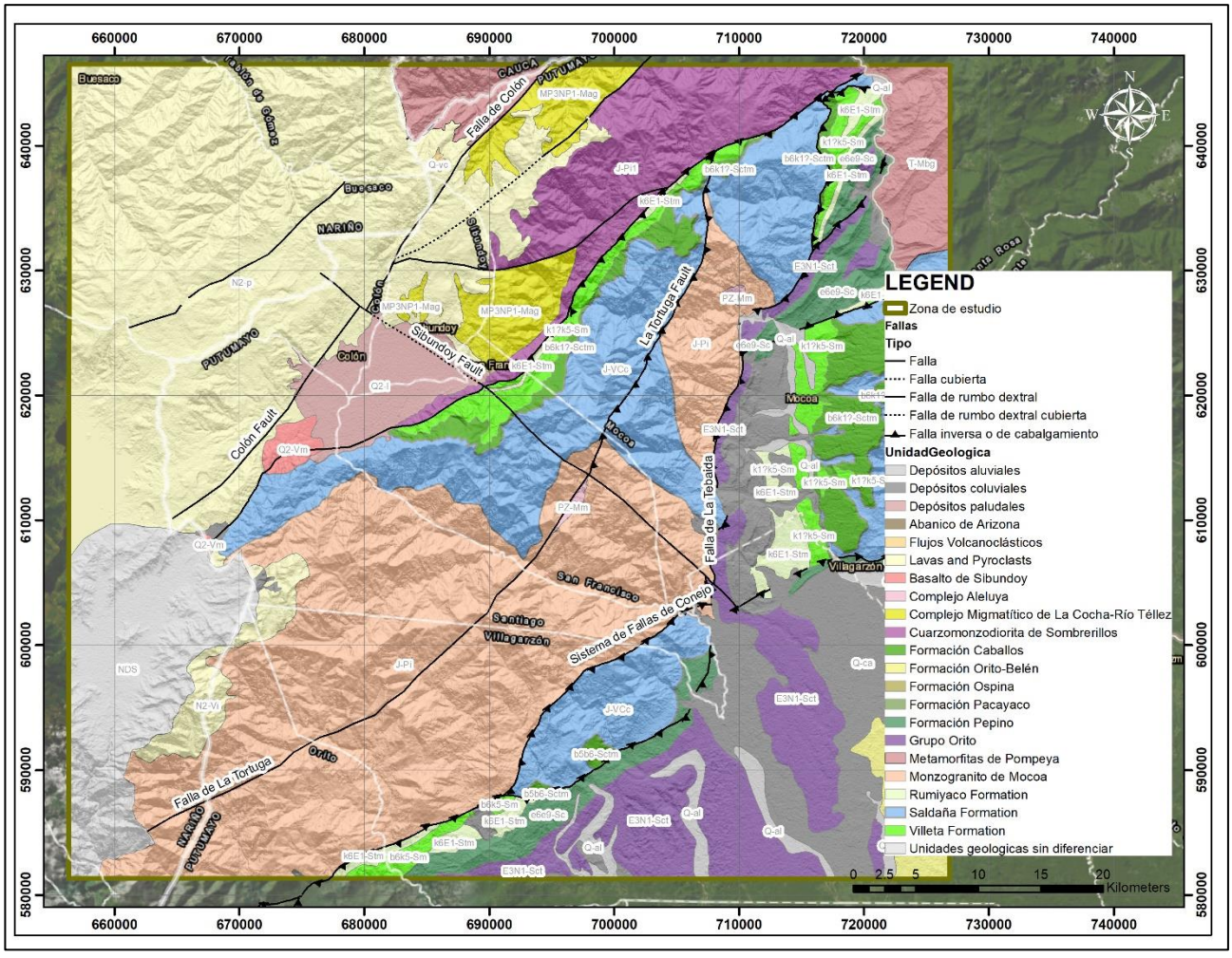

FIGURE 21. LITHOSTRATIGRAPHIC UNITS OF SIBUNDOY VALLEY GEOTHERMAL SYSTEM (SVGS). ADAPTED FROM SGC, 2012; RAMÍREZ ET AL, 2021; LÓPEZ ET AL, 2023.

5.2.Hydrogeochemistry of thermal springs of SVGS

The chemical data of the SV thermal waters was sourced from the National Inventory of Hot Springs (2014) as summarized by the SGC and accessed via the website: http://hidrotermales.sgc.gov.co/. Ramirez et al. (2021) compiled and plotted the data, which was subsequently analyzed for geothermal context by López et al. (2023). The chemical analysis included Sodium (Na^+), Potassium (K^+), Calcium (Ca^{2+}), Magnesium (Mg^{2+}), Lithium (Li^+), Bicarbonates (HCO^-_3), Fluorine (F^-), Sulphate (SO_4^{2-}), and Chloride (Cl^-) for the CBE analysis.

TABLE 4. MAIN CHEMICAL COMPONENTS, PH, AND TEMPERATURE OF SIBUNDOY VALLEY GEOTHERMAL SYSTEM. LABEL ASSOCIATED FOR THE FIGURES. THE SPECIES OF THE SOLUTION IN MG/L. DATA SOURCE FROM COLOMBIAN GEOLOGICAL SURVEY (2012) COMPILED BY RAMIREZ ET AL, 2021.

Sample	pH	CE	Li	Na	K	Ca	Mg	SiO_2	B	Cl	F	SO_4	HCO_3
La Josefina	7.5	820	0.08	104.2	15.06	15.5	10.3	86.84	1.6	60.43	1.26	0.8	372.1
Colón	9.14	1666	0.4	238	2.9	9.3	-	64.07	2.9	293	2.3	202	14.27
Balsayaco	7.33	3190	1	383	40.2	80.6	0.4	111	5.3	564	3.3	291	89.93
Sibundoy	9.71	218	-	27.2	1.5	2.4	0.3	78.09	0.3	2.28	0.61	17.25	-

The thermal water samples collected from the hot springs in the Sibundoy Valley, including Colón, Salado de Balsayaco, and Sibundoy hot spring, are located within the sodium chloride water region on the Piper diagram (Figure 22a), while the La Josefina hot spring falls within the sodium carbonate-dominated water region. The variation in the ionic composition of these samples may arise from two distinct water sources: surface water and volcanic waters (Ramirez et al., 2021). Dissolution/precipitation processes along their flow path or mixing may be influenced by temperature-dependent ions.

In Figure 22b, it is illustrated that the Josefina thermal exhibits behavior characteristic of peripheral water, potentially indicative of a mixture of volcanic and meteoric waters. Conversely, the Sibundoy thermal displays elevated sulfate concentrations, suggesting steam condensation in the water near the surface and relation with volcanic waters (Nicholson, 1993). The Salado de Balsayaco and Colón hot spring exhibit concentrations closer to mature water, typically associated with fractures that facilitate fluid circulation (Kresic & Stevanovic, 2010).

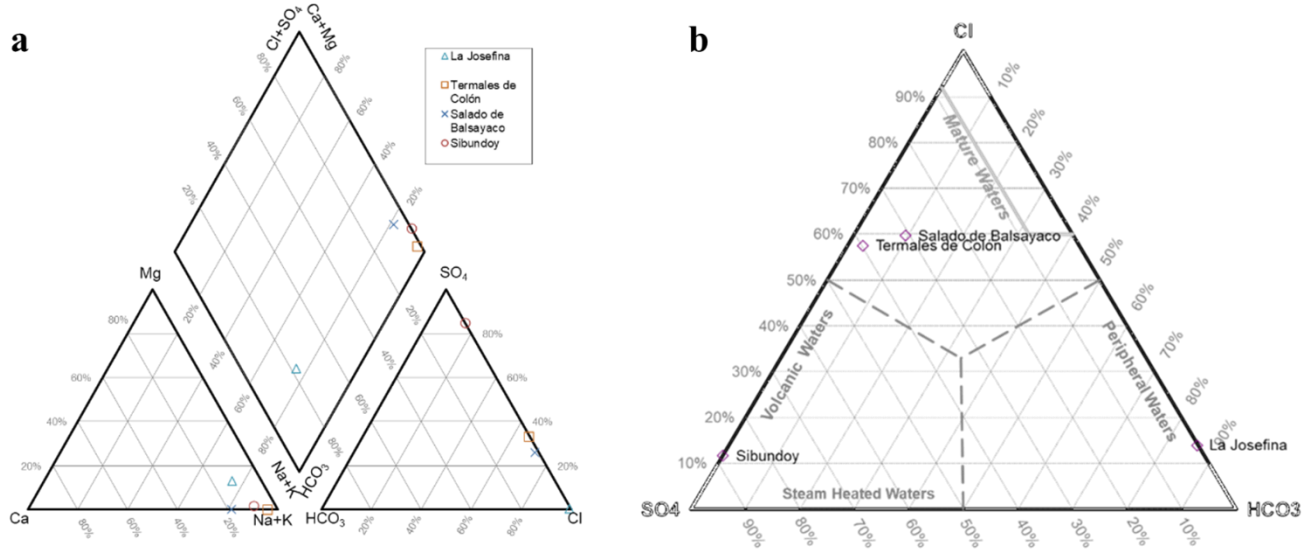

FIGURE 22. PIPER DIAGRAM AND WATER GEOTHERMAL TYPE OF SVGS SPRINGS. SODIUM-CHLORINATED TYPE AND SODIUM BICARBONATE. BLUE TRIANGLE FOR JOSEFINA HOT SPRING, ORANGE RECTANGLE FOR COLÓN HOT SPRING, BLUE X FOR BALSAYACO HOT SPRING AND RED DOT FOR SIBUNDOY HOT SPRING. ADAPTED FROM (RAMIREZ ET AL., 2021). SIBUNDOY VALLEY GEOTHERMAL SYSTEM (SVGS).

The Stiff diagrams clearly depict ion-exchange processes, particularly evident in the Balsayaco, Colón, and Josefina hot springs, where high concentrations of chlorine and sodium suggest lateral flow and direct feeding from the deep reservoir (Nicholson, 1993). Conversely, the Sibundoy thermal exhibits lower chlorine content and reduced sodium and sulfate compared to other hot springs, as depicted in Figure 23.

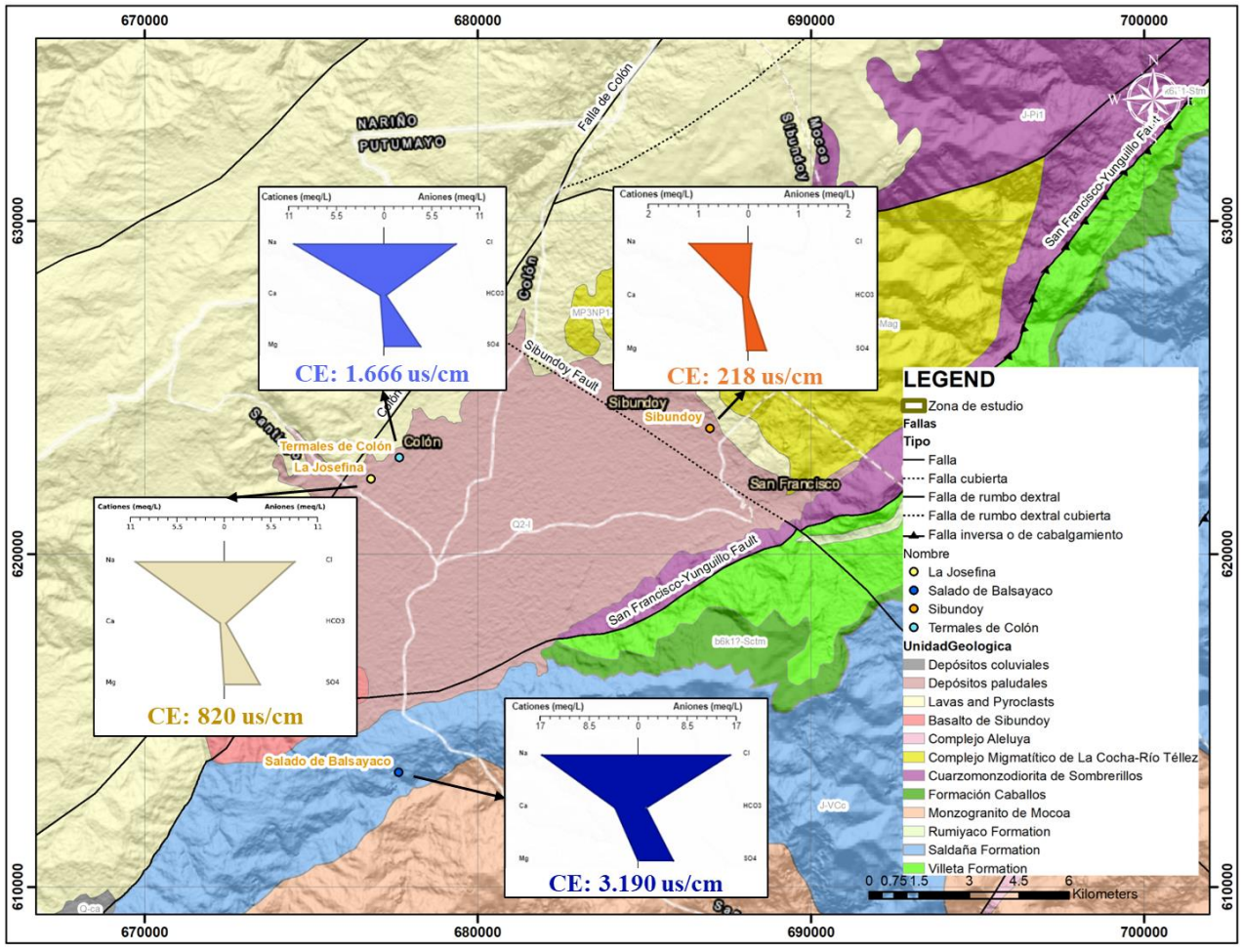

FIGURE 23. STIFF DIAGRAMS OF THE SIBUNDOY VALLEY SPRINGS. SPATIAL DISTRIBUTION ON THE GEOLOGICAL MAP. THE LIGHT BLUE DIAGRAM REPRESENTS THE COLÓN SPRING, THE BLUE DIAGRAM REPRESENTS THE BALSAYACO SPRING, THE LIGHT BROWN REPRESENTS THE JOSEFINA SPRING AND THE RED DIAGRAM REPRESENTS THE SIBUNDOY SPRING. SIBUNDOY VALLEY GEOTHERMAL SYSTEM (SVGS).

The relationship with electrical conductivity in the thermal springs does not exhibit a clear spatial trend, with only the Balsayaco thermal spring suggesting moderate transit conditions in the medium or assimilation of ionic components due to the lithology where its upwelling occurs.

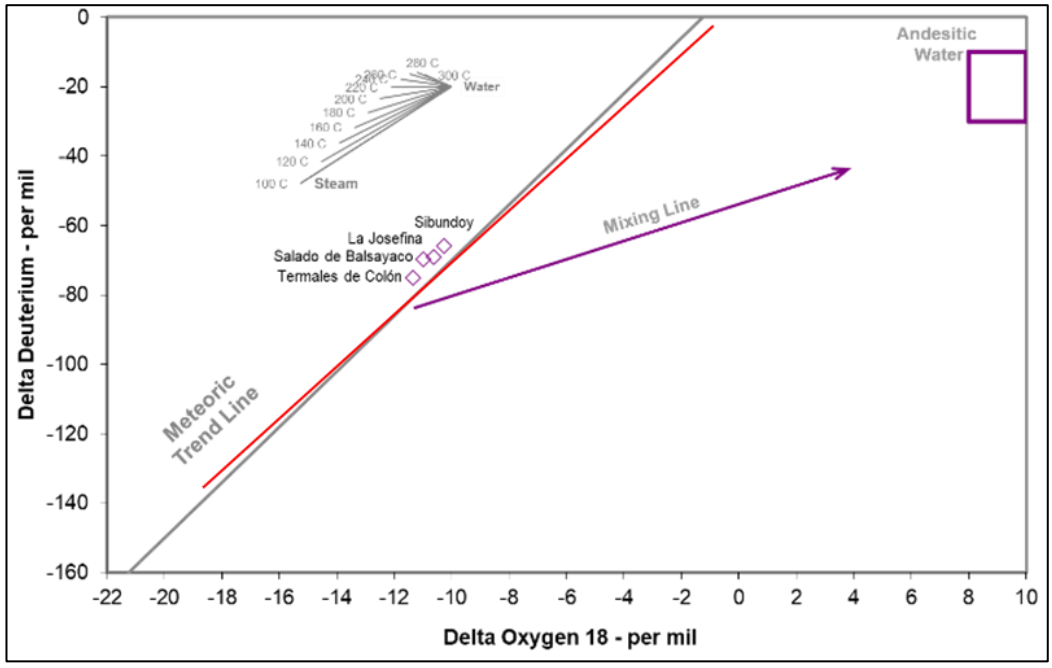

FIGURE 24. DIAGRAM OF STABLE ISOTOPES OF WATER (O18 – OD). THE RED LINE IS THE SEGMENT OF THE COLOMBIA METEORIC LINE (CML) AND THE GRAY LINE IS THE GLOBAL METEORIC WATER LINE (GWM). THE RANGE OF ANDESITIC WATERS PROPOSED BY GIGGENBACH (1992). THE POINTS OF THE SIBUNDOY REFLECTS AN ALIGNMENT PATTERN SIMILAR TO METEORIC WATERS. ADAPTED FROM (RAMIREZ ET AL., 2021). SIBUNDOY VALLEY GEOTHERMAL SYSTEM (SVGS).

López et al. (2023) propose the hypothesis that in a monogenetic field like that of SW Colombia (Sibundoy), the geothermal system is linked to the transfer of heat along the fractured medium (Sibundoy and Colón faults), which in turn controls the mixing of water (meteoric/hydrothermal), depending on the fracturing density. To verify this approach, Figure 24, plotted by Ramirez et al. (2021), shows that the hot springs of the DGS are positioned to the right of the GWML (Global Meteoric Water Line) and CML (Colombia Meteoric Line) with a slight inclination. This result indicates that all the analyzed thermal springs are plotting along the GWML (Global Water Meteoric Line), suggesting a mixing line of volcanic waters and meteoric recharge with a temperature range between 100° and 120° (Ramirez et al., 2021). Although the mixing relationship is not entirely clear, the oxygen depletion could be related to a mixture with little transit in the medium, correlated with the electrical conductivity values.

The Na-K-Mg plot (Figure 25) depicts the positioning of the Sibundoy and La Josefina thermals near the Mg appendix, indicating the presence of immature or mixed waters. No discernible trend is observed, suggesting that these springs may not be well-suited for geothermometers, particularly Na/K

thermometers. The Balsayaco thermal falls within the partially equilibrated region, indicating potential mineral dissolution or the establishment of equilibrium reactions without reaching full equilibrium (Ramirez et al., 2021). On the other hand, the water from the Colon thermal spring falls within the region of complete equilibrium, with an estimated temperature of approximately 110°C according to the graph. Finally, the selected silica geothermometers are shown in Table 5. The silica geothermometers used by Ramirez et al. (2021) include Conductive Quartz and Adiabatic Quartz for the Salado de Balsayaco thermal, and Conductive Chalcedony and Alpha Cristobalite for the presumed low enthalpy deposits. The Na-K-Ca-Mg geothermometer was used as a reference.

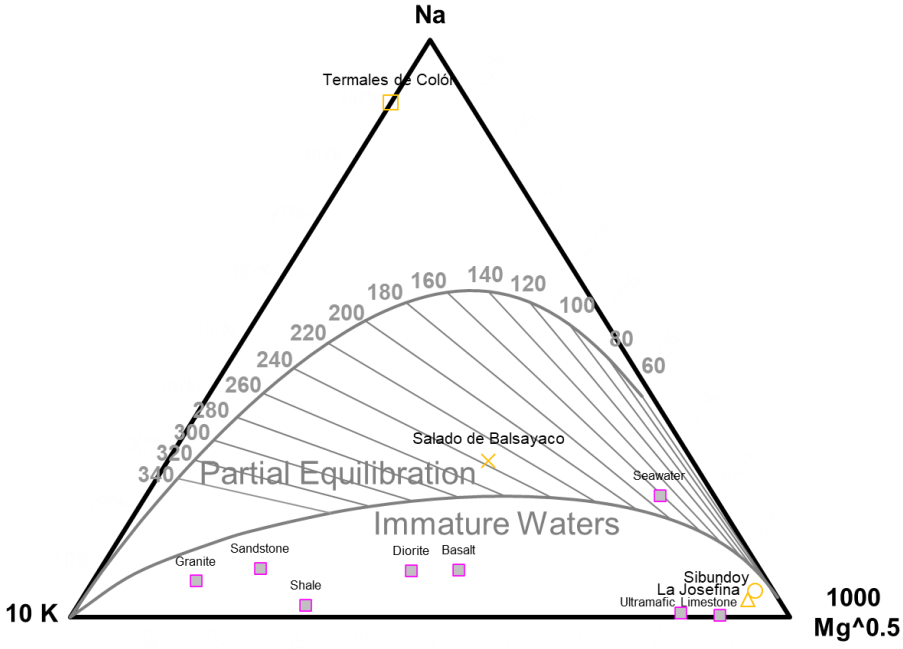

FIGURE 25. NA-K-MG DIAGRAM. THE COLÓN SPRING IS REPRESENTED BY A YELLOW RECTANGLE, BALSAYACO SPRING BY A YELLOW X, SIBUNDOY SPRING BY A YELLOW DOT AND THE JOSEFINA SPRING BY A YELLOW TRIANGLE. GRAPHS WERE MADE USING THE LIQUID ANALYSIS V3 SPREADSHEET (POWELL & CUMMING, 2010).ADAPTED FROM (RAMIREZ ET AL., 2021). SIBUNDOY VALLEY GEOTHERMAL SYSTEM (SVGS).

TABLE 5. RESERVOIR TEMPERATURES (°C) ESTIMATED BY SOLUTE GEOTHERMOMETERS IN THE SVGS. TAKEN FROM (RAMIREZ ET AL., 2021).

Sample name	Alpha Cristobalite Fournier and Potter, 1982	Chalcedony conductive Fournier and Potter, 1982	Na-K-Ca Mg Fournier, 1979	Quartz conductive Fournier and Potter, 1982	Quartz adiabatic Fournier and Potter, 1982
La Josefina	79	102	29	-	-
Termales de Colón	63	85	84	-	-
Salado de Balsayaco	-	-	-	143	138

To adjust the geothermometer data, which appears to be not in equilibrium, we utilize thermochronology data from Villagómez & Spikings (2013), which reports ages of the apatite fission track (AFT) of 13.7 ± 2.2 Ma and 18.7 ± 7.4 Ma. The AHe samples ranged between 3.5 ± 0.3 Ma and 4.5 ± 0.3 Ma. Single-grain Pleistocene ages in apatite (U-Th)/He have been reported by Pérez-Consuegra et al. (2021). Therefore, it can be inferred that, in general, geothermometers appear to be overestimating the temperature of the play. The reported ages of 2.8 Ma (Pérez-Consuegra et al., 2021) may indicate fault movement and/or hydrothermal reset ages, suggesting that since that time, the hot fluids located in that region have been interacting with the host rock at temperatures ranging above 80°C and below 40°C, classifying the SGP as a low to medium enthalpy play.

5.3.Acquisition of satellital information and processing of shaded surfaces

The assessment of relief through quantifiable attributes allows for the characterization, grouping by similarities, and qualification of a system according to the research objectives. This numerical relationship of terrain characteristics reduces subjectivity in the conclusions derived from these attributes and enables a spatial and numerical assessment of the conditions of a particular area (Carvajal, 2012). As outlined in the methodology section, the analysis of the morphometric conditions of the terrain is conducted using geographic information system processing of the information provided by the Digital Elevation Model (DEM) mosaic of the ALOS-PALSAR satellite at a resolution of 12.5 x 12.5 meters. This surface was reprojected and adjusted to the Sibundoy Volcano Area, resulting in a surface of 10 x 10 meters, from which slope orientation models and shadow maps were derived.

Situated on the easternmost slope of the eastern mountain range and the beginning of the Amazon basin, the highest elevations, reaching approximately 3930 meters above sea level, are found on the western and northwestern side of the study area, bordering the departments of Putumayo and Nariño. Conversely, on the eastern and southeastern side, elevations decrease rapidly, reaching as low as 275 meters above sea level, encompassing the municipalities of Mocoa and Villagarzon in the department of Putumayo. The digital elevation model of the zone is depicted in Figure 26.

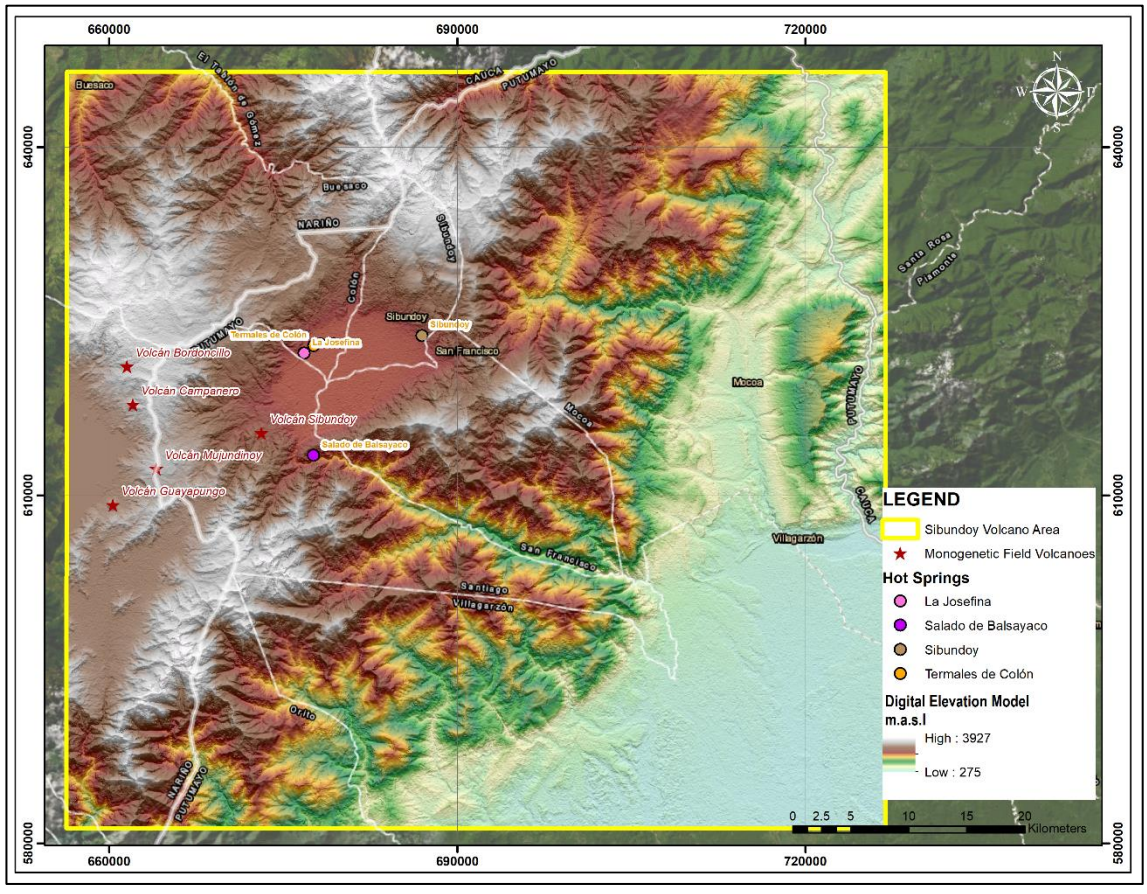

FIGURE 26. DIGITAL ELEVATION MODEL. ALOS PALSAR SURFACE REPROCESSED IN 10 X 10-PIXEL SIZE. HIGHER VALUES IN EARTH COLORS, LOWER VALUES IN PASTEL COLORS. SIBUNDOY VALLEY GEOTHERMAL SYSTEM (SVGS).

In alignment with the proposed methodology, generating the aspect model involves determining the orientation of slopes relative to geographic north. The resulting aspect raster layer ranges from 0° to 360°, representing the slope direction of specific hillsides. Derived from the previously analyzed DEM, this

model assigns values starting from the north (0°) and proceeding clockwise in an azimuthal distribution. Primarily impacting hydrological delimitation rather than hydrogeological delineation, the model highlights two predominant behaviors.

Firstly, it delineates geoforms associated with the San Francisco fault line, directing most northern, northeastern, and central slopes of the study area to drain towards the Sibundoy valley. Secondly, it outlines the main inclination in a south and southeast direction, with some drainage towards the southwest, indicating trends for slopes to drain towards the Putumayo River basin and areas of lower elevations. The spatial distribution of the terrain aspect model is depicted in Figure 27.

A terrain shadow model illustrates the spatial distribution of shadows cast by terrain features, indicating areas of sunlight exposure and those shaded by topographical elements such as hills, valleys, and slopes. This model is generated by analyzing the angle and orientation of terrain surfaces relative to the position of the sun, resulting in a semi-dimensional visualization.

Following the proposed methodology, eight shadow models were created, with orientation intervals every 45° and a consistent inclination of 30°. The results are presented in Figure 28. Surfaces labeled as a, b, g, and h (0°, 45°, 270°, and 315°) represent positive relief features, including elevated topographies like ridges and scarps. Conversely, the remaining orientations (90°, 135°, 180°, and 225°) correspond to negative relief features, typically comprising faults, valleys, trenches, and joints (Radaideh et al., 2016).

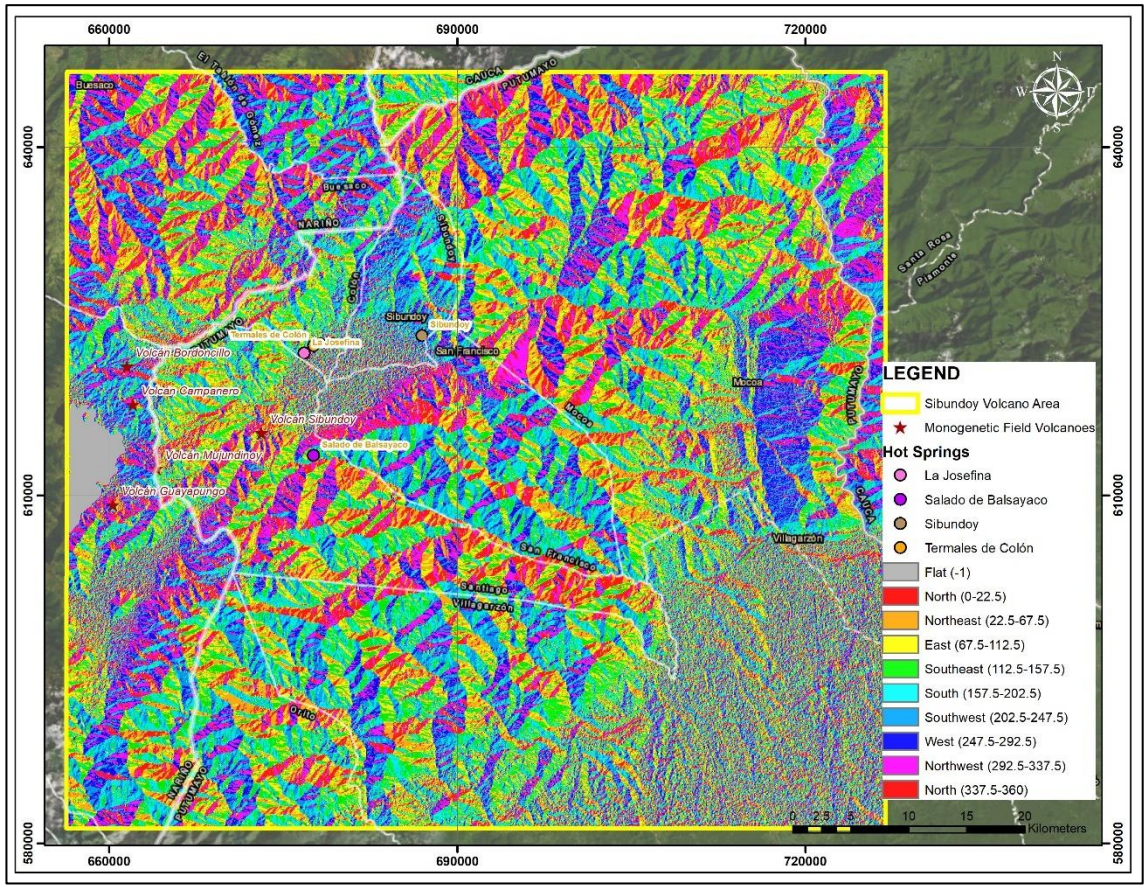

FIGURE 27. ASPECT MODEL. PRODUCT DERIVED FROM ALOS PALSAR SURFACE REPROCESSING IN 10 X 10 PIXEL SIZE. SIBUNDOY VALLEY GEOTHERMAL SYSTEM (SVGS).

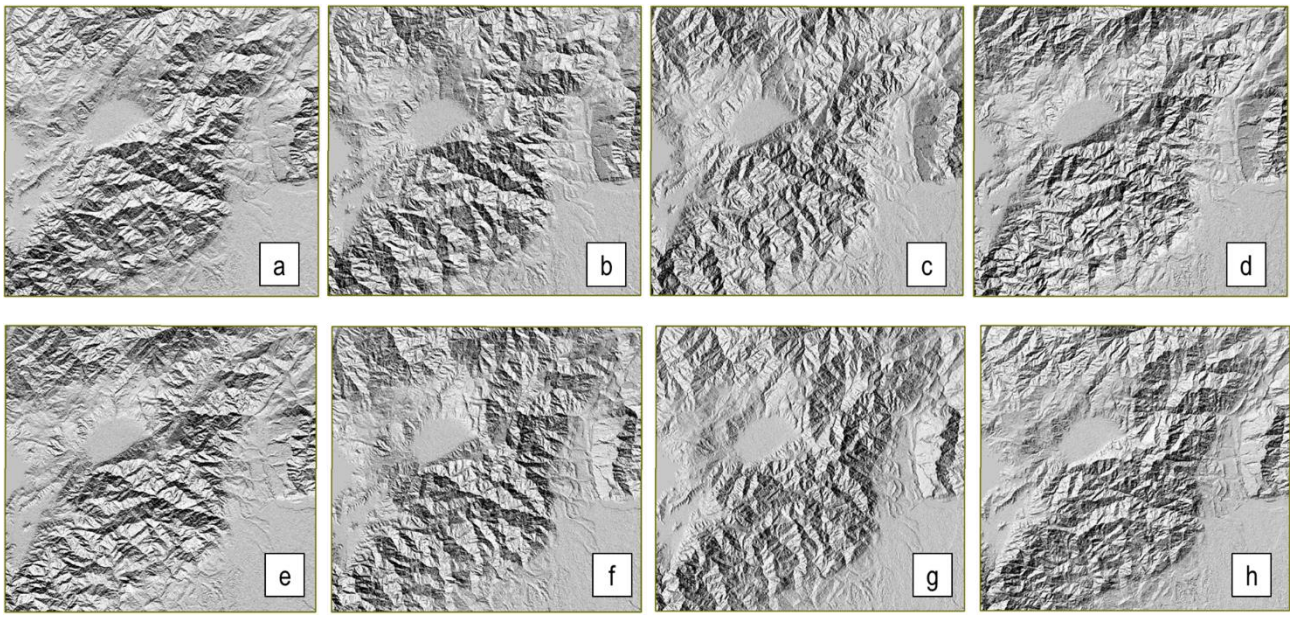

FIGURE 28. SHADOW MODELS EVERY 45° AZIMUTH WITH CONSTANT INCLINATION OF 30°. RIO SUCIO BASIN IN THE DEPARTMENT OF ANTIOQUIA. A. 0° AZIMUTH MODEL. B. MODEL 045° AZIMUTH. C. 090° AZIMUTH MODEL. D. 135° AZIMUTH MODEL. E. 180° AZIMUTH MODEL. F. 225° AZIMUTH MODEL. G. 270° AZIMUTH MODEL. H. 315° AZIMUTH MODEL. SIBUNDOY VALLEY GEOTHERMAL SYSTEM (SVGS).

5.4.Statistical model: Principal Components analysis

To statistically complement the assessment of the shadow surfaces involved in the analysis of automatic lineaments, a PCA (Principal Components Analysis) statistical model is performed to reduce the dimensionality of the eight surfaces, which may show redundancy in terms of frequency associated with a specific direction. PCA statistically groups the data, showing two groups of shadow models from which the final surfaces are derived to replicate the procedure proposed by Mark (1992). The combination of individual shadow maps enhances detail in areas of an image that would otherwise be illuminated by direct light or left in darkness by a single illumination source (Mark, 1992).

It's worth noting that shaded relief maps generated in traditional models emphasize structures that are illuminated obliquely but exclude structures illuminated along the structural domain (Mark, 1992). Following this premise, a statistical analysis begins with a correlation matrix (Figure 29b), composed by 1716 points associated with the centroid of a 1 km x 1 km cell within the zone (Figure 29a). Each model's value returned configures a database of 1716 rows x 8 columns. Values close to 1 and -1 in this matrix indicate surfaces with high correlation, suggesting they are similar. Values close to 0 indicate surfaces that differ from each other, possibly representing terrain features that can be combined when analyzing trends in different directions. Subsequently, using a processing code in MatLab software, two surfaces grouped into two main components are obtained: the first, represented by the combination of the 135°, 180°, 225°, and 270° models, and the second, grouping the 45°, 90°, 315°, and 360° models as a complementary surface, as depicted in Figure 29c.

By processing the shadow models to derive different weights (W) and executing the weighted models, two surfaces are obtained, presented in the Figure 30, summarizing the most expressive features according to different proposals. In Mark's proposal, where light incidence angles correspond mainly to NW-W-SW directions, emphasizing shaded features that depend on weights, the algorithm is induced to capture the main trends along a N-S to NNW-SSE regional axis (Figure 30b). Conversely, the PCA model adapts surfaces with light incidence angles in SE-S-SW directions, which, complementarily to the former surface, highlight shaded features at similar angles to the incidence, with the main trends being NW-SE and E-W (Figure 30a).

Visually, the models respond in a nearly complementary manner, emphasizing features associated with different morphotectonic characteristics. Both multiple illuminated shaded images, when analyzed independently, yield results with noticeable differences. For the purposes of this research, these surfaces are considered visually and statistically complementary, supported by the analysis of the second principal component obtained in the correlation matrix in section 3.3, suggesting PCA-2 type surfaces in the directions proposed by Mark (1992) (225°, 270°, 315°, and 360°).

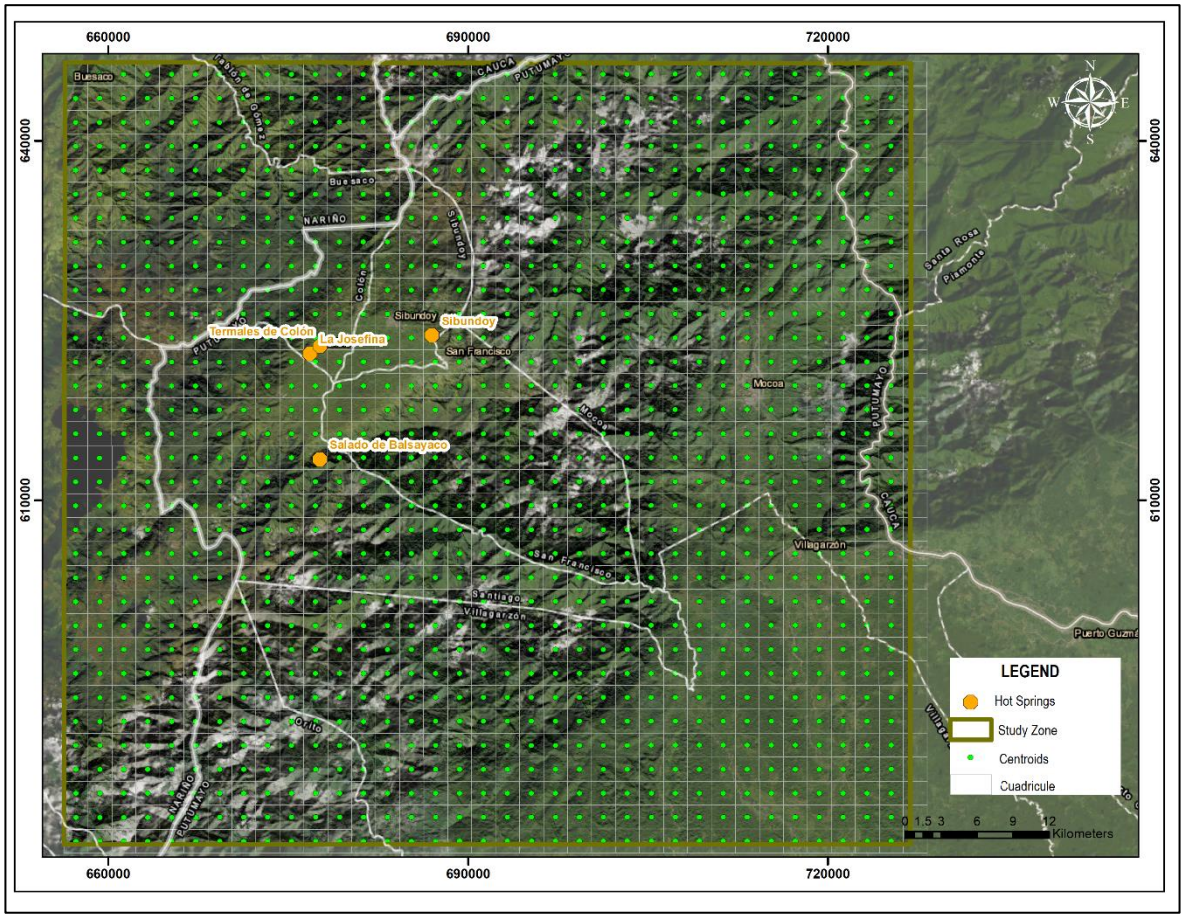

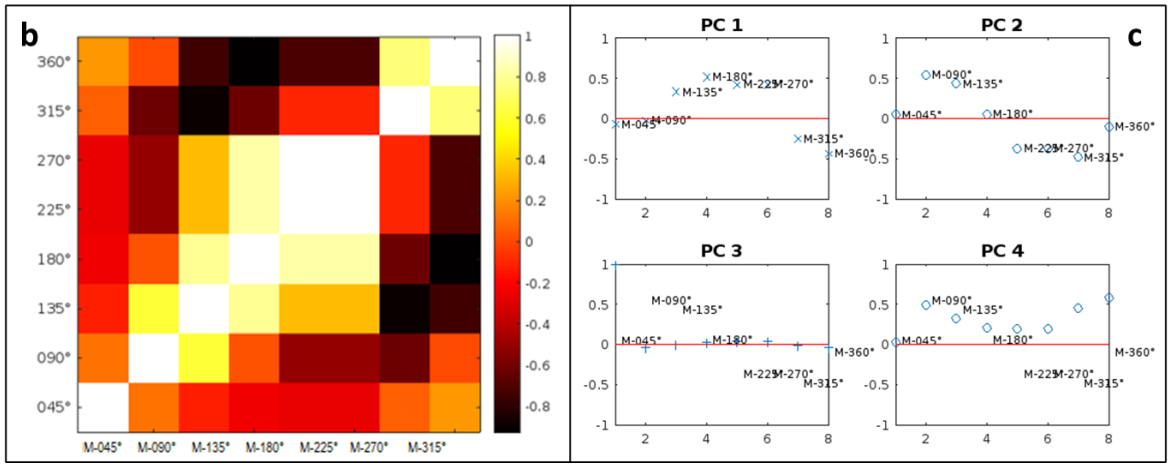

FIGURE 29. PCA ANALYSIS PROCESSING. (A) 1X1 KM GRID AND SAMPLING CENTROIDS. (B) CORRELATION MATRIX FOR THE 8 SHADOW MODELS. (C) PRINCIPAL COMPONENTS AND CLUSTERS OF INTEREST. SIBUNDOY VALLEY GEOTHERMAL SYSTEM (SVGS).

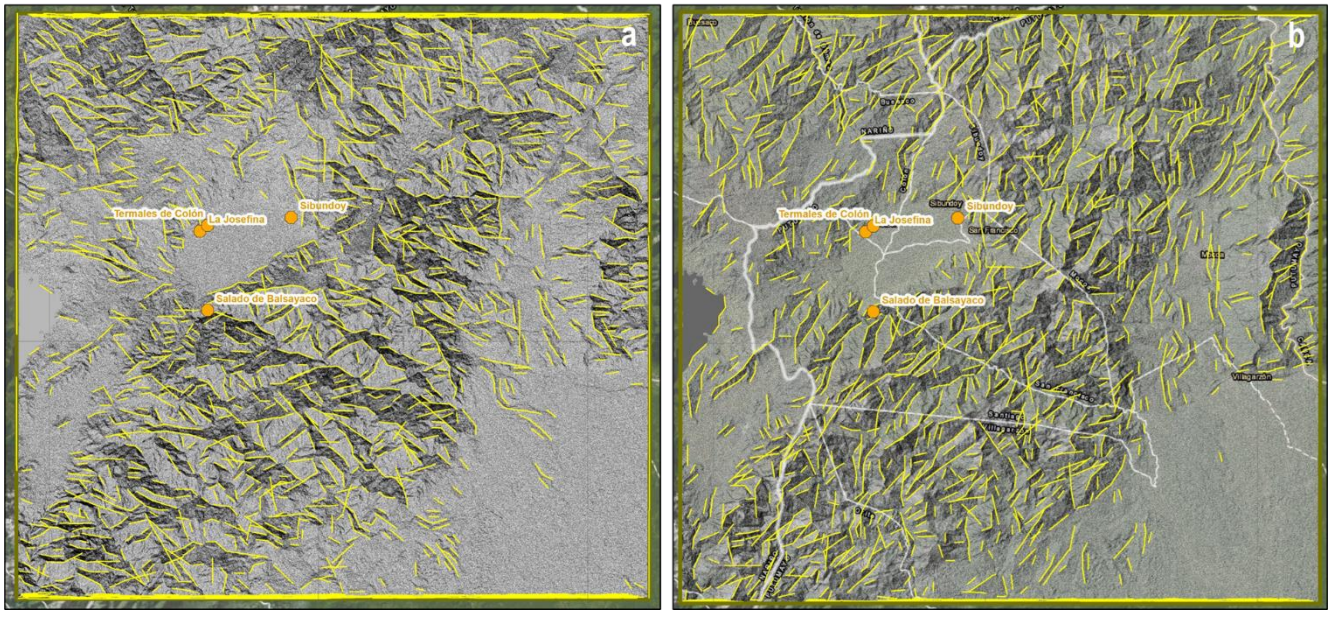

FIGURE 30. WEIGHTED MODELS DERIVED FROM PCA ANALYSIS. (A) WEIGHTED MODEL ACCORDING TO PCA MODEL . (B) WEIGHTED MODEL ACCORDING TO MARK´S PROPOSAL. ADAPTED FROM LÓPEZ ET AL., 2023. SIBUNDOY VALLEY GEOTHERMAL SYSTEM (SVGS).

5.5.Automatic Lineament Model and Analysis of Lineament Trends

In line with the previous procedure, it is essential to clarify that the processing of the acquired lineaments involves merging the linear features of both images, addressing the generated edge noise and eliminating the strokes smaller than 100 meters to maintain a scale ratio of 1:100,000. Additionally, processing is restricted to consolidated lithological units, excluding lineaments derived from recent and sub-recent deposits. Following post-processing, a total of 2724 lineaments were identified, spanning approximately 4527 kilometers within the Sibundoy Area. Overall, the surface depicted in Figure 31 aptly captures the regional NE-SW to N-S structural trend, as delineated geomorphologically by Velandia's proposition (2005). This aligns with a traction basin formed along the dextral displacement of the Algeciras strike-slip fault, ultimately manifesting as a pull-apart basin. These displacements give rise to Riedel, synthetic, and antithetic faults, notably observed in the W-E direction, alongside others such as the Colón fault and the Sibundoy fault exhibiting a NW-SE trend.

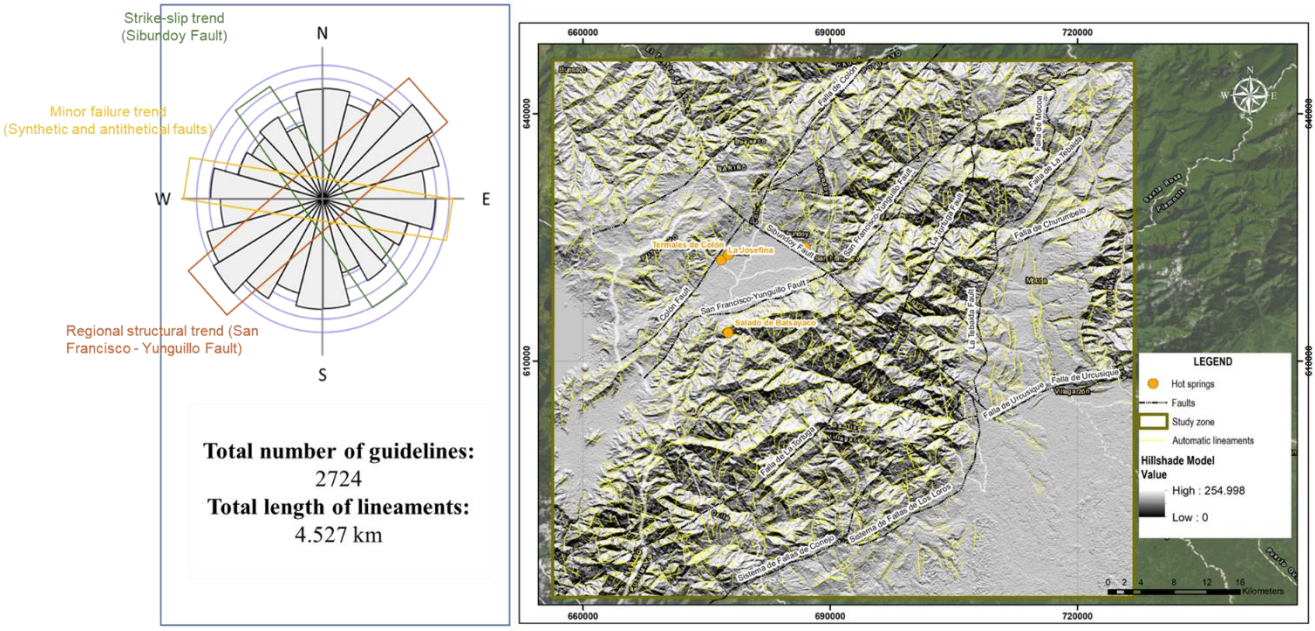

FIGURE 31. ANALYSIS OF AUTOMATIC LINEAMENTS. UNION AND PROCESSING OF WEIGHTED IMAGES. ROSE DIAGRAM FOR THE MAIN TRENDS OBTAINED. SIBUNDOY VALLEY REGION. UPPER PUTUMAYO BASIN. ADAPTED FROM LÓPEZ ET AL., 2023. SIBUNDOY VALLEY GEOTHERMAL SYSTEM (SVGS).

In general, structural trends reflect the rheological behavior of various geological units. It's crucial to discern the outcomes of automatic lineament analysis promptly to categorize behaviors concerning the defined objectives. As proposed by Lopez et al. (2023), the paramount significance lies in the dominance of structural control over water flows in the area. To ascertain the planes where surface structures are oriented and the preferred directions where flow may infiltrate towards the thermal springs, analysis of different orientations for each lithology with their respective persistence lengths was conducted (Singhal & Gupta, 2010).

The structural analyses of each lithology, depicted in Figure 32, reveal three predominant directions. Firstly, a NE-SW trend is observed primarily in Jurassic-age lithologies such as the Mocoa Monzogranite and the Saldaña Formation, with minor directions in the NW-SE orientation. Both the main planes and the minor directions could be correlated with similar poles reflecting the behavior of regional faults, approximately in the E-W and ENE-WSW directions.

Secondly, a dominant N-S direction is mainly associated with the La Concha – Río Téllez migmatitic complex of Proterozoic age, the Villeta Formation of Cretaceous age, and the Cuarzomonzodiorita de Sombrerillos of Jurassic age, all of which are rocks located east of the San Francisco Fault and north of the Sibundoy Fault. Lastly, the ENE-WSW direction is represented by units corresponding to the Sibundoy Basalts from the Holocene, as well as lavas and pyroclasts from the Neogene. It is suggested that these predominant planes generate poles approximately towards the SSE, consistent with the dip direction of the Colón fault.

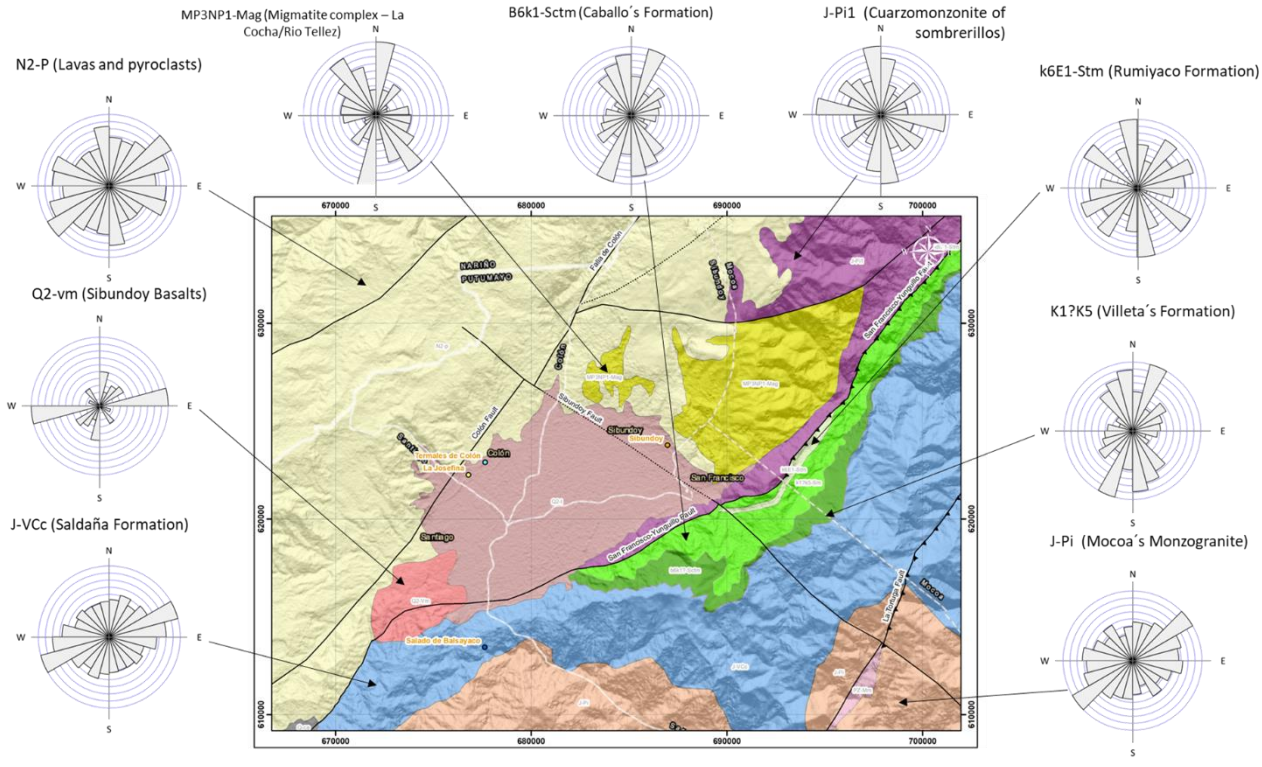

FIGURE 32. BASE GEOLOGICAL MAP AND ROSE DIAGRAMS ASSOCIATED WITH EACH LITHOLOGICAL UNIT. ADAPTED FROM LÓPEZ ET AL., 2023. SIBUNDOY VALLEY GEOTHERMAL SYSTEM (SVGS).

5.6.Distributed Analysis and Lineament Density of structural blocks

To achieve the primary goal of delineating flow zones based on the degree of fracturing within the geothermal system's constituent units, it's crucial to acknowledge that, given its fault and fracture-rich environment, groundwater flow paths are expected to predominantly align with these features. Like the previous approach, to map the three lineament density indices proposed by Saepuloh et al. (2017)—Ll (Lineament Length), Lf (Frequency of occurrence), Li (Intersection density)—ordinary kriging interpolation was conducted, adjusted according to the proposed method using the spherical or exponential model.

As illustrated in Figure 33a, the spatial distribution of lineament length ranges from 0 to 9 km, with higher values observed towards the SW and NE of the SVGS basin, a trend that is mirrored in the number of lineaments with values ranging from 0 to 11. Meanwhile, the number of intersections, spanning a range of 0 to 18, exhibits the highest values in the SW part of the study area (Figure 33b). Across all three lineament density indices, it is evident that the SE zone lacks lineaments, including the point of overlap between the San Francisco fault and the Sibundoy fault, as depicted in Figure 33c. It's important to note that a significant portion of the western sector of the area, a considerable segment of the southeastern mountain foothills, and the Sibundoy valley itself, lack automatic lineaments, either due to the presence of deposits or the absence of elements associated with the regional structural system.

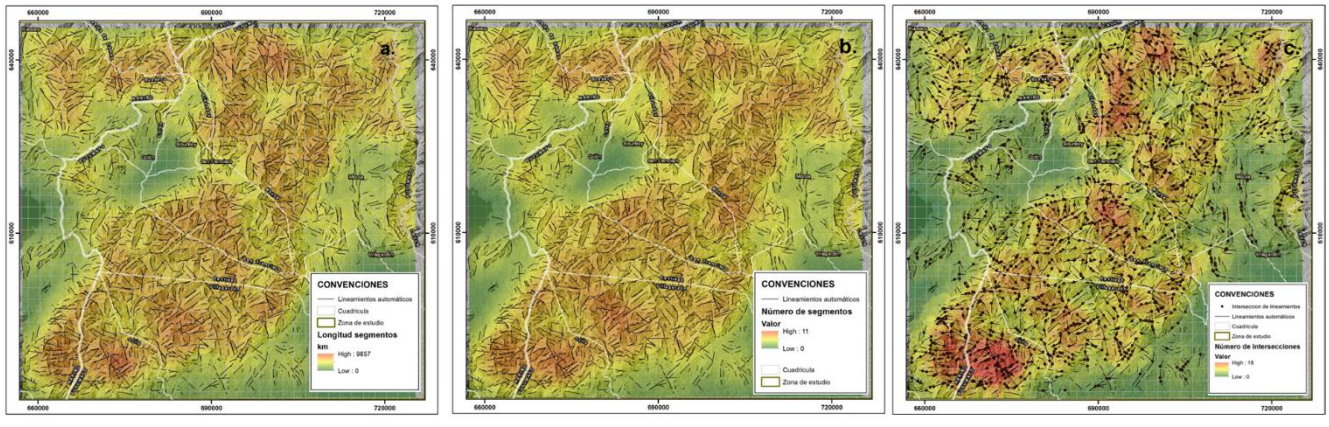

FIGURE 33. MAPS OF FRACTURING DENSITY ANALYSIS OF THE RIO SUCIO BASIN. (A) MAP OF LENGTH OF LINEAMENTS – LL INDEX, (B) MAP OF NUMBER OF LINEAMENTS – LF INDEX, (C) MAP OF NUMBER OF INTERSECTIONS - LI INDEX. SIBUNDOY VALLEY GEOTHERMAL SYSTEM (DGS).

Unlike the conclusion drawn from the analysis of surfaces associated with fracturing density in environments dominated by fractures, where groundwater is expected to rapidly descend into reservoirs along prominent faults and fractures in certain regions, in the case of structures associated with the behavior of the Sibundoy valley system, it is anticipated that regional flow patterns will be more closely associated with structural orientations rather than fracture density itself. However, the density of fractures near discharge areas could generate upward flow influenced by the advective movement of hydrothermal system isotherms, and even control the presence of monogenetic bodies conceptually considered as the heat source of the system.

Although the conceptual hypothesis varies, the approach to the problem involves delimiting a series of structural blocks, considering that the fractured environment influences the processes. The differentiated zoning of these blocks may result from various convergent processes that define the current context of the geothermal system. To adhere to the proposed methodology based on fracture density analysis—interpolating the number of segments for each block of interest and revealing the relationships between the different units within the same tectonic-structural block—a total of four blocks with different behaviors were delineated.

Furthermore, it's important to mention that because the proposed analyses only correspond to fractured lithologies, the definition of the blocks involved in the geothermal system is conceptually supported by the in-depth interpretation of the units, structures, and recent surface deposits, aiming to effectively integrate the conclusions, as depicted in Figure 34. The visual of block III is omitted from the cross-profile.

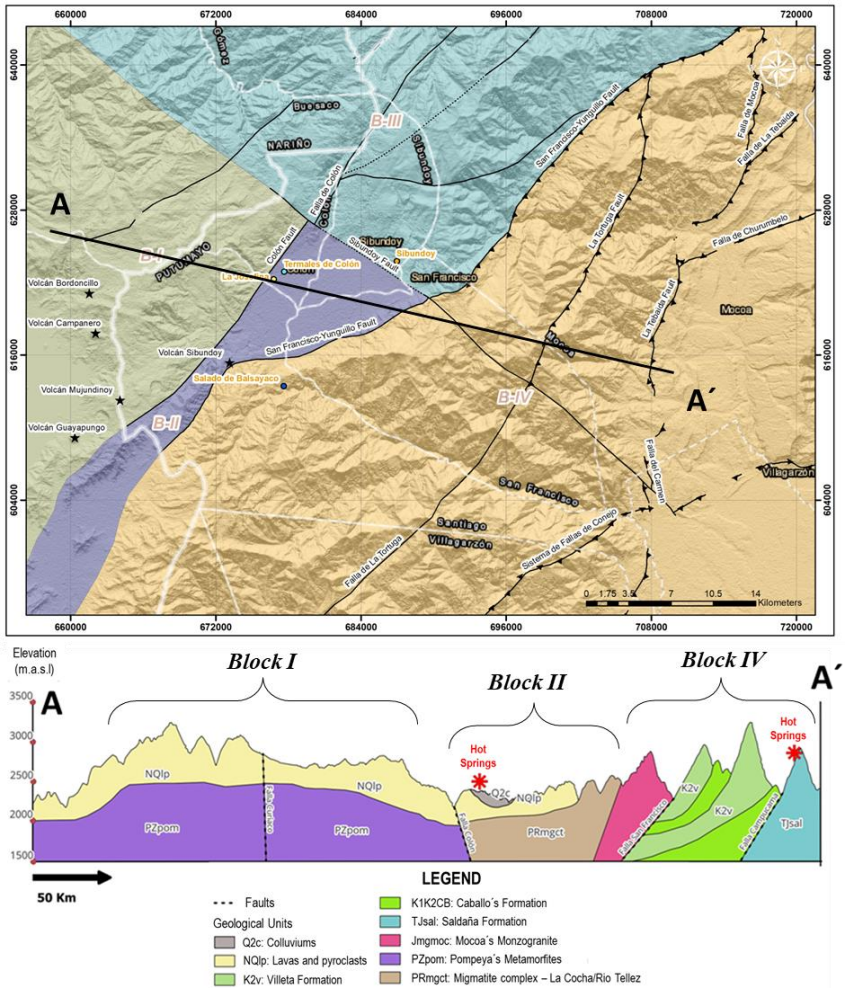

FIGURE 34. STRUCTURAL BLOCKS AND CROSS PROFILE ADAPTED FROM LÓPEZ ET AL, 2023. SIBUNDOY VALLEY GEOTHERMAL SYSTEM (DGS).

The first structural block is associated with lithologies located west of the Colón fault, encompassing a wide extension of lavas and pyroclasts on the surface, with its basement interpreted by López et al. (2023) as rocks associated with the Popeya Metamorphites. The general structural style and fracturing density are analyzed in the Neogene lava and pyroclast units and the Sibundoy Basalts. The predominant directions are approximately ENE-WSW, with minor trends potentially associated with jointing due to cooling superimposed on the structural context.

The analysis of fracturing density reveals a block of moderate to low density, where areas closest to the structural systems derived from the Sibundoy fault to the north of the block register up to 6 structures per

km^2, while towards the center and south of the block, the density is low and very low, respectively, with a slight accumulation of up to 4 structures per km2 in the vicinity of the Colón Fault trace, as presented in Figure 35a.

The second block corresponds to the portion of the valley between the east of the Colón Fault and the west of the San Francisco fault. In this zone, the structural style and fracturing density are analyzed in the outcropping portion of the Migmatite Complex La Cocha-Rio Téllez and the easternmost slope of the basalts generated by the Sibundoy volcano. Despite being the location of 3 of the 4 thermal springs, this block exhibits the lowest fracturing density and extension among the proposed blocks. Only in the center of the block, close to the Sibundoy Volcano, are up to 4 structures per km^2 recorded, within a range of low fracture density.

The structural trends fully coincide with the behavior of the two regional structures, predominantly in a NE-SW direction, with inferred poles to the northwest and west of the valley's lowest area. The spatial distribution associated with Block II of the Sibundoy geothermal system is presented in Figure 35b.

The third block corresponds to lithologies located north and northwest of the Sibundoy Fault, where the structural style is completely dominated by trends generated by strike-slip faulting. This sector comprises rocks of the Cocha-Rio Tellez migmatitic complex, part of the Jurassic body of the Sombrerillos Quartziorite, and a sector where Neogene lavas and pyroclasts emerge. The structural trends are generally associated with a north-south system, but minor trends in a NW-SE direction are noteworthy, coherent with the regional trend of the Fault and suggesting poles in approximately a west and south-southwest direction.

The fracturing density presented in Figure 35c shows one of the blocks with the highest concentration of lineaments near the Sibundoy valley. In general, moderate classification ranges predominate in the north and northeast of the block, with values between 4 and 6 structures per km2, followed by low and very low classifications close to the Sibundoy fault line (between 2 and 6 structures per km^2). The high values, between 6 and 8 structures per km^2, are located on the "wedge" generated between the Sibundoy fault and the San Francisco fault to the north, consistent with the highest elevations of the study area.

The fourth structural block includes lithologies located east of the San Francisco - Yunguillo Fault, primarily consisting of Jurassic rocks from the Saldaña Formation, the Mocoa monzogranite, and

Cretaceous lithologies from the Villeta Formation and the Rumiyaco Formation. The observed trends align with the trace of the regional fault, as well as the orientation and extent of the units within the block. The structures within this block generally trend approximately NE-SW and NW, except for the Rumiyaco Formation, which exhibits multiple orientations. This block exhibits the highest fracture density, predominantly moderate, with lower values in certain areas, and notably high and very high values towards the southwest, near the San Francisco fault line. The spatial distribution of fracture density is presented in Figure 35d.

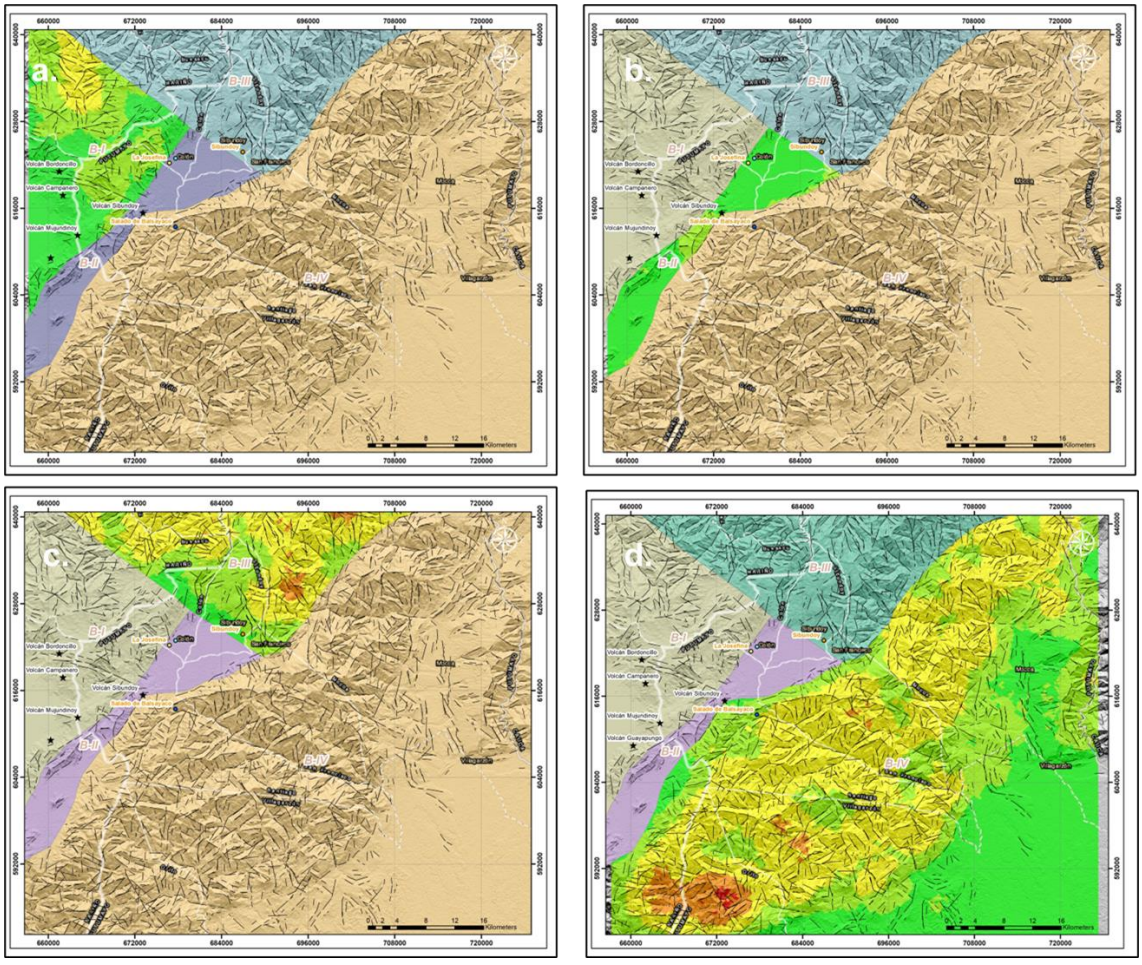

FIGURE 35. STRUCTURAL BLOCKS AND FRACTURE DENSITY OF THE SIBUNDOY VALLEY. (A) FRACTURE DENSITY FOR BLOCK I: COLÓN FAULT SYSTEM. (B) FRACTURE DENSITY FOR BLOCK II: SIBUNDOY VALLEY. (C) FRACTURE DENSITY FOR BLOCK III: SIBUNDOY FALT SYSTEM. (D) FRACTURE DENSITY FOR BLOCK IV: SAN FRANCISCO FAULT SYSTEM. SIBUNDOY VALLEY GEOTHERMAL SYSTEM (SVGS).

5.7.Conceptual model of the Sibundoy Geothermal Play

The geothermal systems associated with volcanic arcs resulting from subduction zones exhibit varying characteristics as we move away from the subduction zone. Small-volume volcanoes are classified as monogenetic or polygenetic based on petrogenetic classification and volcano architecture (Smith & Németh, 2017). Monogenetic fields consist of small volcanoes spaced apart and are often associated with deep magmatic sources, forming small clusters aligned along structural systems over time (Smith & Németh, 2017).

The initial conceptual model proposed for the Sibundoy region aligns with the model introduced by Ramirez et al. (2021), suggesting that the Sibundoy Valley represents a depression resulting from local tension along the fault system overstep, interpreted as a pull-apart basin. Notably, numerous strike-slip faults in the Sibundoy valley exhibit the presence of "echelon" faults and folds. This staggered arrangement of structures, relatively short, overlapping, and nearly parallel to each other, albeit oblique to the linear zone where they are situated (Biddle and Christie-Blick, 1985; Campbell, 1958; Harding and Lowell, 1979).

Predominant structural orientations indicate that the oldest rocks exhibit a NW-SE alignment, corresponding to antithetic faults and other structures formed during the inception of the pull-apart basin. These fractures facilitate the infiltration of meteoric water into the geothermal system and may contribute to the dispersion of heat flow. This pattern correlates with the distribution of surface thermal features, including the Sibundoy, Colón, and La Josefina hot springs.

An illustrative case highlighted by both Ramirez et al. (2021) and López et al. (2023) is the Balsayaco thermal spring, resulting from the advection of isotherms originating in the Saldaña Formation, acting as a hanging wall influenced by the displacement of the San Francisco-Yunguillo thrust fault. Considering the substantial contribution to this approach, the main objective is based on the hypothesis that meteoric water and heat flows are dominated by the structural control of the area. To understand the planes where the surface structures are oriented and the preferential directions for potential infiltration flow towards the thermal springs, an analysis of different orientations for each lithology with their respective persistence lengths was necessary (Singhal & Gupta, 2010) complemented by distributed surfaces.

López et al. (2023) infer that the heat generated by the subduction process is transferred to the surface by the structural systems that control the distribution of the monogenetic field. The heat from the magmatic arc and the structural control in the thrust zones categorize the geothermal system as mixed, where the heat source is associated with the field's own magmatism, but its circulation and dissipation are controlled by the San Francisco, Yunguillo, Colón, and Sibundoy faults.

The discussion on fracture density reveals that areas with the highest fracture density lie southeast of the San Francisco Fault, whereas those with lower density are situated on volcanic formations northwest of the fault. This trend aligns closely with areas of highest infiltration potential identified by López et al. (2023), particularly associated with the Saldaña Formation, validating the significant control exerted by fracture density on mixing processes within the system.

The heat potential in the system is mainly found in the block east of the San Francisco fault. However, the structural configuration proposed in this new model could indicate a condensation of heat flow from adjacent blocks to the thermal springs, with predominant directions generating poles converging towards the Sibundoy valley.

In the Sibundoy Valley Geothermal System (SVGS), we observe a typical mixed system where the heat source stems from a young magmatic source, yet its flow is predominantly governed by deep faults forming the pull-apart basin. These faults not only orient the monogenetic volcanoes of southern Colombia but also influence the distribution of hydrothermal springs within the valley, showcasing the intricate interplay between geological structures and fluid flow patterns. The interaction of geological structures with hydrogeological and geothermal dynamics in various geothermal systems presents intriguing complexities worth exploring. For example, the presence of partial crystallizations associated with monogenetic volcanism, together with the unique geometry of certain calderas, gives rise to seal layers or condensate layers, redirecting both the recharging flows of meteoric water and the flows of volcanic heat itself, influencing the overall hydrogeological and geothermal dynamics of the system.

Furthermore, hypotheses regarding the migration of the monogenetic system in southwestern Colombia contributing to the formation of low-permeability layers and the influence of lithological homogeneity on block formations highlight the importance of understanding the geological context in delineating flow zones and predicting hydrogeological behavior.

5.8.Concluding remarks

The Sibundoy geothermal system is situated within a fractured medium, characterized by homogeneous lithologies and extensive historical volcanism linked to the subduction zone dynamics of the northern Andes. Monogenetic fields, comprising small volcanoes formed by deep magmatic sources, exhibit clustering along structural systems over time. These structural systems, comprising fault lines and fractures, play a pivotal role in governing fluid flow dynamics and heat distribution within the system.

The interaction between geological structures and hydrogeological and geothermal processes results in a series of complex phenomena. Partial crystallizations associated with monogenetic volcanism, along with the geometry of calderas, give rise to seal or condensate layers. These layers, along with fine-sized sediments, influence the redirection of meteoric water recharge and volcanic heat flows, thereby shaping the hydrogeological and geothermal dynamics of the system.

Fracturing density within the study area varies significantly across different structural blocks. Block I, located west of the Colón fault, exhibits moderate to low fracture density, while Block IV, east of the San Francisco - Yungillo Fault, shows the highest fracture density, particularly towards the southwest near the San Francisco fault. Structural trends align closely with regional fault lines, with predominant directions observed approximately ENE-WSW and NE-SW across Blocks I, II, and IV.

The lithologies within each block, spanning Jurassic rocks to Neogene lavas and pyroclasts, influence structural styles and fracture densities. Specific formations, such as the Saldaña Formation and Mocoa monzogranite, correlate with higher fracturing densities in certain blocks. The structural control dominates the SGSV, with meteoric water infiltration in northern thermal springs exhibiting lower temperatures than the Salado de Balsayaco thermal spring, influenced by the advection of isotherms due to the movement of the San Francisco-Yunguillo thrust fault.

In addition to structural controls, geochemical analysis and thermochronology provide valuable insights into the thermal evolution and fluid composition of the SVGS. Geochemical studies reveal the influence of both meteoric and hydrothermal waters on the chemical composition of thermal springs, with variations in major solutes indicating mixing processes and potential steam condensation near the surface. The use

of silica geothermometers and thermochronology data allows for the refinement of temperature estimates and the identification of thermal anomalies within the system.

Thermochronological data, particularly from apatite fission track and (U-Th)/He dates, provide constraints on the thermal history of the SVGS, indicating fault movement and hydrothermal reset ages. These data suggest that the geothermal system has been active since at least the Pleistocene, with interactions between hot fluids and host rocks occurring at temperatures ranging from above 80°C to below 40°C. Integration of geochemical and thermochronological data enhances our understanding of the thermal evolution and fluid circulation within the SVGS, providing critical information for geothermal resource assessment and exploration.

6. DISCUSSION

Dabeiba and Sibundoy are two distinct regions characterized by unique geological and geothermal features. Dabeiba, is known for its local geothermal potential arising from volcanic activity and tectonic processes. Similarly, Sibundoy, situated in the Putumayo department, also exhibits promising geothermal characteristics, attributed to its structural complexities and volcanic history. Despite their geographical and geological differences, both regions share common challenges and opportunities in harnessing geothermal energy for sustainable development. Here after, we propose a discussion related to the methodology, conceptual proposes and integrative results and the main differences between DGS and SVGS.

6.1.General methodological considerations

The discussion surrounding the methodology employed in analyzing terrain characteristics and linear features within the study areas of Sibundoy and Dabeiba reveals several key insights and methodological considerations.

Despite the inherent limitations of resampling for resolution changes, the decision to resample the elevation data to a finer pixel scale of 10 meters significantly improved the accuracy of the representation, particularly in regions with complex tectonic activity. This finer resolution was essential for identifying subtle topographic features and geological structures critical to understanding underlying geological processes and avoiding noise in subsequent analyses.

The utilization of analytical relief shading techniques, such as hill-shading and aspect analysis, proved effective in identifying linear features with specific orientations. These techniques are fundamental in geoscientific research for delineating geological structures and fault lines influenced by tectonic processes. Analyzing terrain response under varying angles of light incidence provided valuable insights into the morphology and spatial distribution of geological features, aiding in the interpretation of structural complexities.

Moreover, the application of Principal Component Analysis (PCA) to reduce the dimensionality of shadow surfaces generated by relief shading techniques demonstrated the efficacy of statistical modeling in identifying distinct groups of shadow models. By statistically grouping the data, PCA facilitated a more precise understanding of directional frequency, improving the accuracy of analysis and terrain interpretation.

Digital processing methods, such as Multidirectional Oblique Weighted Shading (MDOW) relief shading, enabled the simulation of artificial light from multiple azimuthal angles, uncovering diverse spatial patterns of linear features not discernible with traditional shaded relief maps. However, it is crucial to acknowledge the limitations of automated lineament extraction, including difficulties in distinguishing geological from non-geological features, which may introduce inaccuracies in mapping linear structures.

The calculation of lineament density indices, including length, frequency, and density of linear features, provided quantitative measures of spatial distribution and abundance within the study areas. These indices offer valuable insights into the structural complexity and tectonic activity, guiding future research and exploration efforts in geoscience and geothermal resource assessment.

In conclusion, the integration of analytical relief shading techniques, statistical modeling, and digital processing methods represents a robust approach for terrain analysis and identification of linear features in investigating geothermal systems associated with fractured media. The findings contribute to a deeper understanding of geological structures, their relationship with tectonic processes, and the potential of geothermal resources, facilitating informed decision-making in resource exploration and development.

6.2.Conceptual proposals and integrative results

The discussion surrounding the structural trends as delineators of weakness planes within a fractured medium, particularly within the Dabeiba system, sheds light on zones facilitating both the advection of isotherms and the potential ingress of meteoric water into the system. The poles identified indicate flows from the surface, while areas of high fracture density represent potential conduits for heat ascent via advective processes related to a suturing zone. The effective combination of both analyses is essential to understand the processes considered as bidirectional.

The research's discussion outcome entails the distributed understanding of fracture density and its relationship with water flows originating from potential recharge zones, which traverse the medium and serve as precursors to mixing processes. Hydrochemical evidence supports the hypothesis discussed of the Dabeiba Geothermal System (DGS).

Following this line of thought, the fundamental premise postulates that the DGS is probably related to a Miocene extensional event, which allowed the formation of sedimentary rocks of the Guineales Formation. Subsequently, an emplacement event associated with the accretion of the Panama-Chocó block resulted in a series of high-angle normal faults, with fluid flow along them controlled by stress states in the different tectonic zones proposed.

The interpretation of the system could be proposed as a regional graben, dominated by high-angle faulting, and along these traces of normal behavior, coupled with the notable vergence of structures and the characterization of high fracture density found in the current research, suggests that strike-slip components associated with the vergence of the collision front to the southeast reactivated the system until reaching the current configuration. It is not ruled out that further evidence of hydrothermal waters may be found along the zone of high local fracturing.

The flow of groundwater could be associated with the regional fault system, which, along with various automatic trend analyses, reflects a predominantly N-S direction with a slight NE vergence as we approach the proposed collision front. These systems affect the rocks of the Mandé Batholith, the Nutibara Member (K2cn), the Barroso Formation (K2bb) and the Urrao Member of the Cañasgordas Complex (K2alu), making them rocks with high secondary porosity of interest to understand the functioning of the flows in the system. They share the same structural patterns in their drainage, alignments, and general regional orientation of geological units.

The Guineales Formation (E3n1g) is of hydrogeological and geothermal interest, as the primary porosity resulting from diagenetic processes is augmented by the presence of an overlaying fracture density, indicating structural control marked by an orientation of 340° and a density of up to 10 structures per km2. This orientation aligns with the location of the three thermal water sources on the surface, suggesting that the transfer of heat from the deep source to thermal emanations is strongly influenced by deep and intermediate subsurface flows accumulated within levels of this unit.

The hydrogeochemical characterization suggests that the Chobar and Guineales springs are situated at the margin of the system where they are most affected by lateral flow, while the Mohán spring appears to be more linked to upward flow (Montoya et al., 2019). This observation is corroborated by the identification of intermediate flows in specific sectors of the basin, giving rise to hanging water tables that primarily contribute to feeding the base flows of major streams, such as the Río Sucio. These two sources closest to the hydrological body after which the basin is named are directly related to such processes, whereas the concentration of Cl, SO_4, and B in all samples, but especially in the Mohán thermal spring, indicates that the system is influenced by a deep source with minimal dilution and infers that the system is interacting with magma degassing from an intrusive (possibly the Mandé batholith or its satellite bodies), contributed by sedimentary layers or a process of water release due to metamorphism of marine sediments.

Understanding the functioning of isotherms and the processes responsible for their ascent depends on the genesis and evolution of the structural system. The automatic lineament model obtained shows an area with high general fracturing but with density concentrations over areas of greater hydrothermal interest. Thus, the regional morphostructural behavior causes the geothermal gradient to increase around the Chimurró normal fault and to concentrate in areas where the same thermal emanations occur (Figure 36).

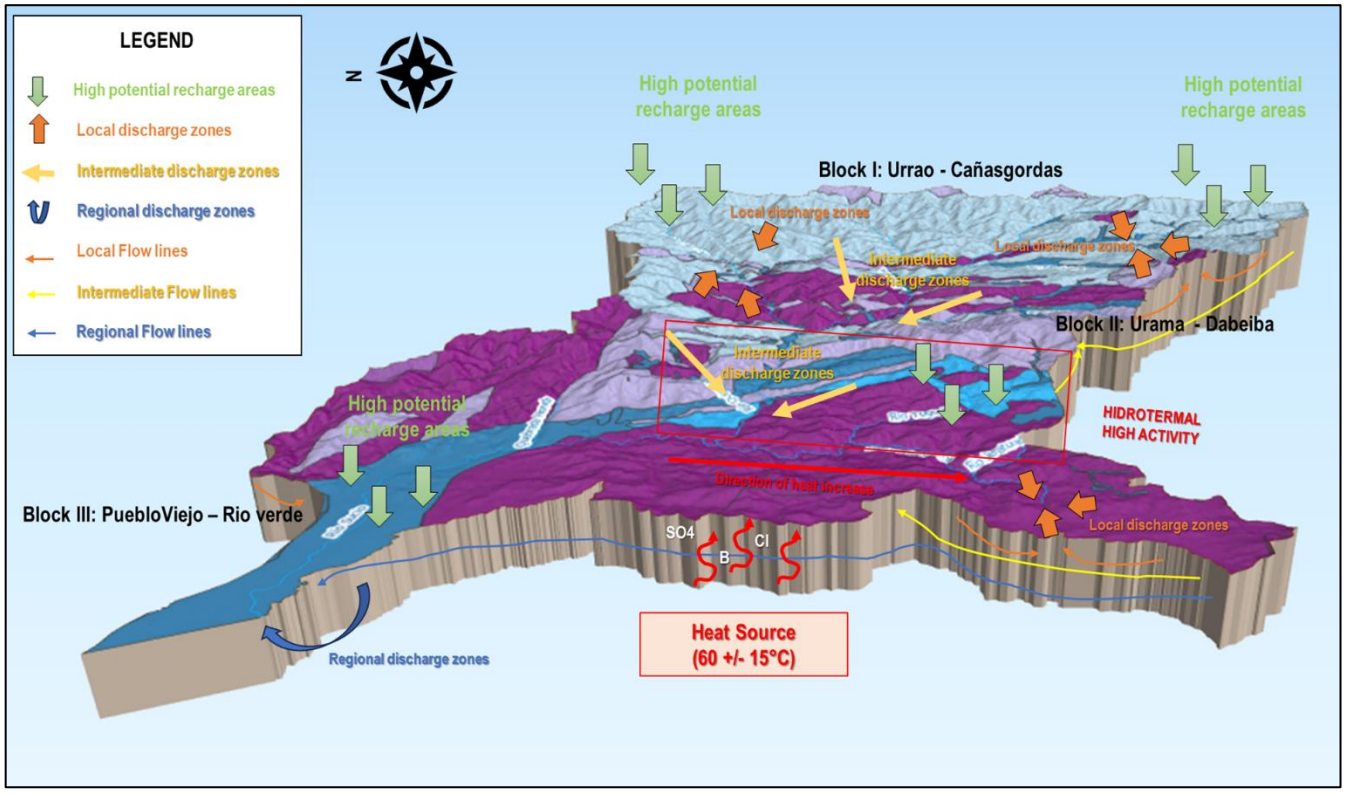

FIGURE 36. CONCEPTUAL DIAGRAM BLOCK OF THE HYDROGEOLOGICAL AND GEOTHERMAL ELEMENTS WITHIN THE RIO SUCIO BASIN IN THE DEPARTMENT OF ANTIOQUIA. DABEIBA GEOTHERMAL SYSTEM (DGS).

The discussion surrounding the structural blocks identified within the SVGS provides insights into the complex interplay between fracturing density, regional flow patterns, and geothermal behavior. While traditional analyses often prioritize fracture density as a primary determinant of groundwater movement, the unique geologic context of the SVGS suggests a more heterogeneous relationship. In contrast to environments where fractures serve as conduits for rapid groundwater descent, such as in fracture-dominated settings, the Sibundoy valley exhibits a more intricate pattern where regional flow patterns align closely with structural directions rather than fracture density alone. However, the density of fractures proximal to discharge areas may induce upward flow, influenced by advective movement of hydrothermal isotherms, potentially controlling the presence of monogenetic bodies acting as heat sources. Despite the conceptual disparity, the methodology hinges on delineating structural blocks, underscoring the fractured environment's role in conditioning processes. The differentiated zoning of these blocks likely results from a convergence of various processes shaping the current geothermal system context. The preservation of

the proposed methodology, employing fracture density analysis and interpolation techniques, allows for the elucidation of relationships among different geological units within each tectonic-structural block.

It is noteworthy that the proposed analyzes belong exclusively to fractured lithologies, and the definition of the blocks of the geothermal system is conceptually supported by a comprehensive interpretation of the geological units, structures and surface deposits. By integrating these conclusions, a clearer understanding of the system's behavior emerges, as shown in the figures provided throughout the document.

The delimitation of four structural blocks reveals different behaviors, each characterized by different fracture densities and geological compositions. From the lithologies west of the Colón fault to those easts of the San Francisco-Yungillo fault, a pattern in fracture density is presented, with implications for regional flow directions and geothermal potential. The association of structural trends with fault orientations further underlines the control exerted by regional tectonic characteristics on the distribution of fractures and, consequently, on the dynamics of groundwater flow, which is assumed to be generated in remote areas. from the point of emergence and consequently due to the presence of partial crystallizations associated with monogenetic volcanism, added to the unique geometry of certain calderas, gives rise to seal layers or condensate layers. These layers, when combined with fine-sized sediments, redirect both the recharge flows of meteoric water and the flows of volcanic heat itself, influencing the general hydrogeological and geothermal dynamics of the system that tend to accumulate over block II of the Valley of Sibundoy like as presented in the Figure 37.

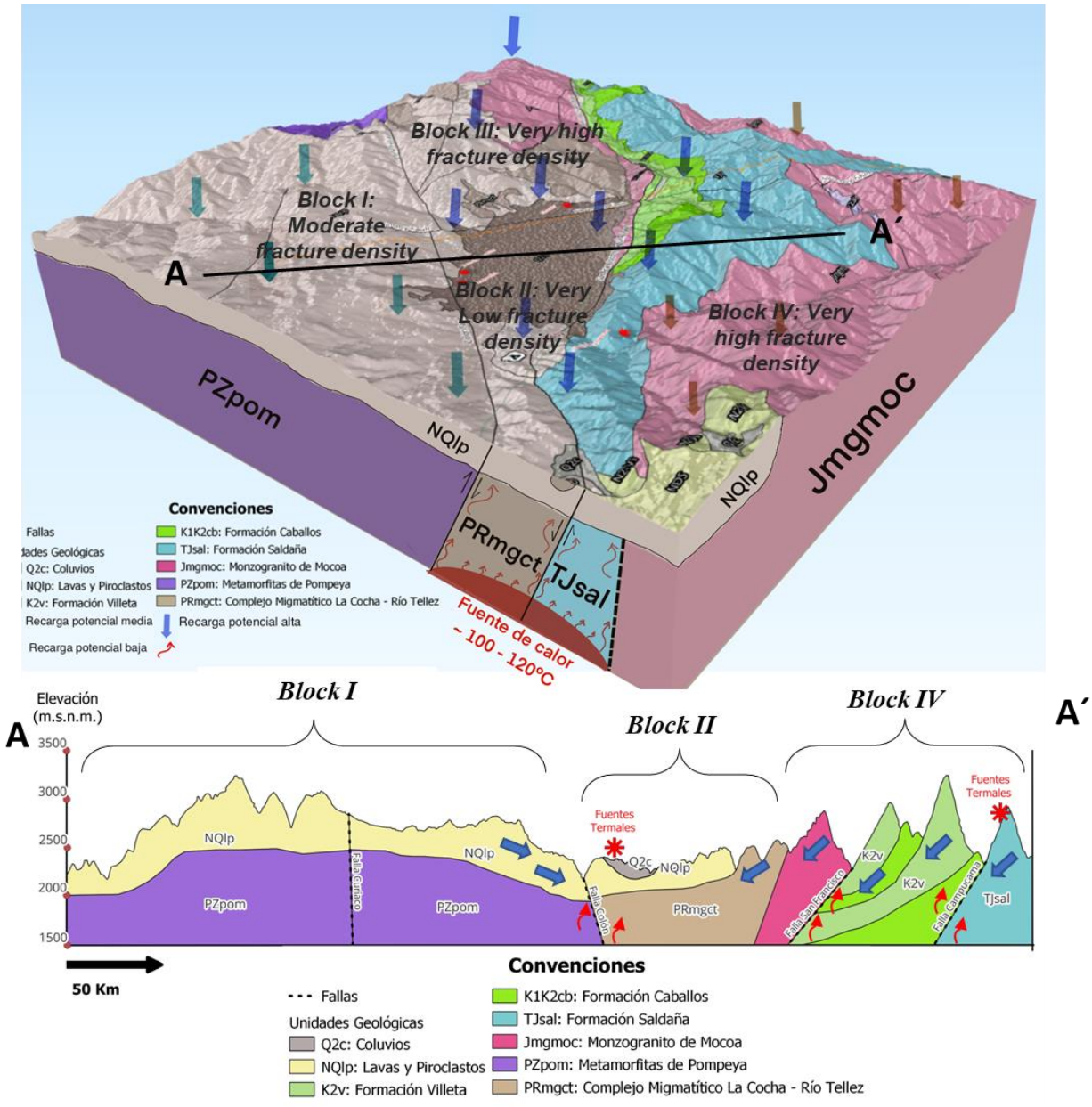

FIGURE 37. CONCEPTUAL DIAGRAM BLOCK - GEOTHERMAL MODEL. SIBUNDOY VALLEY – UPPER PUTUMAYO BASIN. ADAPTED FROM LÓPEZ, 2023. SIBUNDOY VALLEY GEOTHERMAL SYSTEM (SVGS).

The integration of chemical analyzes with thermochronological data provides more information on the behavior of the Sibundoy Valley Geothermal System (SVGS). The variation in ionic composition suggests contributions from surface waters and volcanic sources, with dissolution/precipitation and mixing processes influenced by temperature-dependent ions.

Stiff diagrams clarify ion exchange processes, particularly in hot springs such as Balsayaco, Colón and Josefina, where high concentrations of chlorine and sodium imply lateral flow and direct feeding from deep reservoirs. On the contrary, the Sibundoy thermal exhibits a lower chlorine content, which indicates a possible condensation of vapor near the surface, probably related to volcanic waters, and a possible regional connection with higher power volcanic systems such as the Doña Juana Volcanic Complex north of the area of interest. Furthermore, stable isotope analysis reveals a pattern of mixing of meteoric and volcanic waters, supported by the positioning of hot springs along the Global Meteoric Water Line (GWML). Although the mixing ratio is not entirely clear, oxygen depletion suggests limited transit in the medium, correlated with electrical conductivity values.

The Na-K-Mg plots further delineate the geochemical characteristics of the hot springs, with the Sibundoy and La Josefina hot springs indicating the presence of immature or mixed waters. The Balsayaco thermal spring is located within the partially balanced region, while the Colón thermal spring exhibits complete equilibrium, providing information on reservoir temperatures estimated through solute geothermometers.

The presence of the Balsayaco thermal spring to the east of the fault, influenced by isothermal advection controlled by the fault movement, highlights the complex interaction between structural controls and fluid circulation processes, and is considered within the research as the sector with the greatest geothermal potential considering current information.

6.3. Main differences between DGS and SVGS

The structural characteristics and geochemical signatures of the Dabeiba and Sibundoy geothermal systems underscore the significance of regional tectonic settings in understanding groundwater flow and heat transfer processes. In Dabeiba, structural trends delineate weakness planes within a fractured medium, influencing the advection of isotherms and meteoric water ingress. Fracture density, particularly in high-density areas, plays a crucial role in facilitating heat ascent processes. The genesis of the Dabeiba system likely relates to Miocene extensional events, followed by emplacement events associated with the accretion of the Panama-Chocó block, resulting in high-angle normal faults. The regional graben structure, dominated by faulting, indicates a predominantly N-S direction of groundwater flow, influenced by structural controls and hydrogeological features like the Guineales Formation. Hydrochemical evidence supports lateral and upward flow patterns, contributing to the system's complexity. Thermochronological data from apatite fission track and (U-Th)/He dating provide constraints on the thermal history of the Dabeiba system, indicating fault movement and hydrothermal reset ages, suggesting activity since at least the Pleistocene with interactions between hot fluids and host rocks occurring at temperatures ranging from above 80°C to below 40°C.

In contrast, the Sibundoy valley system exhibits a more intricate pattern, where regional flow aligns closely with structural directions rather than fracture density alone. The delineation of structural blocks reveals varying fracture densities and geological compositions, influencing regional flow patterns and geothermal potential. Chemical analyses coupled with thermochronological data provide insights into water sources, mixing processes, and reservoir temperatures. The presence of immature or mixed waters in certain hot springs suggests complex fluid circulation pathways, influenced by fault-controlled isothermal advection. Thermochronological data from apatite fission track and (U-Th)/He dating in the Sibundoy system similarly provide constraints on its thermal history, indicating fault movement and hydrothermal reset ages, suggesting activity since at least the Pleistocene with interactions between hot fluids and host rocks occurring at temperatures ranging from above 80°C to below 40°C.

Both cases underscore the importance of integrating geological, geochemical, thermochronologicl and hydrogeological data to develop comprehensive conceptual models for geothermal exploration and resource assessment. Further research is needed to elucidate the complex interaction between structural

patterns, fluid circulation processes, and heat mechanisms in these geothermal systems. Additionally, the characterization of these systems as low to medium enthalpy systems highlights their potential for sustainable geothermal energy development in the context of renewable energy transitions.

While the Dabeiba system emphasizes the role of fracture density and regional fault systems in controlling groundwater flow and heat transfer, the Sibundoy system highlights the interplay between structural controls, fracture density, and geochemical signatures in shaping hydrothermal behaviors.

7. CONCLUSIONS

The integration of remote sensing data with geothermal analysis has proven to be an effective approach in identifying structural features and understanding their influence on geothermal processes. The trend of the lineaments observed by remote sensing indicates their potential role in both surface water dynamics and subsurface fluid flow patterns.

The use of complementary surface models, including Mark's proposal (1992) and the PCA shadow model, has provided valuable insights into both regional and local structural features. While Mark's model captured broader regional structures, the PCA model revealed more localized features associated with jointing and volcanic influences. These identified lineaments align closely with geological structures such as faults and fractures, emphasizing the importance of considering both geological and geomorphological factors in geothermal studies.

The evidence supports the hypothesis of a Dabeiba Geothermal System (DGS) linked to a Miocene extensional event. Fault structures, particularly those associated with the Guineales Formation, play a critical role in controlling fluid flow, with potential contributions from meteoric water infiltration and upward heat flows. Geological units like the Guineales Formation exhibit high hydrogeological importance due to primary and secondary porosity, with fracture orientation influencing heat transfer and the emergence of thermal water sources on the surface.

The complex structural zones observed within the study area, with different blocks displaying varying degrees of deformation and structural influence on fluid flow, highlight the need for further field investigations to confirm and refine the findings. Detailed field measurements, including fracture density assessments, along with additional geological and geophysical data, are essential for a comprehensive understanding of the geothermal system.

Understanding the characteristics of the geothermal system is crucial for sustainable resource management. The identified structural features and potential flow pathways should be considered in environmental impact assessments and future geothermal resource development plans.

In conclusion, the integrated approach presented here lays the groundwork for advancing our understanding of the geological and hydrogeological controls on the Dabeiba Geothermal System. These

findings provide valuable insights for future research and underscore the importance of interdisciplinary approaches in geothermal exploration and sustainable resource management.

The analysis of structural blocks within the Sibundoy geothermal system also offers significant insights into fracture distribution, density, and orientation, highlighting the intricate interplay between geological structures and hydrothermal dynamics. These findings are essential to inform geothermal resource evaluation and development strategies, emphasizing the need to integrate geological, hydrochemical and hydrogeological data to optimize efforts during the exploration and characterization stages of a geothermal reservoir.

Additionally, thermochronological analysis has provided valuable insights into the thermal history and evolution of both the Dabeiba and Sibundoy geothermal systems. Thermochronological data, particularly from apatite fission track and (U-Th)/He dating, offer constraints on fault movement and hydrothermal activity ages, suggesting that these geothermal systems have been active since at least the Pleistocene. This information enhances our understanding of the temporal evolution of fluid circulation pathways and heat transfer processes within these systems. Integration of thermochronological data with geological and geochemical analyses further refines our understanding of the geothermal resource potential and aids in the identification of optimal drilling targets for future exploration efforts.

8. REFERENCES

Alfaro, C., Rueda-Gutiérrez, J. B., Casallas , Y., Rodríguez, G., & Malo, J. (2021). *Approach to the geothermal potential of Colombia.*

Álvarez, A., & González, M. (1978). *Geología y geoquímica del Cuadrángulo I–7 (Urrao).* Informe técnico interno, CORPOURABA.

Álvarez, J. (1970). *Mapa geológico generalizado y localización del muestreo geoquímico de la Cordillera Occidental, departamentos de Chocó y Antioquia.* Medellín: INGEOMINAS- Memorias inéditas.

Batson, R., Edwars, E., & Eliason, E. (1975). *Computer generated shaded relief images.* J. Res US. Geol. Surv. 3 (4), [401-408].

Betancur , & Martinez . (2022). *Potential and prospects for hydrogeological exploration according to lithostructural criteria in Antioquia department, Colombia.*

Biddle, K. T., & Christie-Blick, N. H. (1985). *Basin formation. structural traps, and controls on hydrocarbonocurrence along wrenchfault zones.*

Bonforte, A., Federico, C., Giammanco, S., Guglielmino, F., Liuzzo, M., & Neri, M. (2013). *Soil gases and SAR measurements reveal hidden faults on the sliding flank of Mt. Etna (Italy).* J. Volcanol Geotherm. Res. 251, 27–40. http://dx.doi.org/10.1016/j.jvol.

Botero, G. M. (2018). *Proveniencia y estilo estructural de la Formación Penderisco y las sedimentitas de Beibaviejo: Relación con el bloque Panamá-Choco (PCB).* Medellín : Grupo de Estudios Tectónicos (GET)-Universidad Nacional De Colombia.

Calle, B., & Salinas, R. (1986). *Geología y geoquímica de la Plancha 165, Carmen de Atrato.* Medellín: INGEOMINAS-Informe de presentación. 140p.

Campbell, J. D. (1958). *En echelon folding: Economic Geology.*

Carvajal, J. (2012). *Propuesta de Estandarización de la cartografía Geomorfológica en Colombia.* Bogota D.C: Servicio Geológico Colombiano: https://doi.org/10.32685/9789589952825.

Chandrasekharam, D., & Bundschuh, J. (2008). *Low-enthalpy geothermal resources for power generation.* Leiden: The Netherlands, CRC Press/Balkema. D'Amore, F., and Truesdell, AH-1985.

Corgne, S., Magagl, R., Yergea, M., & Sylla, D. (2010). *An integrated approach to hydrogeological lineament mapping of a semi-arid region of West Africa using Radarsat-1 and GIS.* Remote Sens Environ. 114, 1863–1875. http://dx.doi.org/10.1016/j.rse.2010.03.

CORPOAMAZONIA. (2006). *Plan de manejo ambiental de los humedales de la parte plana del valle del Sibundoy .*

CORPOURABA. (2018). *Diagnóstico Ambiental de la Cuenca Alta del Río Sucio Alto. Informe técnico,.* pp. 45-58.

Deon , F., Moeck, I., Jaya, M., Wiegand, B., Scheytt , T., & Putriatni, D. (2012). *Preliminary assessment of the geothermal system in the Tiris volcanic area, East Java, Indonesia.* Copenhagen, Denmark: Proceedings of the 74th EAGE conference and exhibition. EarthDoc EAGE Publications.

Ehlers, T. A., & Chapman, D. S. (1999). *Normal fault thermal regimes: conductive and hydrothermal heat transfer surrounding the Wasatch fault, Utah.* Tectonophysics, Volume 312, Issues 2–4, 5 November 1999, Pages 217-234.

Faulds, J., Bouchot , V., Moeck, I., & Oguz, K. (2009). *Structural controls of geothermal systems in western Turkey: a preliminary report.* Geotherm Resou CouncTrans 2009; 33: 375–83.

Flynn, G., & Ghusn, J. (1983). *Geologic and hydrogeologic research in the Moana geothermal system, Washoe County, Nevada.* Geotherm Resou Counc Trans 1983; 7:417–21.

Genter, A., Cuenot, N., Goerke , X., Melchert, B., Sanjuan, B., & Scheiber , J. (2012). *Status of the Soultz geothermal project during exploitation between 2010 and 2012. In: Proceedings of the 37th workshop on geothermal reservoir engineering.* Stanford,California: Stanford University - 2012 January30–February 2: SGP- TR-194,12p.

Giggenbach, W. (1991). *Isotopic shifts in waters from geothermal and volcanic systems along convergent plate boundaries and their origin.* EPSL 113, 495-510.

Gómez , E. (2019). Low Enthalpy Geothermal System at Dabeiba, Colombia; an Assessment Through the Hydrogeochemistry of Thermal Water. *Workshop on Geothermal Reservoir Engineerin. Stanford University.* , 2-6.

Gómez Díaz, E. (2017). *POTENCIAL GEOTERMICO EN EL SUR DE COLOMBIA A PARTIR DE ANÁLISIS GEOQUÍMICOS DE FUENTES TERMALES: CASO DE ESTUDIO VOLCÁN PURACÉ Y EL COMPLEJO DOÑA JUANA .*

González, H. (1997). *Mapa geológico generalizado del Departamento de Antioquia. Escala 1:400.000.*

Gorynski , K., Walker, D., Stockli , D., & Sabin, A. (2014). Apatite (U–Th)/He thermochronometry as an innovative geothermal exploration tool: A case study from the southern Wassuk Range, Nevada. *Journal of Volcanology and Geothermal Research 270*, 99-114.

Haeruddin Haeruddin, Saepuloh Asep, Mohamad Nur Heriawan, Taiki Kubo, Katsuaki Koike, & Dwiyogarani Malik. (2017). *Application of lineament density extracted from dual orbit of synthetic aperture radar (SAR) images to detecting fluids paths in the Wayang Windu geothermal field (West Java, Indonesia).* Volume 72, March 2018, Pages [145-155].

Hardin, T. P., & Lowell, J. D. (1979). *Structural styles, their plate-tectonic habitats, and hydrocarbon traps in petrolum provinces.*

Hochstein, M. (1988). *Assessment and modelling of geothermal reservoirs (small utilization schemes).* Geothermics 1988;17(1):15–49.

Horn, B. (1981). *Hill shading and reflectance map.* Proc. IEEE 69 (1), [14-47.

Hung, L., Batelaan, O., & De Smedt, F. (2005). Lineament extraction and analysis, comparison of LANDSAT ETM and ASTER imagery. Case study: Suoimuoi tropical karst catchment, Vietnam. SPIE-5983, Remote Sensing for Environmental Monitoring, GIS Applications,. *http://dx.doi.org/10.1117/12.627699. ALOS/PALSAR characteristics and status. In: CEOS SAR Workshop Proc. Tokyo*, 191–194.

IDEAM. (2018). *Estudio nacional del agua .* Bogotá: Ideam: 452 pp.

IDEAM. (2018). *Estudio nacional del agua (ENA-Colombia).*

IGAC. (2007). *Estudio general de suelos y zonificación de tierras departamento de Antioquia.* Bogotá D.C: DB-IGAC 1-00869. Instituto geográfico Agustín Codazzi.

IGAC-INGEOMINAS. (2001). *Comprehensive Research of the Colombian Pacific Platform. Cartographic sources of geology, geomorphology, soils, and threat sheets 101, 102, 103, 104, 112, 113, 128. Urabá, Antioquia.*

INGEOMINAS . (2009). *Geological mapping and geochemical sampling of sheets 144, 145, 128, 129, 113 and 114.*

INGEOMINAS. (1987). *Geology and geochemistry of sheet 115-Toledo. Scale 1:100.000 .*

Kenya, M., & Oham, N. (2009). *Application of geophysics to geothermal energy exploration and monitoring of its exploitation.* Lake Naivasha: KenGen P.O. Box 765.

Koch, M., & Mather, P. (1997). Lineament mapping for groundwater resource assessment: a comparison of digital Synthetic Aperture Radar (SAR) imagery and stereoscopic Large Format Camera (LFC) photographs in the Red Sea Hills. Sudan. *Int. J. Remote Sens. 18*.

Kresic, N., & Stevanovic, Z. (2010). *GROUNDWATER HYDROLOGY OF SPRINGS .* Burlington: Brithish Library-BH-USA.

Leech, D. P., Treloar, P. J., Lucas, N. S., & Grocott, J. (2003). *Landsat TM analysis of fracture patterns: a case study from the coastal cordillera of northern Chile.* Int. J. Remote Sens. 24 (19), 3709–3726.

López Zuluaga , A. (2023). *Zonificación del potencial de infiltración y lineas de flujo en el play geotermico del Sibundoy .*

Marin-Cerón, M. I., Bernet, M., & Leal Mejia, H. (2019). *Late Cenozoic to Modern-Day Volcanism in the Northern Andes: A.* Geology and Tectonics of Northwestern South America [PP 603–648].

Mark, R. (1992). *Multidirectional, oblique-weighted, shaded-relief image of the Island.* U.S. Geological Survey.

McCoy-West, A., Milicich, S., Robinson , T., Bignall, G., & Harvey, C. (2011). *Geothermal resources in the Pacific Islands: The potential of power generation to benefit indigenous communities.* Stanford, California: In: Proceedings of the 36th workshop on geothermal reservoir engineering.

Moeck, I. (2014). *Catalog of geothermal play types based on geologic controls.* Renewable and Sustainable Energy Reviews 37 (2014) [867–882].

Moeck, I., Bendall, B., Minnig, C., Manzella, A., & Yasukawa, K. (2020). *Geothermal Play Typing – Current Development and Future Trends of a Modern Concept.* Proceedings World Geothermal Congress 2020, Reykjavik, Iceland, April 26 – May 2, 2020.

Monsalve Bustamante, M. L., Gómez , J., & Nuñez Tello, A. (2020). *Rear–arc small–volume basaltic volcanism in Colombia: Monogenetic volcanic fields.* The Geology of Colombia, Volume 4 Quaternary. Servicio Geológico Colombiano, Publicaciones Geológicas Especiales 38, [353-396].

Montoya Londoño, N., Parra Londoño, M. C., & Marín-Cerón, M. I. (2019). *Preliminary geothermal conceptual model.* (Trabajo de grado- Universidad EAFIT).

Muhammad, M. M., & Awdal, A. H. (2012). *Automatic Mapping of Lineaments Using Shaded Relief Images Derived from Digital Elevation Model (DEM) in Erbil-Kurdistan, Northeast Iraq.* Advances in Natural and Applied Sciences, 138-146.

Neuendorf, K., Mehl Jr., J., & Jackson , J. (2005). *Glossary of Geology.5th ed. .* Alexandria VA: American Geosciences Institute.

Nicholson , K. (1993). *Geothermal fluids: Chemistry and exploration techniques.* Berlin-Heidelberg: Springer 263.

(1993). *Nicholson K. Geothermal fluids: Chemistry and exploration techniques. .*

Nukman , M., & Moeck, I. (2013). *Structural controls of a geothermal system in the Tarutung Basin, North Central Sumatra.* Journal of Asian Earth Sciences 74.

Pérez-Consuegra, N., Hoke, G. D., Mora, A., Fitzgerald, P., Sobel, E. R., & Sabdoval, J. R. (2021). *The case for tectonic control on erosional exhumation on the tropical Northern Andes base on thermochronology data .*

Powell , T., & Cumming, W. (2010). *Spreadsheets for Geothermal Water and Gas Geochemistry. Proceedings.* California: Thirty-Fifth Workshop on Geothermal Reservoir Engineering. Stanford University. PP 4-6.

Radaideh, O. M., Grasemann, Bernhard, Melichar, Rostislav, & Mosar. (2016). *Detection and analysis of morphotectonic features utilizing satellite remote sensing and GIS.* Geomorphology 275 [p.58–79].

Ramirez E, C. (2021). *Preliminary geothermal conceptual model at the Sibundoy geothermal play, SW Colombian volcanic arc. A conventional or non-conventional geothermal play?*

Reed, M. (1983). *Assessment of low-temperature geothermal resources of the United States.* USGS Circular 1983; 892:73.

Rodríguez , G., & Zapata, S. (2012). *Características del plutonismo Mioceno Superior en el segmento norte de la Cordillera Occidental e implicaciones tectónicas en el modelo geológico del noroccidente colombiano.* Informe técnico, CORPOURABA.

Rodríguez, G., & Arango, M. (2012). *Formación Barroso: Arco volcánico toleítico y Diabasas de San José de Urama: un prisma acrecionario T-MORB en el segmento norte de la Cordillera Occidental de Colombia. En Geología del municipio de Urrao, Departamento de Antioquia.* (pp. 7-53). INGEOMINAS, Servicio Geológico Colombiano.

Rodríguez, G., & Arango, M. I. (2013). *Formación Barroso: Arco Volcánico Toleitico Y Diabasas De San José De Urama: Un Prisma Acrecionario T-Morb En El Segmento Norte De La Cordillera Occidental De Colombia. .* Bogotá: Boletín Ciencias de La Tierra, 33, 17–38. .

Rodríguez, G., & et al. (2013). *Cartografía geológica del municipio de Frontino, Departamento de Antioquia.* INGEOMINAS, Servicio Geológico Colombiano, 79-134.

Rodríguez, G., & Zapata, G. (2012). *Características del plutonismo Mioceno superior en el segmento Norte de la Cordillera Occidental e implicaciones tectónicas en el modelo geológico del Noroccidente Colombiano.* Bogotá: Boletin de Ciencias de La Tierra, (31)- 5.22. .

Rodriguez, G., Zapata, G., & Gomez, J. F. (2012). *Plancha Geológica 114, Dabeiba, Antioquia.* Medellín: Servicio geológico colombiano. .

Roulleau, E., Bravo, F., Pinti, D., Barde-Cabusso, S., Pizarro, M., Tardani, D., & Morata, D. (2017). *Structural controls on fluid circulation at the Caviahue-Copahue Volcanic Complex (CCVC) geotermal area (Chile-Argentina), revealed by soil CO2 and temperature, self potential, and helium isotopes.* Journal of Vulcanology and Goetertmal resarch 241, 104-118.

Sanyal, S. (2005). *Classification of Geothermal systems – a possible scheme.* Stanford, CA: In: Proceedings, 30th Workshop on Geothermal Reservoir Engineering Stanford University;, SGP-TR-176.

Sarp, G. (2005). *Lineament Analysis fromSatellite Images, North-west of Ankara* . (M.Sc Dissertation) School of Natural and Applied Science, Middle East Technical University, Ankara (76 p.).

Servicio Geológico Colombiano . (2014). *Geology and geochemistry of sheet 114-Dabeiba. Scale 1:100.000.*

Servicio Geológico Colombiano . (2014). *SGC Hot Springs Inventory. Location and physico-chemical description of the three hot springs of the Dabeiba thermal system.*

Servicio Geológico Colombiano. (2003). *Regional geological reconnaissance of sheets 411 La Cruz, 412 San Juan de Villalobos, 430 Mocoa, 431 Piedmont, 448 Monopamba, 449 Orito and 465 Churuyaco. Departments of Caquetá, Cauca, Huila, Nariño and Putumayo. Scale: 1:100,000.*

Servicio Geológico Colombiano. (2005). *Geology and geochemistry of sheet 129-Cañasgordas. Scale 1:100.000.*

Servicio Geológico Colombiano. (2016). *Geology and geochemistry of sheet 130-SantaFe De Antioquia. Scale 1:100.000.*

Servicio Geológico Colombiano. (2021). *Plancha Geologíca 430 Mocoa* .

Setyawan, A., Yudianto, H., Nishijama, J., & Hakim, S. (2015). *Horizontal Gradient Analysis for Gravity and Magnetic Data Beneath Gedongsongo Geothermal Manifestations Ungaran-Indonesia.* Melbourne: ELSEVIER.

SGC. (2014). *Inventario nacional de fuentes termales-Reporte básico. Medellín : Manantial Termal de Guineales.* Dabeiba - Antioquia : Servicio geológico Colombiano.

Sibson, R. H. (1996). *Structural permeability of fluid-driven fault-fracture meshes.* Journal of Structural Geology 18(8):1031-1042.

Singhal, B., & Gupta, R. P. (2010). *Applied Hydrogeology of Fractured Rocks.* DOI:10.1007/978-90-481-8799-7.

Smith, I. E., & Németh, K. (2017). *Source to surface model of monogenetic volcanism: a critical review.*

Soengkono, S. (1999). TeKopia geothermal system (New Zealand)—the relationship between its structure and extent. *Geothermics 28, 767–784. http://dx.doi.org/10.1016/S0375-6505(99)00042-5.*, 767-784.

Velandia , F., Acosta, J., Terraza Melo, R., & Villegas, H. (2005). *The current tectonic motion of the Northern Andes along the Algeciras Fault System in SW Colombia.* Tectonophysics 399(1-4) [313-329].

Villagómez, D., & Spikings, R. (2013). *Thermochronology and tectonics of the central and western Cordilleras of Colombia: Early cretaceous tertiary evolution of the Northern Andes.*